

University of Louisville

ThinkIR: The University of Louisville's Institutional Repository

Electronic Theses and Dissertations

12-2021

Investigation of mitochondrial inheritance in the smut fungus *sporisorium reilianum*.

Hector Eduardo Mendoza
University of Louisville

Follow this and additional works at: <https://ir.library.louisville.edu/etd>



Part of the [Molecular Genetics Commons](#)

Recommended Citation

Mendoza, Hector Eduardo, "Investigation of mitochondrial inheritance in the smut fungus *sporisorium reilianum*." (2021). *Electronic Theses and Dissertations*. Paper 3748.
<https://doi.org/10.18297/etd/3748>

This Doctoral Dissertation is brought to you for free and open access by ThinkIR: The University of Louisville's Institutional Repository. It has been accepted for inclusion in Electronic Theses and Dissertations by an authorized administrator of ThinkIR: The University of Louisville's Institutional Repository. This title appears here courtesy of the author, who has retained all other copyrights. For more information, please contact thinkir@louisville.edu.

INVESTIGATION OF MITOCHONDRIAL INHERITANCE IN THE SMUT
FUNGUS *Sporisorium reilianum*

By

Hector Eduardo Mendoza

B.A., CUNY Queens College, 2015
M.Sc., University of Louisville, 2018

A Dissertation
Submitted to the Faculty of the
College of Arts and Sciences of the University of Louisville
in Partial Fulfillment of the Requirements
for the Degree of:

Doctor of Philosophy in Biology

Department of Biology
Division of Molecular, Cellular and Developmental Biology
University of Louisville
Louisville, Kentucky

December 2021

INVESTIGATION OF MITOCHONDRIAL INHERITANCE IN THE SMUT

FUNGUS *Sporisorium reilianum*

By

Hector E. Mendoza

B.A., Queens College, 2015
M.Sc., University of Louisville, 2018

A Dissertation Approved on

November 19th, 2021

by the following Dissertation Committee:

Dr. Michael Perlin, Dissertation Chair

Dr. David Schultz

Dr. Michael Menze

Dr. James Graham

Dr. Dae-Sung Hwangbo

DEDICATION

En memoria de Rosario “Charito” Escobedo Oblitas,
cuya amistad y amor por la ciencia han sido
las fuentes más valiosas de inspiración y fortaleza.

ACKNOWLEDGMENTS

Inception of the present work would not have been possible without the unwavering support of Dr. Michael Perlin, who from day one has been a source of motivation to pursue high-quality science and to disseminate it effectively and freely. His mentorship and friendship have been essential in my personal and professional growth. Likewise, I would also like to thank the rest of my committee members, Dr. David Schultz, Dr. Michael Menze, Dr. James Graham, Dr. Dae-Sung Hwangbo and Dr. Susanna Remold, whose expertise in their respective areas of study bolstered the continuous reevaluation and improvement of this work.

My experience as a graduate student would not have been as prolific and pleasant without the constant encouragement from the Perlin laboratory. I am honored to have learned from Margaret Wallen, whose assiduous and caring disposition made my first two years in the program productive and uncomplicated. I also would like to express my appreciation for Sunita Khanal, whose kind and invigorating advice has been critical during taxing circumstances. In the same manner, I am indebted to the rest of my colleagues, Nelson Tsai, William Beckerson, Joseph Ham, Roxanne Leiter and Shikhi Baruri, who further contributed to a convivial and fruitful laboratory experience. Finally, I would like to

thank Roberk Skolik and Clinton Belott from the Menze laboratory for their assistance with respirometry and confocal microscopy, respectively, which was crucial for the culmination of the alternative respiration studies.

The most rewarding experiences in the Perlin laboratory have always involved mentorship, a trait that I now consider indispensable for a well-rounded scientist. Accordingly, I would like to acknowledge Caroline Culver, Emma Lamb and Luke Schroeder, who put their trust in me to guide them through their own scientific journeys and who invested their valuable time and effort carrying out countless experiments. As part of the Perlin team, I was also fortunate enough to learn from our collaborators in Jena, Germany. The three months I spent away from my friends and family were undoubtedly gratifying thanks to Dr. Jan Schirawski, Nisha Agrawal and Christian Müller, whose generosity and hospitality made my first time in Europe comforting and rewarding.

This project would not have been possible without the financial support of the National Science Foundation (NSF), the Southern Regional Educational Board (SREB) and the Graduate School and the College of Arts & Sciences at the University of Louisville. I also would like to express my gratitude to the faculty and administrative staff of the Biology Department at the University of Louisville, who provided me with the necessary resources for a smooth and edifying experience in the doctoral program. I want to also thank my parents and brother, whose continued encouragement and unconditional love have been constant reminders of perseverance and determination, and to my uncle Dr. Javier García, who has been a role model since my earliest encounters with science.

No least of all, I am indebted to my partner Maxwell Jones, who has also experienced the ups and downs of my doctoral journey from day one without hesitation and whose love and patience have always provided a much-needed sense of normalcy to the rather intense experience of graduate school. Upon self-reflection, I would have been unable to be where I am today without Max's support, and I am enthusiastic for the life we will build together.

ABSTRACT

INVESTIGATION OF MITOCHONDRIAL INHERITANCE IN THE SMUT

FUNGUS *Sporisorium reilianum*

Hector E. Mendoza

November 19th, 2021

An important goal in evolutionary biology is to address the origin of Earth's immense biodiversity through the evolution of complex sexual reproduction mechanisms in eukaryotes. Inheritance of mitochondria during sexual reproduction has received special attention in recent years, as these organelles cannot be synthesized *de novo* and must be transmitted from parent to offspring. The importance of these organelles far exceeds its common function as the energy-producing "powerhouse" of the cell, as it has been found to also be involved in fundamental processes like apoptosis, aging and metabolic homeostasis. Thus, appropriate inheritance of mitochondria is essential for growth and development of progeny.

Sexually reproducing eukaryotes present a variety of mechanisms that allow mitochondria from a single parent to be passed on to the offspring (homoplasmy). However, biparental inheritance of mitochondria has also been described in other systems, in which offspring inherit mitochondrial genomes from both parents (heteroplasmy). Presence of different mitochondrial genomes

within the same cytoplasm may result in the dissemination of deleterious mutations arising from the individual nature of each mitochondrial genome (e.g. different DNA replication rates, susceptibility to oxidative damage, etc.). The smut fungus *Sporisorium reilianum* f. sp. *zeae* is a pathogen of maize that exhibits a dimorphic lifestyle, being able to switch from budding yeast-like haploid sporidia to pathogenic filamentous dikarya that eventually develop into diploid teliospores. Notably, this smut fungus is equipped with genes for the appropriate segregation of mitochondria during sexual reproduction. Mating in *S. reilianum* may occur between three parental type strains, a1, a2 and a3, of which only a2 contains genes that promote inheritance of its own mitochondrial genetic material. Accordingly, mitochondrial inheritance in offspring resulting from a cross with the a2 parent is expected to follow a uniparental pattern. However, what happens in a cross between the a1 and a3 partners remains unclear.

The present work explores the uniparental inheritance system of mitochondria in *S. reilianum* through the development of reliable and low-cost diagnostic methodologies to discern between mitogenomes. The study was dependent on the investigation of the genetic diversity of different *S. reilianum* strains through whole-genome sequencing and gene synteny analysis, which proved to be more reliable, and led to cost-effective methodologies for the detection of polymorphisms. Multiple sequence alignment revealed a slew of mutations throughout the mitochondrial DNA molecule. Mutations that were detected in protein-encoding regions needed further investigation, as they could have detrimental consequences on their predicted polypeptides. Furthermore,

unique DNA sequence was detected in the *cox1* gene of the Chinese isolate mitogenome, with high percent identity to other species related to *S. reilianum*. This remarkable finding may hint at a complex evolutionary history of *S. reilianum*, influenced by potential inter- and intraspecific exchange of mitochondrial genetic material.

The distinct polymorphic region detected in Chinese strains of *S. reilianum* also provided the ideal groundwork for the development of simple diagnostic methods to discern between mitotypes following a mating event in the context of mitochondrial inheritance. Exploration of the mitochondrial inheritance mechanism of *S. reilianum* was based on previous findings from the closely related species, *Ustilago maydis*, which involves a degradation-mediated mechanism that renders inheritance uniparental. The diagnostic methods developed were based on Polymerase Chain Reaction (PCR) technology and suggested deviation from predicted inheritance patterns in which the Chinese mitotype was always favored. Additionally, this deviation was not affected in the absence of the Lga2/Rga2 system.

Finally, the electron transport chain of *S. reilianum* was further explored. Bioinformatic analysis and growth inhibition assays using specific respiratory inhibitors revealed the presence of a putative alternative oxidase (AOX), which is associated with alternative respiration in the face of inhibition of one or more of the classical mitochondrial complexes. AOX may play a more prominent role in the pathogenic stage of the fungus, as its absence significantly reduced disease severity. Moreover, expression analysis revealed that alternative oxidase is

upregulated in the diploid teliospore stage of the fungus. Compared to haploid sporidia that bud or the dikarya that grow filamentously, such teliospores may benefit from reduced respiratory rates due to their mostly quiescent nature. Combined with the findings regarding mitochondrial inheritance, the characterization of alternative routes facilitated by nuclearly-encoded components like alternative oxidase provide an additional perspective from which to study genomic conflicts during sexual reproduction.

TABLE OF CONTENTS

DEDICATION.....	iii
ACKNOWLEDGEMENTS.....	iv
ABSTRACT.....	vii
LIST OF TABLES.....	xv
LIST OF FIGURES.....	xvi
CHAPTER I: AN OVERVIEW OF MITOCHONDRIAL INHERITANCE IN PHYTOPATHOGENIC FUNGI.....	1
Chapter Overview.....	1
Introduction.....	2
The mitochondrion as the prominent cellular organelle.....	4
Origin of mitochondria.....	7
Cellular distribution of mitochondria.....	9
The stability of the mitochondrial genome.....	16
Regulation of mitochondrial inheritance.....	20
<i>Saccharomyces cerevisiae</i> : location-dependent mitochondrial inheritance.....	24
<i>Ustilago maydis</i> : degradation-mediated uniparental mitochondrial inheritance.....	25
<i>Microbotryum violaceum</i> : doubly uniparental inheritance of organelle.....	29

<i>Cryptococcus neoformans</i> : genetic and physical constraints during uniparental mitochondrial inheritance.....	30
<i>Sporisorium reilianum</i> : challenging uniparental inheritance patterns.....	33
Research questions.....	34
CHAPTER II: ANALYSIS OF MITOGENOMIC DATA OF DIFFERENT STRAINS OF <i>Sporisorium reilianum f. sp. zea</i>	37
Chapter Overview.....	37
Introduction.....	38
Materials and Methods.....	41
Strains and growth conditions.....	41
Molecular techniques and bioinformatic analysis.....	42
Results.....	44
Gene synteny analysis.....	44
Confirmation of <i>nad6</i> deletion.....	46
Verification of <i>cox1</i> polymorphic region.....	48
Development of diagnostic PCR for the determination of fungal mitotype.....	51
Discussion.....	51
CHAPTER III: CHARACTERIZATION OF THE Lga2/Rga2 MITOCHONDRIAL INHERITANCE SYSTEM IN <i>Sporisorium reilianum f. sp. zea</i>	59
Chapter Overview.....	59
Introduction.....	60
Materials and Methods.....	64

Strains and growth conditions.....	64
Molecular techniques.....	67
Expression analysis.....	70
Mating assays.....	71
Stress assays.....	71
Pathogenicity assays and teliospore harvesting.....	71
Results.....	73
Lga2 and Rga2 are not essential components of the mating program, are not involved in overall cell viability and do not affect pathogenicity	
Absence of Lga2 and Rga2 changes expected mitochondrial inheritance patterns.....	73
Absence of Lga2 and Rga2 changes expected mitochondrial inheritance patterns.....	74
Screening of <i>cox1</i> polymorphic region.....	78
Discussion.....	80
CHAPTER IV: IDENTIFICATION AND FUNCTIONAL CHARACTERIZATION OF A PUTATIVE ALTERNATIVE OXIDASE (AOX) IN <i>Sporisorium reilianum f. sp.</i> <i>zeae</i>	84
Chapter Overview.....	84
Introduction.....	85
Materials and Methods.....	88
Strains and growth conditions.....	88
Bioinformatics.....	90

Molecular techniques.....	90
Mating assays.....	96
Stress assays.....	96
Growth inhibition assays.....	96
Pathogenicity assays.....	97
Expression studies.....	97
Microscopy.....	98
Results.....	99
Identification of a putative alternative oxidase in SRZ.....	99
Mating capability is not affected in the absence of AOX.....	101
AOX does not influence overall cell integrity and viability.....	102
AOX provides an alternative route for the transport of electrons during oxidative phosphorylation.....	103
Secondary respiration is involved in pathogenicity of SRZ.....	107
AOX expression is upregulated during the teliospore stage of the fungal life cycle.....	109
SRZ AOX localizes to the mitochondrial membrane.....	110
Discussion.....	111
CHAPTER V: CONCLUSIONS.....	115
REFERENCES.....	121
APPENDIX.....	135
CURRICULUM VITAE.....	152

LIST OF TABLES

Table 2.1 SRZ strains used in Chapter 2.....	42
Table 2.2 Primers used in Chapter 2.....	43
Table 2.3 Summary of mutations detected in mitogenomes sequenced in reference to SRZ2.....	46
Table 3.1 SRZ strains used or generated in Chapter 3.....	65
Table 3.2 Plasmids used or generated in Chapter 3.....	65
Table 3.3 Primers used in Chapter 3.....	66
Table 4.1 SRZ strains used or generated in Chapter 4.....	89
Table 4.2 Plasmids used or generated in Chapter 4.....	90
Table 4.3 Primers used in Chapter 4.....	95

LIST OF FIGURES

Figure 1.1 Mechanisms of mitochondrial inheritance in fungi.....	23
Figure 2.1 Gene synteny analysis of SRZ strains.....	45
Figure 2.2 Verification of <i>nad6</i> deletion via PCR and sequence alignment.....	48
Figure 2.3 Verification of <i>cox1</i> polymorphic region via PCR.....	49
Figure 2.4 Polymorphic region in <i>cox1</i> of German and Chinese strains.....	51
Figure 3.1 Proposed mitochondrial inheritance patterns in SRZ.....	62
Figure 3.2 Gene disruption in the <i>a2</i> locus of by homologous recombination....	63
Figure 3.3 Plasmids containing <i>Lga2/Rga2</i> deletion constructs.....	68
Figure 3.4 Symptomatic profile of SRZ infection of maize.....	72
Figure 3.5 Determination of teliospore mitotype.....	77
Figure 3.6 Primer binding areas around the <i>cox1</i> polymorphic region.....	79
Figure 4.1 AOX-mediated respiration.....	87
Figure 4.2 Plasmid containing the AOX deletion construct.....	91
Figure 4.3 MUSCLE analysis of amino acid sequence of putative SRZ AOX against known polypeptides.....	100
Figure 4.4 Mating reactions of SRZ.....	102
Figure 4.5 Growth of SRZ on stress media.....	103
Figure 4.6 Growth inhibition assay of SRZ.....	106

Figure 4.7 Assessment of pathogenicity of SRZ on maize.....108

Figure 4.8 Fold-change differences of AOX expression in teliospores and haploid cells of SRZ.....110

Figure 4.9 Localization of AOX in SRZ.....111

CHAPTER I¹

AN OVERVIEW OF MITOCHONDRIAL INHERITANCE IN PHYTOPATHOGENIC FUNGI

Chapter Overview

Mitochondrial functioning and maintenance are essential for fueling metabolic processes in the eukaryotic cell. Mitochondrial DNA replication is independent of the replication control of nuclear DNA and as such, mitochondria may behave as selfish elements that need to be controlled, maintained, and reliably distributed to progeny. Sexual reproduction entails compatibility between two cellular partners that may undergo fusion to produce genetically recombinant progeny able to adapt to an unpredictable environment. This compatibility checkpoint is further exacerbated when considering inheritance of organellar material, which deviates from Mendelian principles of segregation and independent assortment by transmitting the organellar genetic material of only

¹ This chapter was previously published in the open access International Journal of Molecular Science and has been modified to meet dissertation formatting guidelines and content, with the permission of the co-authors and publisher.

Mendoza, H., Perlin, M.H., Schirawski, J. "Mitochondrial Inheritance in Phytopathogenic Fungi-Everything Is Known, or Is It?" *Int J Mol Sci.* 2020 May 29;21(11):3883. doi: 10.3390/ijms21113883. PMID: 32485941; PMCID: PMC7312866.

one parent to the offspring. This uniparental pattern of inheritance of organelles is generally accepted among most eukaryotes and may be crucial for the prevention of any adverse effects brought on by heteroplasmy and other genomic conflicts. Phytopathogenic fungi meet with special environmental challenges within the plant host that might depend on and influence mitochondrial functions and services. Accordingly, phytopathogenic fungi provide excellent biological systems in which mitochondrial inheritance can be further explored. The following chapter explores the ample literature on mitochondrial evolution, structure, function, and organization that exacerbate its relevance as the most important organelle in the eukaryotic cell. Special attention is placed on the molecular mechanisms that drive mitochondrial inheritance, with emphasis on the biological systems discovered in phytopathogenic fungi.

Introduction

Mitochondria are essential organelles in most eukaryotic cells. They ensure the supply of energy in the form of ATP that can be used for cellular processes. Energy for metabolic reactions is gained from substrates that phytopathogenic fungi take from live or freshly killed plant material. Substrate acquisition will depend on environmental conditions that are highly variable and constantly change with the growth of the fungus. Biotrophic fungi that spread within live plants will face different conditions depending on the invaded tissue, which poses high demands on proper mitochondrial functioning. Mitochondrial

function is highly dependent on nuclear gene expression since most of the mitochondrial proteins are encoded in the host cell nucleus. Despite this high dependence, mitochondria are also highly independent and behave like selfish replicative elements. They possess their own genomic DNA (gDNA) that replicates independently of the nuclear cell cycle, is subject to higher mutation rates, and encodes specific tRNAs for the translation of mitochondrially-encoded proteins. Mitochondria are also highly dynamic. They may occur as egg-shaped compartments in the cytoplasm, or they may fuse to form a filamentous network spanning the whole cell. The interplay and regulation of transition between these different forms must be coordinated and integrated so that cellular physiology can respond to rapid changes in the needs of a cell. Regulation of these processes requires the action of evolutionarily conserved activities governing mitochondrial fusion and fission, as well as motility and tethering of mitochondria to the cytoskeleton. During cell division, whole mitochondrial organelles are inherited by the new cell. In addition to the mechanical process of distribution between mother and daughter cells, mitochondrial inheritance is regulated in many fungi, and often associated with mating type, being inherited from one parent only. In cases with uniparental inheritance patterns, individual offspring contain mitochondria of a single parent, and heteroplasmy (the occurrence of different types of mitochondria in the same cell) is usually avoided. This introductory chapter will summarize what is known about function and inheritance of these important organelles and highlight the knowledge gaps in the field.

Mitochondria also pose an additional complex layer of interactions that needs to be considered to fully understand the evolutionary history of host and pathogen.

The mitochondrion as the prominent cellular organelle

Mitochondria are essential organelles of eukaryotic cells that provide them with chemical energy in the form of ATP. ATP is generated by the cooperation of several protein complexes that form higher supramolecular structures called respirasomes and function in the inner mitochondrial membrane to oxidize NADH and to transfer electrons to a final electron acceptor, most often oxygen (1).

These respirasomes are highly conserved among eukaryotes and are comparable to the membrane-bound electron transport systems found in bacteria and archaea that may use nitrate, fumarate or oxygen as the final electron acceptor (2). Electron transport results in a transfer of protons across the inner mitochondrial membrane into the intermembrane space, which generates an electrochemical gradient (proton motive force or pmf). The accumulated protons flow back to the mitochondrial matrix along the concentration gradient and through a membrane-spanning enzyme complex called ATP synthase that uses the flow of protons for the generation of ATP (3).

Respirasomes of some eukaryotes contain alternative components that compensate for lack or non-functionality of classical complexes of the eukaryotic electron transport chain. One such alternative component is NADH dehydrogenase that is capable of oxidizing extracellular NADH. NADH

dehydrogenases were first identified in higher plants (4) and later in fungi (5,6). A combination of internal and external alternative NADH dehydrogenases is present in *Saccharomyces cerevisiae*, where complex I is completely absent (7). Alternative components of the mitochondrial respiratory chain can be found in many pathogenic fungi, although further studies are needed to understand their structures and specific functions as part of the respirasome (8).

Proper mitochondrial functioning is extremely important, and a defect in mitochondrial function can result in serious disease. In humans, a multitude of mitochondrial disorders has been described that cover genetic disorders occurring at birth due to mutations of nuclear genes, as well as those that are based on mutation of mitochondrial genes and that can occur at any age (9). Some nuclear mitochondrial genes have a role in common diseases like Parkinson's disease, where a defect in the PTEN-induced kinase 1 (PINK1) or in the E3 ubiquitin ligase, Parkin, lead to a lack of mitochondrial quality control (10). Symptoms induced by a lack of mitochondrial function are heterogeneous and vary from patient to patient, however, some clinical features are common among affected humans. These include ptosis (dropping eyelids), external ophthalmoplegia (weakening of eye muscles), proximal myopathy (muscle weakness of upper or lower limbs), cardiomyopathy (weakness of heart muscles), and exercise intolerance among others (9). Mitochondrially encoded genetic diseases usually do not occur at birth, and affected individuals carry a mixture of healthy and mutated mitochondrial genomes (11). The presence of different mitochondrial genomes within the same cytoplasm may result in the

dissemination of deleterious mutations arising from the individual nature of each mitochondrial genome (*e.g.*, different DNA replication rates, increased susceptibility to oxidative damage, etc.) (12-15). The concentration of the mutation needs to exceed a certain threshold level to manifest a disease (16), and this level may vary from person to person and from tissue to tissue (17) explaining the varied clinical phenotypes of individuals affected by a mutation in the mitochondrial DNA (mtDNA) (9). Mitochondrial heteroplasmies and copy number variations have also been associated with several cancers, including hepatocarcinomas, lung cancers, and breast cancers (13,14,18,19). Determination of the exact cause of a nuclear-encoded genetic mitochondrial disorder is also challenging, because more than 1000 mitochondrially located proteins are encoded in the nuclear genome. The nuclear genome controls essential processes needed for proper functioning of mitochondria, like mtDNA maintenance, mitochondrial protein synthesis, coenzyme Q10 biosynthesis and assembly of respiratory chain complexes (9).

Mitochondrial defects are tolerated differently depending on the complexity of the organism, as it is the case of some unicellular organisms. For instance, in unicellular obligate aerobic eukaryotes, mitochondrial defects are rarely tolerated because the resulting fitness defect of the cell will lead to its rapid extinction. Under controlled laboratory conditions however, such mitochondrial mutants can be cultivated and studied. A famous example involves the *S. cerevisiae* petite mutants that form much smaller colonies on nutrient agar than their wild type ancestors (20). The petite mutants lack all (ρ^0) or a large portion (ρ^-) of their

mtDNA. Such mutants lose their ability to respire, as well as their ability to grow on ethanol or glycerol as sole carbon sources.

Origin of mitochondria

Today's mitochondria are the result of several billion years of co-evolution within eukaryotic cells. Originally proposed in 1967 by Lynn Sagan Margulis, the emergence of the mitochondrion was a direct result of the need to adapt to an oxygen-containing atmosphere (21). With the establishment and advancement of phylogenetics and mitogenomics, it was recognized that mitochondria are related to a now extinct alpha-proteobacterial lineage (22,23), a conclusion that allowed further development of the endosymbiont hypothesis generally accepted today.

Despite being a ubiquitous organelle in eukaryotes, the mitochondrion still retains a certain level of sovereignty, as it contains its own independently replicating genetic material, protected by a double membrane of comparable composition to the cellular membrane. mtDNA contains protein-encoding genes for key components that make up the respirasome. This apparent independence from nuclear DNA (nDNA) is further accentuated by numerous reports of alternative mitochondrial genetic codes across species (24).

The transition from symbiont to mitochondrion involved gradual gene loss and acquisition events. For instance, proteomic studies comparing the ancient symbiont with modern alpha-proteobacteria reveal the loss of proteins involved in replication, transcription and cell division, while retaining those involved in protein

synthesis and energy conversion (25). Perhaps the most exciting finding regarding the evolution of mitochondria is phylogenomic evidence revealing the presence of genes encoding flagellar components, suggesting that the pre-mitochondrion symbiont was free-living (26,27). Such changes would have generated intermediate states of the organelle-to-be differing in metabolic capacity, until reaching the most suitable levels of synergy with its eukaryotic host.

mtDNA genomes across species also present vast diversity in size and structure, ranging from a mere ~6000 bp in *Plasmodium falciparum* (28) to an impressive ~7 Mbp organized as circular-mapping chromosomes, in *Silene noctiflora* (29). The mitochondrial genome of *S. cerevisiae* is much larger than that of mammals (85 kb vs. 16 kb), however, the coding potential is almost the same. The extra sequences mainly stem from the existence of extensive introns and intron-encoded endonucleases. Given this remarkable heterogeneity of the genome of an organelle that is found in almost all eukaryotes (30) and that is derived from a single common ancestor, it can be safely presumed that the most important symbiotic relationship of life itself was not harmonious after all.

The metabolic niche of mitochondria renders mtDNA more vulnerable to mutations than nDNA and this vulnerability is exacerbated by the lack of efficient repair machinery and the simple plasmid-like architecture of mtDNA. Mutations can happen simultaneously in different mtDNA molecules and thus, can rise in frequency and outcompete wild type mtDNA. This is often referred to as the “tragedy of the cytoplasmic commons”, in which rapid and efficient replication of

mutant mtDNA benefits the individual organelle genome but may represent a detriment for the general welfare of the cell (31). As previously mentioned, generation of a heterogeneous genomic population is linked to the emergence of mitochondrial disorders; however, it has been previously reported to occur at low frequencies (microheteroplasmy) in healthy yeast cells (32) and *Drosophila* (33) and may be even linked to aging processes in humans (34).

Cellular distribution of mitochondria

With the exception of a few cell types (*e.g.*, mature red blood cells of mammals or phloem cells of plants) and of a few organisms (*e.g.*, a species of the *Monocercomonoides*, where the essential mitochondrial functions have been replaced by a bacterial-like cytoplasmic sulfur mobilization system (30) and a parasite of salmon, *Henneguya salminicola*, that lacks a mitochondrial genome (35)) mitochondria are exclusively eukaryotic organelles. But how many mitochondria are in one cell? Although this question can be answered for certain cell types and temporal states, determined numbers greatly vary (from zero to millions), depending on the type of method used for mitochondrial quantification, the type of organism studied, the type of tissue investigated, the nutritional and developmental state of the investigated cells and the stress experienced by the cells under investigation (36). In addition, the shapes and sizes of mitochondria greatly vary not only between different species but also within one species during different developmental processes. Therefore, mitochondrial number is regulated

by fission and fusion events and is tied to developmental processes like the cell cycle.

A dynamic fission and fusion process determines the number of mitochondria per cell at any given time. These dynamics are essential for the maintenance of mitochondrial structural integrity, function, and appropriate distribution within the cell. The process is required for the optimization of, among other things, the energy output for a given environmental context. Mitochondrial morphology is therefore also highly dynamic. Depending on the cell type or state of the organism, mitochondria may be small oval-shaped organelles, short tubules or even networks spanning the whole cell. They are continuously dividing and fusing, thereby exchanging both soluble and membrane components (*e.g.*, DNA, protein, lipids). The fusion process allows for communication between mitochondrial compartments, which can shield against transient defects in mitochondrial function (37). In parallel, fission provides a mechanism for the transport, distribution, and quality control-mediated degradation of the organelle (37).

The core machinery for mitochondrial division is evolutionarily conserved and involves dynamin related proteins, whose GTPase activity provides for membrane conformational changes. The dynamin related GTPases Drp1 (mammals) / Dnm1p (yeast), and Dyn2 are involved in fission, whereas fusion is promoted by the GTPases Mfn1, Mfn2 (mammals) / Fzo1 (yeast), and OPA1 (mammals) / Mgm1 (yeast).

For mitochondrial fission, the Dnm1p/Drp1 protein is essential. Dnm1p is normally found in the cytosol and must be recruited to the mitochondrial outer membrane for division (38). Dnm1p has been shown to form spirals that can bind, constrict, and fragment mitochondrial liposomes *in vitro* (39). The presence of such helices only at later stages of mitochondrial constriction suggested the roles of additional proteins that assist in the process of pinching off or severing membranes (37).

For *S. cerevisiae*, additional components of the complex involved in mitochondrial fission include Fis1p, Mvd1p, and Caf4p (37,40). Fis1 is a mitochondrial outer membrane protein with a single transmembrane segment. Its main protein part is oriented towards the cytosol, and it has been shown to recruit the Mvd1p adaptor protein (41). Mvd1p ensures binding of Dnm1p and the assembly of Dnm1p spirals that encircle and divide the mitochondrial compartment (42). In contrast, Caf4p has a relatively minor role in Dnm1p assembly. In *S. cerevisiae*, Dnm1p has been shown to interact with Num1p, a protein originally known to be necessary for nuclear migration. Both Num1p and Dnm1p are required for proper mitochondrial inheritance (43). An additional outer membrane protein, Mdm36p, helps to stabilize the Dnm1p/Num1p interaction and links mitochondria to the cell cortex (44). Association with the cortex may play a role in mitochondrial inheritance being equal during cell division, since in the absence of Dnm1p and Num1p, all mitochondria are transferred to the daughter cells, and none remain in the mother cells (43,44).

In mammals, Fis1p is not required for recruitment of Drp1 (45), and human Fis1p (hFis1p) mediated-mitochondrial fragmentation occurs in the absence of Drp1 and Dyn2 (46). Instead, hFis1 has been shown to bind to and inhibit the GTPase activity of Mfn1, Mfn2, and OPA1, the dynamin related GTPases necessary for mitochondrial fusion. Thus, hFis1 supports mitochondrial fission by blocking the fusion machinery (46).

The fusion of the mitochondrial outer membrane is mediated by the mitofusin proteins Fzo1 (in yeast) and Mfn1 and Mfn2 (in mammals). These proteins also mediate the mitochondrial cross talk with other mitochondria and with other organelles (47). Fusion of the inner mitochondrial membrane is brought about by Mgm1 (in yeast) and Opa1 (in mammals). Opa1 exists in eight isoforms that are proteolytically cleaved into longer membrane-anchored forms and shorter soluble forms found in the intermembrane space (48). Through its decisive role in mitochondrial fusion, Mgm1/Opa1 is important for regulating the number of mitochondria per cell.

Mitochondrial fusion and fission events are intimately tied to the cell cycle. During the G1/S transition of the cell cycle, mitochondria elongate and fuse to form a hyperfused giant mitochondrial network, whereas mitochondria fragment at the onset of mitosis (49). Mitochondrial hyperfusion can be induced by inhibition of Drp1 and coincides with a buildup of cyclin E that normally regulates the cell cycle progression through G1/S (49). In contrast, mitochondrial morphology is not associated with a specific nuclear division state in the filamentous fungus *Ashbya gossypii* (50). In *A. gossypii*, mitochondria exhibit

substantial heterogeneity in both morphology and membrane potential within a single multinucleated cell. Heterokaryons with wild type nuclei and nuclei lacking the mitochondrial fusion/fission genes *DNM1* and *FZO1* exhibit altered mitochondrial morphology. This suggests that in *A. gossypii*, the gene products may be required locally near their expression site rather than diffusing widely in throughout the cell (50).

During cell division, mitochondria are partitioned between mother and daughter cells and require their association with cytoskeletal elements. In some fungi, such as *Aspergillus* or the budding yeast, or in plant cells, mitochondrial motility is largely actin-based (51). In yeast, some mitochondria are retained at the base of the mother cell distal to the bud (the “retention zone”), where they colocalize with actin cables (52). Interaction with actin cables is also necessary for movement of mitochondria into the daughter bud (52). Indeed, though mitochondria are actively transported along the actin cytoskeleton to the growing bud site in a Myo2-dependent manner, the tethering of specific mitochondria to either the mother or daughter cell is required to ensure proper distribution. An interesting aspect of this process is that daughter cells maintain a constant mitochondria-to-cell size ratio, as well as having “younger” mitochondria, implying communication leading to mitochondrial biogenesis that is coordinated with cell growth (53). In fact, the mitochondria in the daughter cells have higher redox and membrane potentials than mitochondria retained in the mother cell; the mitochondria in daughter cells also have lower levels of superoxide dismutase.

Such age asymmetry is disrupted when Mmr1, the bud-specific tether for Myo2-mitochondria interaction, is missing (54,55).

In mammals, mitochondria are transported to the cleavage furrow during cytokinesis in a microtubule-dependent manner (56). An association of mitochondria with astral microtubules of the mitotic spindle during cytokinesis was observed via super-resolution microscopy. Dominant-negative mutants of KIF5B, the heavy chain of kinesin-1 motor, and of Miro-1, the evolutionarily conserved mitochondrial Rho GTPase, abrogated mitochondrial transport to the furrow (56). However, even in systems where microtubules are the primary means of long-distance mitochondrial transport, the actin cytoskeleton is required for short-distance mitochondrial movements and for immobilization of the organelle at the cell cortex (51).

In addition to proper distribution and localization, mitochondrial contact with other organelles is critical for appropriate communication, usually via a tether-mediated contact that influences the behavior or function of one or both organelles (57). Among the many intracellular contacts made by mitochondria with other organelles, important ones include mitochondrial positioning by dynein anchoring at the plasma membrane during development and differentiation. Mitochondria also make contact with endosomes for iron transfer, and vacuoles and lysosomes for possible lipid and amino acid transport and for mitochondrial division. Finally, contact with the endoplasmic reticulum (ER) is involved in mitochondrial fusion/fission, mtDNA replication and distribution, autophagy, lipid transport, and Ca^{2+} transfer (57). Indeed, the ER-mitochondria contacts influence

the processes that affect both mitochondrial outer and inner membranes during division.

Integrity of mitochondria and their DNA is provided, not only via fusion-fission dynamics and proper transport, but also by mitophagy and genetic selection of functional genomes (58). Mitophagy is mediated by autophagosomes, whereby the mitochondria are first segregated in preparation for their degradation in lysosomes. The goal of this process is to remove defective mitochondria, especially under certain cellular conditions. This is distinct from the bulk autophagy response, where functional and dysfunctional mitochondria are indiscriminately removed. This occurs, for example, during nitrogen starvation in *S. cerevisiae* (59); on the other hand, if cells starved for nitrogen are maintained on a carbon source requiring mitochondrial function, mitophagy is reduced, but not autophagy.

Defects in mitophagy can lead to disease. Mutations in the *PINK1* and *parkin* genes are associated with familial Parkinson's disease. Parkin protein, an E3 ubiquitin ligase, is downstream of PINK1 in the pathway in *Drosophila*. In mammalian cells, PINK1 is required for Parkin to translocate from the cytosol to the mitochondrial outer membrane, leading to polyubiquitination of outer membrane proteins. An additional component of this process is played by the AAA ATPase p97, thought to help extract proteins from the outer membrane and make them accessible to the proteasome (58).

Another important factor influencing the distribution and transmission of mitochondria is genetic selection. While genetic selection should be influenced

by the relative functionality of individual mitochondria, other factors may also contribute to selection. A severe bottleneck of mtDNA distribution appears to be operating during oogenesis such that only a small percentage of mtDNA molecules winds up in the mature egg. Examples from mice, cows, and humans (58) show rapid segregation of heteroplasmic mtDNA haplotype ratios. Even in cases where a mother has low heteroplasmy, homoplasmic offspring for the rare genotype can be produced (60). One possible explanation for such bottlenecks involves the independence of mtDNA replication from the overall cell cycle. Thus, a few mitochondrial genomes in the developing oocyte could be preferentially replicated, whether or not such selective replication is biased towards particular haplotypes.

The stability of the mitochondrial genome

mtDNA is replicated within the mitochondria by a special set of nuclear-encoded proteins. mtDNA replication is best understood in mammals. Mammalian mtDNA is a small (16.6 kb) double-stranded circular DNA molecule. One of the two strands is richer in guanine bases, making it possible to differentiate a heavy from a light strand. mtDNA replication is mainly carried out by the nuclear-encoded mitochondrially-located DNA polymerase γ (POL γ). While at least four additional polymerases have been shown to also have a role in mitochondria, none of them can replace POL γ (61). POL γ works together with the helicase TWINKLE that unwinds the double strand in front of POL γ and the

mitochondrial single-stranded DNA-binding protein mtSSB that protects the single-stranded DNA against nucleases (62). The human mtDNA carries two replication origins, O_H , for initiation of heavy strand replication, and O_L , located 11 kb downstream of O_H , where light strand replication is initiated. Replication starts at O_H and proceeds by strand replacement, generating a long stretch of single-stranded template that is only replicated once the replication fork has unwound the sequences at O_L . Initiation of light strand replication starts by the action of the mitochondrial RNA polymerase POLRMT that starts to synthesize a very small transcript that is then used by POL γ for light strand synthesis (62). RNA primers will later be removed by RNASEH1. When POL γ has completed one round of replication and meets with the DNA strand that it has just polymerized, it starts a process called idling, where it alternates functionally from 5'-3' exonuclease and 3'-5' polymerase activities. Idling is necessary for strand ligation by DNA ligase III. Without the 5'-3' exonuclease activity, the replicated strand can be replaced, and circularization of the DNA molecule cannot take place (63). Daughter molecules may be intertwined during or after replication, and such hemicatenanes need to be resolved by the mitochondrial topoisomerase Top3 α (64).

Interestingly, mtDNA replication in yeast follows a different mechanism to that in mammals. For one, enzymes important for replication in mammals are absent from the yeast genome. The yeast genome does not contain genes for a mitochondrial primase, a ribonuclease H, or a topoisomerase. Therefore, it seems that replication of yeast mtDNA does not depend on the existence of

classical replication origins but is origin-independent. Recent findings led to a reanalysis of previous data and favored a model by which replication of mtDNA in yeast is primed by recombinational structures and proceeded by rolling circle replication and template switching. This allows replication of both leading and lagging strands independent of specific origins and various replicative components needed during conventional DNA replication (65).

mtDNA is packed into compact nucleoprotein complexes visible as mitochondrial nucleoids that usually contain one DNA molecule each (66). The main protein component is the high mobility group (HMG)-box domain-containing protein TFAM that binds DNA non-specifically via two binding sites at a density of about one protein per 16-17 bp of mtDNA (67). Compact and less compact nucleoids exist in each mitochondrion, showing that DNA replication and transcription of mtDNA is not synchronized within mitochondria. Less compact nucleoids have been observed to occur preferentially at sites of mitochondrial contact to the ER. These mitochondria-ER contact sites have been identified as the sites where mitochondrial division takes place, linking mitochondrial division to mtDNA replication. This may ensure an even distribution of newly replicated mtDNA molecules within the mitochondrial network (62,68).

Replication of the mtDNA via POL γ is very precise, since POL γ is a polymerase with proofreading activity that has a low inherent error rate of less than 10^{-6} (69). However, in *Rhynchosporium* species the mitochondrial mutation rate was found to be higher than the nuclear mutation rate by more than 70 times (70). The higher increased mutation rate of mtDNA could be due to an increased

concentration of reactive oxygen species (ROS) that are generated at the mitochondrial membrane, and mutations are likely due to an inefficiency of the mtDNA repair system (71). Point mutations in mtDNA will accumulate with age and an increase in mtDNA mutations may also play a vital role in the aging process (71). A second type of common mutations in mitochondrial genomes are rearrangements and deletions that could result from errors in replication, double strand breaks or a shortage of repair mechanisms (71). Deletions that invariably remove essential regions that can compromise cell survival usually occur during heteroplasmic events.

In eukaryotic cells, mechanisms exist that allow mitochondrial quality control. Studies from mice suggest that removal of highly defective mitochondria from oocytes occurs in an age-dependent manner, with mitochondria that bear more deleterious mutations being effectively removed with increasing maternal age. Such purifying selection would require monitoring of both the functional capability and the quality of the respective mitochondrial genomes. Interestingly, the removal of mitochondria whose mtDNAs contained non-deleterious polymorphisms seems to be much less efficient (72). What is particularly interesting about these experiments is that the mechanism of such purifying selection appears to operate at a sensitivity well beyond the initially observable effects of even some seriously deleterious mutations affecting, for example, oxidative phosphorylation. Some severe mutations do not appear to affect function of this critical process until the effects have accumulated beyond a certain threshold (73). Perhaps whatever is making the decision on removal of

defective mitochondria relies on the increased levels of ROS associated with certain mtDNA mutations; such a process might be used in conjunction with targeted mitophagy of individually identified defective mitochondria.

Regulation of mitochondrial inheritance

Although many sexually reproducing eukaryotes utilize uniparental mitochondrial inheritance, biparental inheritance of mitochondria has been previously described in other systems such as *S. cerevisiae* and in diverse animal groups (74). While exclusive maternal inheritance of mitochondria in humans has been the accepted dogma, paternal leakage of mitochondria and persistent heteroplasmy are not rare (75,76). Some degree of biparental inheritance has been found in a wide array of animals (*e.g.*, mammals, arthropods, fish, birds). Specifically, biparental inheritance has been observed in both intra- and inter-specific matings (74).

A unique feature of sexual reproduction is the prevalence of compatibility between two cellular entities, which will undergo fusion to produce genetically recombinant progeny that are able to adapt to an unpredictable environment (77). A crucial aspect of sexual reproduction is the inheritance of organelles, with emphasis on the transmission of the genetic material of mitochondria (and chloroplasts in the case of plants). The process of segregation of genetic material of organelles was first described in 1909 by Carl Correns and Erwin Baur, who observed different foliage phenotypes in the progeny of *Pelargonium* crosses.

Further crossing of this progeny revealed that plastids are segregated from each other during vegetative growth and that they are inherited from only one parental strain (78). It is now known that most angiosperms employ this system, in which plastid DNA (cpDNA) and mtDNA are inherited from the maternal strain (79). In contrast, gymnosperms have been shown to have maternal inheritance of mtDNA but paternal inheritance of cpDNA (80).

Correns and Baur's observations embrace an anisogamous scheme of sexual reproduction, in which there is clear discrimination between gametes (e.g., morphology, size, motility, etc.). Gamete asymmetry represents the first checkpoint by which organelle inheritance can be strictly uniparental. In mammals, large size differences exist between the ovum and the spermatozoon: the diameter of the egg is approximately 10^4 times larger than the length of a fully mature sperm cell. Accordingly, there is a striking disparity in cytoplasmic contributions. Alternatively, isogamous systems, in which there is no clear distinction between sex cells, may also present pre-determined patterns of organelle inheritance. Isogamous systems are suggested to be the ancestral foundation from which sexual reproduction and sex differentiation emerged (81).

Uniparental inheritance is found throughout eukaryotes, ranging from those with similar-sized mating cells, to those with extreme differences in gamete size. The role of uniparental inheritance in selecting against deleterious mutations, as well as in restricting nuclear/mitochondrial and mitochondrial/mitochondrial conflict cannot be overstated. The mating type contributing most mitochondria to the next generation is "maternal", while the

other is “paternal”. Control of mitochondrial inheritance can similarly be maternal or paternal. Maternal control involves destruction of the partner’s mitochondria after fertilization, whereas in paternal control, nuclear genes in one mating type control destruction of its own mitochondria during gamete formation. Such controls may be found in unicellular organisms where the mating cells are of similar size, but for multicellular organisms where there is gamete asymmetry, maternal control would amount to the targeting and elimination of mitochondria from sperm post-fertilization.

In contrast, under paternal control, the exclusion or disabling of mitochondria occurs during spermatogenesis (before entering the oocyte) (74). Male organelles are prevented from entering the oocyte in *Ascidian* tunicates, while, in the fungal plant pathogen *Ustilago maydis*, the maternal (*i.e.*, *a2* mating type) mtDNA is protected and there is selective elimination of opposite mating type mtDNA after fusion. However, paternal mtDNA may be eliminated without any involvement of the maternal mating type as it is the case in *Drosophila melanogaster*, fish and mice, in which mtDNA is actively degraded during spermatogenesis (82-84). Control can also involve both parents, as seen in bovine and primate sperm where mitochondria are modified with ubiquitin during spermatogenesis, leading to selective degradation after gamete fusion. In fungi, mitochondrial inheritance has been investigated in some detail in only a few species. However, these investigations provided a large variation in different inheritance mechanisms. Recent results on mitochondrial inheritance mechanisms in *Saccharomyces cerevisiae*, *Ustilago maydis*, *Microbotryum*

violaceum and *Cryptococcus neoformans* each provide unexpected solutions to the problem of mitochondrial inheritance as summarized in Figure 1.1.

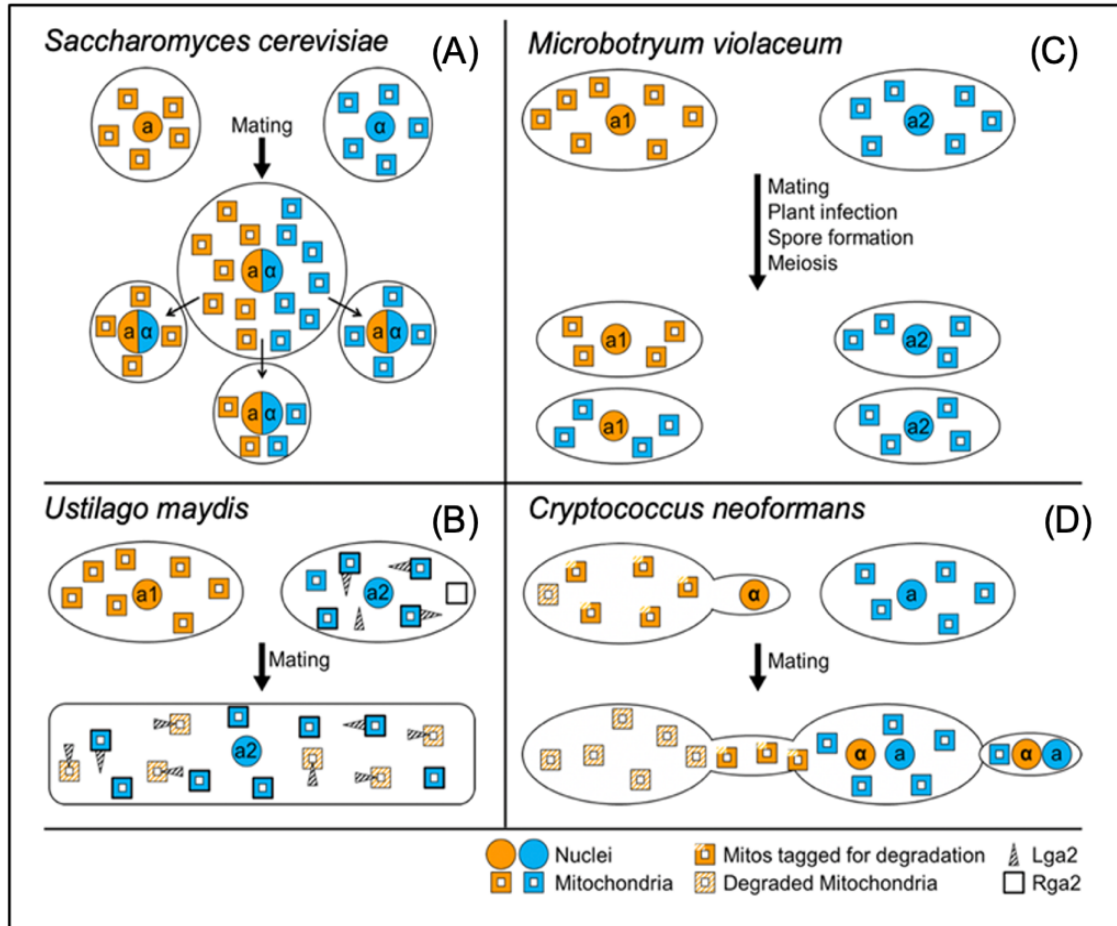


Figure 1.1 - Mechanisms of mitochondrial inheritance in fungi. (A) In *S. cerevisiae*, a and α type mitochondria remain relatively evenly distributed upon zygote formation. Whether offspring contain a or α type mitochondria or a mixture of both depends on the local position of the emerging bud. Figure modified from (91). (B) In *U. maydis*, two proteins encoded in the a2 mating type locus are responsible for uniparental mitochondrial inheritance. Rga2 shields mitochondria from the degradative effect of Lga2. Upon dikaryon formation, Lga2 leads to degradation of unprotected a1 type mitochondria. Figure modified from (96). (C) In *M. violaceum*, sexual development results in offspring where a1 type cells contain either a1 or a2 type mitochondria and a2 type cells contain only a2 type mitochondria. The mechanism of this doubly uniparental inheritance pattern is unknown. Figure modified from (119). (D) In *C. neoformans*, two effects might lead to uniparental mitochondrial inheritance. During pheromone stimulation, α type mitochondria might be tagged for degradation and be degraded during zygote formation. Only α type cells form conjugation hyphae through which the α type nuclei migrate into the zygotes. The zygote buds off at the opposite pole, thus further reducing the chance of inheriting α type mitochondria. Figure modified from (112).

***Saccharomyces cerevisiae*: location-dependent mitochondrial inheritance**

S. cerevisiae is a single-celled eukaryote widely used as a model organism to study the relationships between genes and proteins and extrapolate them into more complex organismal systems. The life cycle comprises haploid and diploid stages, in which reproduction can be achieved through vegetative propagation (budding) or sexual fusion between compatible mating types. The sexual stage of yeast is controlled by the mating type locus *MAT*. Two nonhomologous alleles or “idiomorphs” of this locus, *MAT_a* and *MAT_α*, determine the cell mating type, and fusion will only occur between an *a* and an *α* partner. Nuclear magnetic resonance and mass spectrometry studies have revealed that the *MAT_a* cells produce a pheromone (the *a* factor) that carries characteristic post-translationally attached farnesyl residue and a terminal methyl ester group (85), and that *MAT_a* cells produce cell surface receptors (encoded by *STE3*) specific for *α* pheromones. Similarly, the *MAT_α* cells produce the *α* factor and proteins that activate the expression of cell surface receptors (encoded by *STE2*) specific for *a* pheromones (86). The *MAT* locus itself encodes regulatory transcription factors, rather than the pheromone or receptor directly. Compatible partners are arrested in the G1 phase of the cell cycle, and pheromone signaling triggers the formation of polarized structural projections, known as “shmoo”, that point towards each other (87). Time-lapse digital imaging microscopy has revealed that this process is dependent on the coordinate assembly and disassembly of microtubular complexes (88).

Successful mating between haploid yeast cells produces a heteroplasmic diploid zygote, which contains a mixture of mtDNA from both parental strains. The *MATa/MATα* diploids are unresponsive to pheromone signaling and will only undergo meiosis to produce four haploid daughter cells through sporulation. Transition to the sporulation program is mediated by repressing *rme1* (repressor of meiosis 1), a haploid-specific gene that normally represses meiosis and promotes mitosis (89). Distribution of mtDNA among daughter cells is limited to the budding extension point (90,91). In other words, cells that originate from buds from either end of the mother cell will inherit mtDNA from one parental strain; whereas cells that originate from a midpoint will inherit a mixture (Figure 1A). *In vitro* studies have shown that yeast displays mostly biparental inheritance of mtDNA (92). However, this pattern is lost after approximately twenty rounds of mitotic cell division, restoring and selecting for homoplasmic daughter cells. An interesting mitochondrial inheritance pattern is observed in the petite mutants (*rho*⁻) of *S. cerevisiae*, that lack large fractions of their mtDNA leading to a respiration deficiency. When wild type cells are crossed with hyper-suppressive *rho*⁻ petite mutants, the progeny are exclusively of the *rho*⁻ mitotype. This observation suggests an extremely biased inheritance pattern for the hyper-suppressive *rho*⁻ mitotype (93).

***Ustilago maydis*: degradation-mediated uniparental mitochondrial inheritance**

U. maydis is one of the best characterized fungal plant pathogens. This smut fungus only infects corn (*Zea mays*) and its progenitor (teosinte) and has allowed the study of recombination, plant-pathogen interactions, mating type loci and, among others, inheritance of mtDNA. Haploid cells (sporidia) of this unicellular eukaryote are generated through meiosis of germinated diploid teliospores and proliferate by budding. For plant infection and pathogenic development, mating-compatible sporidia need to fuse. Fusion and the maintenance of the subsequently formed dikaryotic filaments is controlled by two unlinked mating type loci: the *a* locus that encodes a precursor for a small lipopeptide pheromone and a seven transmembrane G-protein coupled pheromone receptor (94), and the *b* locus that encodes the two subunits of a heterodimeric regulatory protein responsible for infectious development (95).

The *a* locus exists in two non-homologous idiomorphs (*a*₁ and *a*₂), while the *b* locus is multiallelic, existing in at least 23 different forms (94). Successful mating will only occur between cells of different mating types for both *a* and *b* loci and is initiated by pheromone signaling that leads to the formation of conjugation tubes. Conjugation tubes from mating-compatible sporidia fuse at their tips, which leads to plasmogamy and the formation of stable dikaryotic hyphae. Dikaryotic hyphae proliferate within the plant tissue, lead to the local induction of tumors, and after fusion of the nuclei develop into diploid teliospores that can spread, upon tumor bursting, and germinate under favorable conditions to give birth to haploid sporidia of different mating types.

The study of mitochondrial inheritance was possible by the discrimination of different mitotypes following the identification of a polymorphic region within the LSU rRNA region of mtDNA in different *U. maydis* strains (96). Crossing experiments of strains with different mitotypes showed that most offspring only contain mitochondria of one of the two parental strains and that the donating parent was of the a2 mating type, suggesting that in *U. maydis*, uniparental mitochondrial inheritance takes place (96). The a2 locus contains two genes not present in a1, *lga2* and *rga2* (97). To test whether they are involved in the regulation of mitochondrial inheritance deletion strains were created. Deletion of *lga2* resulted in biparental inheritance of mtDNA (96). Interestingly, the *lga2* deletion also led to the generation of recombinant mtDNA molecules. The inheritance of these novel mitotypes was favored when the strains were of the a2 mating type. In contrast, deletion of *rga2* favored the inheritance of a1 mitotypes. Expression of *rga2* in the a1 mating partner resulted in biparental inheritance of mtDNA (96). These results are best explained by a model in which the direct or indirect role of Rga2 is protection of mitochondria or mtDNA from the direct or indirect action of Lga2 (Figure 1B). Lga2 would have a direct or indirect role in degradation of mtDNA that is not protected by the action of Rga2 (96). Lga2 was found to interfere with mitochondrial fusion. This process of Lga2-induced mitochondrial fission is in part mediated by the dynamin-related GTPase Dnm1 known to be involved in mitochondrial fission but not by a possible influence of Lga2 on stability of the fusion protein Fzo1 (98).

The discovery of recombination within the mtDNA molecule raises questions regarding other recombination hot spots and at what frequencies they occur. mtDNA recombination has been previously reported in numerous pathogenic fungi and is suggested to be essential for the purging of deleterious mutations from a lineage (99).

The process of uniparental inheritance of mitochondria mediated by active degradation is common among most eukaryotes that promote the inheritance of maternal mtDNA. For instance, in mammals, numerous studies have described that degradation of paternal mtDNA is achieved through ubiquitination of mitochondria in the sperm prior to fertilization (100-102). As a result, upon cytoplasm fusion, paternal mitochondria are targeted for destruction by the proteasome or the lysosome. In *Caenorhabditis elegans*, paternal mtDNA degradation is regulated by autophagy, as revealed by fluorescence microscopy experiments, in which paternal mitochondria are sequestered by autophagosomes upon injection into the egg's cytoplasm (103). Mutations in autophagy-related genes led to persistence of paternal mitochondria during late embryogenesis stages. In *D. melanogaster*, degradation of paternal mtDNA was observed to occur during gametogenesis (82). During tail formation, mitochondria of the sperm cell fuse to form an elongated organelle with multiple nucleoids containing the genetic material. An endonuclease produced during the maturation of the sperm cell targets mtDNA. In this manner, only maternal mtDNA will be inherited in the zygote following fertilization.

***Microbotryum violaceum*: doubly uniparental inheritance of organelle**

M. violaceum is an obligate pathogen of the carnation family/"Pinks" (Caryophyllaceae) that sterilizes its host by replacing pollen on the anthers of inflorescences with teliospores, hence its moniker "anther smut". The pathogenic development of this fungus highly resembles that of *U. maydis*, thus its previous categorization as *Ustilago violacea*. Phylogenetic studies, as well as studies based on spore morphology and host specificity, led to the development of the new genus *Microbotryum* (104). Teliospores of *M. violaceum* are transmitted by pollinators to healthy hosts, followed by germination and meiosis to produce haploid sporidia.

M. violaceum has a heterothallic bipolar mating system, in which successful mating of haploid sporidia is determined by a specific mating type locus (*a*). This locus exists in two forms, *a*₁ and *a*₂, and determines the mating type of the parental strains. Upon interaction, the compatible partners will trigger a pheromone reaction and the formation of conjugation tubes. Both *a* forms encode specific pheromone receptors that show significant homology to Ste3 pheromone receptors of *S. cerevisiae* (105). The pheromone components of the mating locus remain uncharacterized, although a synthetic pheromone has been produced and used experimentally (106). Upon fusion of haploid sporidia, dikaryotic hyphal growth is triggered, allowing the pathogen to penetrate the plant tissue and produce a systemic infection. The fungus overwinters in the

meristematic tissue of its host until flowering, during which diseased inflorescences emerge.

Early studies using mtDNA restriction fragment length polymorphisms revealed that *M. violaceum* presents a special type of uniparental mitochondrial inheritance (107). In these early experiments, progeny of the a1 type inherited mtDNA from either parental strain, while progeny of the a2 type only acquired mtDNA from the a2 parental strain (Figure 1C) (107). The mechanism of this special type of uniparental mitochondrial inheritance, termed doubly uniparental inheritance is not well understood in *M. violaceum* as the necessary molecular and biochemical studies are lacking. However, doubly uniparental inheritance of mitochondria has been previously described in some bivalve mollusks as a process for sexual differentiation (108,109), providing an excellent model to study mitochondrial function in determination and maintenance of sex.

***Cryptococcus neoformans*: genetic and physical constraints during uniparental mitochondrial inheritance**

C. neoformans is a basidiomycete fungus that exhibits a dimorphic lifestyle, being able to switch from a unicellular budding yeast form to filamentous hyphal growth. Sexual dimorphism has been previously linked to the virulent nature of *C. neoformans* based on its ability to produce infectious spores from filamentous hyphae, on the genetic variability that sexual reproduction provides as a basis for increasing fitness and virulence, and on the importance of mating

type loci in both mating and infection. *C. neoformans* exists as both a free-living form and in association with a variety of plant and animal hosts. More importantly, this fungus behaves like an opportunistic pathogen when infecting immunocompromised animal hosts. The fungus is the causative agent of cryptococcosis, a defining opportunistic infection of AIDS that may lead to life-threatening meningoencephalitis.

C. neoformans mating is regulated by a bipolar mating system, *MAT*, that defines each mating type (a or α) (110). As it is the case in other heterothallic fungi, mating in *C. neoformans* can only occur between compatible cells. This mating reaction is regulated by pheromone and pheromone receptor genes (P/R) encoded within the *MAT* locus (111). In addition to pheromone and pheromone receptor genes, the *MAT* locus also contains genes encoding homeodomain (HD) transcription factors Sxi1 α and Sxi2a that exert conspicuous regulation over sexual development (112).

Mitochondrial inheritance in *C. neoformans* is predominantly uniparental, as demonstrated by evidence of post-mating hyphal growth with mitochondria originating from the MATa parent only (113). The uniparental inheritance pattern is also observed in interspecific crosses (*C. neoformans* vs. *C. deneoformans*) (114). Deletion of either Sxi1 α or Sxi2a results in mitochondrial leakage from the MAT α parent, while exchange of the Sxi2a gene for the Sxi1 α gene in the MATa parent had no effect, suggesting the involvement of other genes that have yet to be identified (115).

A study in 2013 identified Mat2, a transcription factor not encoded within the MAT locus, as being activated in MAT α cells during pheromone signaling, and as being involved in tagging mitochondria for preservation by an unknown mechanism (116). In the MAT α parent, Mat2 activation leads to the formation of a conjugation tube towards the MAT α parent. Upon plasmogamy, a Sxi1 α /Sxi2 α complex arbitrates the activation of downstream factors that lead to the elimination of α mitochondria (Figure 1D). Mat2 activity can be influenced by environmental factors, leading to a leaky mitochondrial inheritance pattern (117). Additionally, unisexual crossings between MAT α cells have been reported to result in a biparental mitochondrial inheritance pattern (114), suggesting different Mat2 regulation in MAT α and MAT α cells.

In addition to genetic control mechanisms, organelle inheritance in *C. neoformans* may also depend on physical constraints during mating. For instance, conjugation tube formation is asymmetrical, emerging from the MAT α parent and polarizing the soon to be zygote. Subsequent hyphal growth from the zygote always occurs at a site opposite from the conjugation side (the “a” side; Figure 1D) (118). These mechanisms impose physical restrictions on the introgression of α mitochondria into the MAT α parent and have been observed in other species like *Agaricus bitorquis* (119) and *Coprinus cinereus* (120).

One possible selective advantage for the uniparental controls of mitochondrial inheritance exhibited by *C. neoformans* may have to do with protection against selfish DNA elements found in mtDNA. As previously mentioned, deletion of either *sxi1 α* or *sxi2 α* gene led to a biparental inheritance

pattern. A recent study revealed that deletion of *Sxi1 α* also resulted in recombinant mtDNA genotypes associated with COX1 introns (121). Since the recombinant COX1 introns are associated with homing endonuclease genes, mobile genetic elements that may exhibit non-Mendelian transmission frequencies and incur no particular benefit other than their own spread, uniparental control may thereby protect *C. neoformans* offspring from homing endonuclease genes. As such, *C. neoformans* appears to be properly equipped with the molecular armament to prevent the spread of such selfish genetic elements.

***Sporisorium reilianum*: challenging uniparental inheritance patterns**

The smut fungus *Sporisorium reilianum* is a closely related species of *U. maydis*, with a comparable life cycle and two host-adapted varieties that infect maize (*S. reilianum* f. sp. *zear*) and sorghum (*S. reilianum* f. sp. *reilianum*) (122). Like many other smut fungi, *S. reilianum* mating is governed by a tetrapolar system composed of two unlinked genomic regions, a and b, which are involved in pheromone recognition and transition to the pathogenic stage, respectively. However, unlike *U. maydis*, the a locus of *S. reilianum* has been found to exist as three alleles, a1, a2 and a3, with the a2 partner also housing gene orthologs for the Lga2/Rga2 inheritance system (123). The requirement of opposing cell mating types fusing together to give rise to the pathogenic dikaryon still holds

true. However, no further studies have been carried out to characterize the inheritance mechanism of mitochondria in a system with three parental strains.

Based on what was found in *U. maydis*, a cross between the a2 partner and the a1 or a3 partner will follow uniparental inheritance patterns, resulting in offspring of the a2 mitotype. However, no formal hypotheses have been generated as to what happens in a cross between a1 and a3 parental strains. Preliminary studies have confirmed that the resulting progeny of this last cross is viable and stable, however, screening of mitotypes has not been performed. In theory, the absence of the Lga2/Rga2 inheritance system should not impose any obstacles for mitochondria to be inherited biparentally. The mating program of *S. reilianum*, thus, poses interesting queries regarding heteroplasmy and mitotype variation as selective forces for selection.

Research questions

Mitochondria are ancient organelles with a long history and an elemental impact on evolution. In this light, it is not surprising that mitochondrial functions are highly conserved among eukaryotes. A lot of what is understood today about mitochondria, their role, their function, their composition, their morphology, their replication, their organellar interactions, their evolutionary and functional constraints, was elucidated in very few organisms and is assumed to be universal. However, even very basic processes like mtDNA replication differ greatly between mammals and yeast. The greatest variation of mechanisms has

been found in mtDNA inheritance and these mechanisms are especially diverse in fungi. For a few proteins, their role in the dynamic modulation of mitochondria has been studied, but for the vast majority of mitochondrially-located proteins no function is known so far.

The evolution of sexual reproduction cannot exclude the emergence of distinct mechanisms of inheritance of organelles. Mitochondria represent pseudo-independent structures within the eukaryotic cell that may disrupt the process by which a cell divides to produce viable offspring. As a result, it is widely accepted that uniparental inheritance of mitochondria provides a selective advantage by preventing the horizontal transfer of selfish genomic elements that may have adverse effects on the overall welfare of a cell. This hypothesis, however, lacks evidence as selfish mitochondrial genes have not been studied more extensively.

Another advantage of uniparental inheritance of mitochondria involves averting the disruption of beneficial organelle genotypes due to outcrossing and recombination, which are common processes in fungal systems. However, in the absence of variation due to outcrossing and recombination, as is the case with asexual organisms, should in theory be less affected by natural selection and be less adaptable to changing environments. This last problem is aggravated when considering phenomena like Muller's ratchet, which links uniparentally inherited genomes to higher mutation rates. Along the life cycle of an organism, these genetic aberrations can persist and accumulate from generation to generation, with the potential to overwhelm the organelles that house them.

The present work scrutinizes a fungal mitochondrial inheritance mechanism to further explore the controversy around heteroplasmy. *S. reilianum* is an ideal model system to conduct this study, as its life cycle and mating system have been extensively studied in the related species, *U. maydis*. Additionally, *S. reilianum* provides the quintessential conditions to examine if biparental inheritance is inevitable in the absence of a uniparental control mechanism and if it has direct repercussions on the fitness of the resulting offspring. The subsequent three chapters focus on the functional characterization of the Lga2/Rga2 mitochondrial inheritance system and the bioinformatic analysis of mitogenomic data in *S. reilianum* for the development of diagnostic tools to discern among different mitotypes within a population. The preliminary data generated in this study will serve as the foundation for future work that considers the evolutionary consequences of biparental inheritance of mitochondria on organismal fitness.

CHAPTER II

ANALYSIS OF MITOGENOMIC DATA OF DIFFERENT STRAINS OF

Sporisorium reilianum f. sp. *Zea*e

Chapter Overview

Modern understanding of the concept of genetic diversity must include the study of both nuclear and organellar DNA, which differ greatly in terms of their structure, organization, gene content and distribution. The following chapter comprises an analysis of the genetic diversity of the smut fungus *Sporisorium reilianum* from a mitochondrial perspective. Whole-genome sequencing data was generated from biological samples collected from different geographical regions and gene synteny analysis of the mitochondrial DNA was performed. Multiple sequence alignment revealed an array of polymorphisms along the mitochondrial DNA molecule, with some requiring further verification through polymerase chain reaction and Sanger sequencing. Notably, unique sequence was detected in all samples collected in China in *cox1*, a mitochondrial gene encoding for one of the subunits that make up complex IV of the mitochondrial electron transport chain. This unique sequence had high percent identity to the mitogenome of the related species *Sporisorium scitamineum* and *Ustilago bromivora*, hinting at potential

horizontal gene transfer or recombination events during the evolutionary history of these species. More importantly, the distinct polymorphic region detected in the Chinese mitogenome provides the ideal foundation to develop a diagnostic method to discern between mitotypes and further explore the mitochondrial inheritance mechanism in *S. reilianum*.

Introduction

Conservation biology aims at the comprehension and protection of Earth's biological variety and variability. The concept of biodiversity is rather complex, and usually invokes investigation based on geographic areas, ecosystems, ecological communities, and species. With the advent of the genomic revolution, genetic diversity has become a crucial component of conservation research, focusing on DNA sequence alterations caused by natural selection, recombination, gene flow and environmental factors and how they impact adaptation. Most studies on genetic diversity, however, focus on nuclear DNA (nDNA) and often ignore organellar DNA (oDNA) which, in contrast to nDNA, differs significantly in structure, organization, size, gene distribution and content and mutational rate (124).

Given the importance of organelles that still preserve their own DNA, like chloroplasts and mitochondria, the concept of genetic diversity can no longer be reduced to a unidimensional approach. Moreover, recent mitogenomic studies have emphasized the importance of mitonuclear (bigenomic) communication in

the regulation of gene expression (125,126), exacerbating the need for both nuclear and mitochondrial perspectives for a broader and unhindered understanding of an organism's genetic structure and evolutionary history. Mitochondrial genome evolution diverges significantly among eukaryotes in terms of size, intron abundance, gene content and order, and rate of mutation (127). Fungal mitogenomes are of particular interest, as they have remained largely unexplored and have the potential to uncover the mysteries of organelle evolution.

A study in 2012 developed a classification system based on mitochondrial DNA (mtDNA), emphasizing intron abundance, size, shape and organization (128). Accordingly, fungal mtDNA displays diversity types 2, 3 and 5, with gene content largely conserved, but with high order variability. Interestingly, fungal mtDNA is more like plant mtDNA, displaying more signals of recombination and highly variable intron content, which in turn influences mitogenome sizes. Fungal introns may also exhibit autonomous proliferation via self-splicing and sequence homing, facilitated by homing endonucleases (HEs) that catalyze site-specific intron integration (129). Finally, fungal mtDNA is also characterized by its highly variable distribution and editing of mitochondrial tRNAs, which allows fungi to participate in extremely rare horizontal gene transfer events (130). These special features of fungal mtDNA provide additional molecular markers that can be used in the study of genetic diversity and evolutionary history.

The following chapter examines mitogenomic diversity in the context of the inheritance mechanisms that determine its distribution in sexually reproducing

eukaryotes. As previously mentioned, *Sporisorium reilianum f. sp. zeae* (SRZ) proves to be an excellent biological system from which to study mitochondrial inheritance patterns, given its tetrapolar mating type system and proposed degradation-mediated uniparental inheritance mechanism (123). The analysis of the mitogenomic diversity of SRZ is crucial for the detection of distinct polymorphisms that allow mtDNA discrimination among a cell population. Previous studies, using relatively costly and time-consuming methods, in the related species, *Ustilago maydis*, confirmed a nearly perfect uniparental mode of inheritance of mitochondria (96,98). A more recent study further confirmed the uniparental inheritance pattern of *U. maydis* mtDNA through the collection and analysis of mitogenomic data from samples distributed throughout Mexico, of which 75% displayed the a2 allelic variant. This study also hints at factors influencing dispersion and distribution of genetically diverse populations across the region (131).

The present study introduces a mitogenomic approach, based on whole genome sequencing (WGS) data and gene synteny analysis, for the identification of polymorphic regions in strains of SRZ. The fungal samples chosen for the study were of Chinese or German origin, as it is highly improbable that their natural populations would have encountered each other, hence leaving the respective mitogenomic diversities intact. The bioinformatic analysis revealed a myriad of mutations throughout the mtDNA. Most notably, a massive deletion in the *cox1* gene of Chinese SRZ mtDNA was initially detected and predicted to have serious consequences on its corresponding polypeptide and in turn, on

mitochondrial maintenance and function. Further investigation revealed what appeared to be a massive deletion was, in fact, unique insertion of DNA sequence not found in the SRZ genomic database and provided an optimal region from which to design a simple and effective PCR-based diagnostic methodology to discern between German and Chinese SRZ mitochondria. The bioinformatic data generated in this study introduces a new evolutionary context from which to study mitogenomic diversity in SRZ, in addition to providing the foundation for the verification of the predicted uniparental pattern of mitochondrial inheritance in SRZ.

Materials and Methods

Strains and growth conditions. The SRZ strains used in this study are listed in Table 2.1 and were kindly provided by Jan Schirawski's laboratory in the Matthias Schleiden Institute of Genetics at the Friedrich-Schiller University (Jena, Germany). The strains included in this study were selected due to their genotypes that allow for compatible crossing, as well as their different geographic origins to further increase the probability of mitochondrial polymorphisms. Haploid strains were grown in potato dextrose (PD) broth on a rotary shaker at 200 rpm at 28°C or on solid PD agar at 28°C. Strains were maintained in PD glycerol (20%) medium at -80°C for long-term storage or on PD agar at 4°C for no longer than 7 days.

Table 2.1 – SRZ strains used in Chapter 2.

Strain	Genotype	Source	Origin
SRZ1	a1b1	(123)	Hohenheim, Germany
SRZ2	a2b2	(123)	Hohenheim, Germany
SRZCXI2	a3b3	Unpublished	China “sample 1”
SRZCXII2	a3b1	Unpublished	China “sample 2”
SRZCXI3	a2b3	Unpublished	China “sample 1”
SRZ55III10	a1b2	(123)	From SRZ1 x SRZ2 teliospores

Molecular techniques and bioinformatic analysis. DNA isolation from SRZ haploid cultures were carried out as previously described for *U. maydis* (132). WGS was performed by CD Genomics (Shirley, NY, USA) using the Illumina HiSeq Sequencing Platform. The raw sequencing data was then assembled and aligned in reference to the annotated mtDNA sequence of SRZ2 (NCBI Accession No. GCA_000230245.1) in SnapGene 5.3.2 (Insightful Science, LLC). Gene synteny analysis was performed based on the concatenated alignment of fourteen mitochondrial protein-coding genes: *atp6*, *atp8*, *atp9*, *cob*, *cox1*, *cox2*, *cox3*, *nad1*, *nad2*, *nad3*, *nad4*, *nad4L*, *nad5* and *nad6*. Confirmation of putative polymorphic regions was achieved with sequential Sanger sequencing (“Primer Walking”) (Eurofins, Louisville, KY, USA). Protein sequence alignments were performed by Multiple Sequence Comparison by Log-Expectation (MUSCLE) in SnapGene 5.3.2 (Insightful Science, LLC).

Polymerase chain reaction (PCR) was carried out in a T100 Thermal Cycler (Bio-Rad Laboratories) with Ex Taq Hot Start DNA Polymerase (TaKaRa Bio Usa, Inc), PrimeSTAR Max DNA Polymerase (TaKaRa Bio USA, Inc) or DreamTaq Hot Start PCR Master Mix (Thermo Fisher Scientific). PCR cycling conditions for the Hot Start polymerases involved an initial denaturation step at

94°C for 4 minutes, followed by 34 cycles of a three-step process (denaturation at 94°C for 30 seconds, annealing at 58-62°C for 30 seconds and extension at 72°C for 1 minute per 1 kb of anticipated product) and a final extension step at 72°C for 10 minutes. PCR cycling conditions for PrimeSTAR Max DNA Polymerase involved an initial denaturation step at 98°C for 2 minutes, followed by 34 cycles of a three-step process (denaturation at 98°C for 10 seconds, annealing at primer 58-62°C for 15 seconds and extension at 72°C for 30-45 seconds) and a final extension at 72°C for 5 minutes. Primers used in this study are listed in Table 2.2. Purification of DNA from agarose gels was achieved using the Zymoclean Gel DNA Recovery Kit (Zymo Research) and followed the manufacturer's instructions.

Table 2.2 – Primers used in Chapter 2.

Running #	Sequence (5' → 3')	Purpose
oHM112	GCCGACGGTCTTTATACGAA	Diagnostic
oHM113	GCGCCTTCTTTTCTTGAATG	Diagnostic
oHM114	TCTTGCTGAAGGACCCCTTA	Diagnostic
oHM115	TAACGGAAAAATGCGAGGTC	Diagnostic
oHM119	TAGCTCGTTTTTCGGCCTTTA	Diagnostic
oHM120	CGAAACCCAGGAATGACACT	Diagnostic
oHM121	AAAGCGCGATCTACAAGACC	Diagnostic
oHM122	TTTGCCCAACATACCCTGAT	Diagnostic
oHM133	TGGGGACTCTATCTTCATCCA	Primer Walking
oHM134	GGCAATTCGAAATGGGATAG	Primer Walking
oHM135	CACCCTCTTTATGAAAAATGACAA	Primer Walking
oHM136	AGGCTACACGCGAAACAAC	Primer Walking
oHM137	AAGCTACGATCCGGAGCTAAA	Primer Walking
oHM138	TCAATGGTCTGTGCAAAGTAAGA	Primer Walking
oHM139	CGTAGGGCATAACAGATCCTCA	Primer Walking

Results

Gene synteny analysis. Concatenated alignments of the fourteen mitochondrially-encoded mitochondrial genes are illustrated in Figure 2.1. The analysis was made in reference to the mtDNA of SRZ2, *U. maydis* (NCBI Accession No. NC_008368.1) and *S. scitamineum* (NCBI Accession No. CP010939). Genome sizes of German strains (SRZ1 and SRZIII10) were closer to that of the reference strain, while Chinese strains (SRZCXI2, SRZCXII2 and SRZCXI3) were closer in size to that of *S. scitamineum*.

As expected, gene order conservation occurred intraspecifically, but not interspecifically. Individual gene analysis was performed in reference to SRZ2 and revealed an array of insertions, deletions and substitutions, as represented by color shade variation in the corresponding genes. Table 2.3 summarizes these base variations and includes analysis of mitogenomes in their entirety. Most of these deletions occur in non-coding regions of mtDNA, which is why they were not subjected to further investigation as they should have little to no effect on mitochondrial function.

Differences among all sequences included a single base-pair insertion in *cob* (m.4315_4317T), a single base-pair deletion in *nad6* (m.633delG) and two point mutations in *cox1* (m.708_710insA, m.2237delC). The mutations in *cob* and *cox1* occur in intronic regions, having no effect on the predicted polypeptide sequence, whereas the mutation in *nad6*, a gene with no introns, is predicted to cause a frameshift. Additionally, the Chinese strains displayed a unique mutation,

with what appeared to be a massive deletion of 1611 bp (m.2988_4598del) detected for all three strains. This last sequence variation spans intronic and gene-coding regions and, if proven accurate, can cause significant modifications on its respective polypeptide sequence.

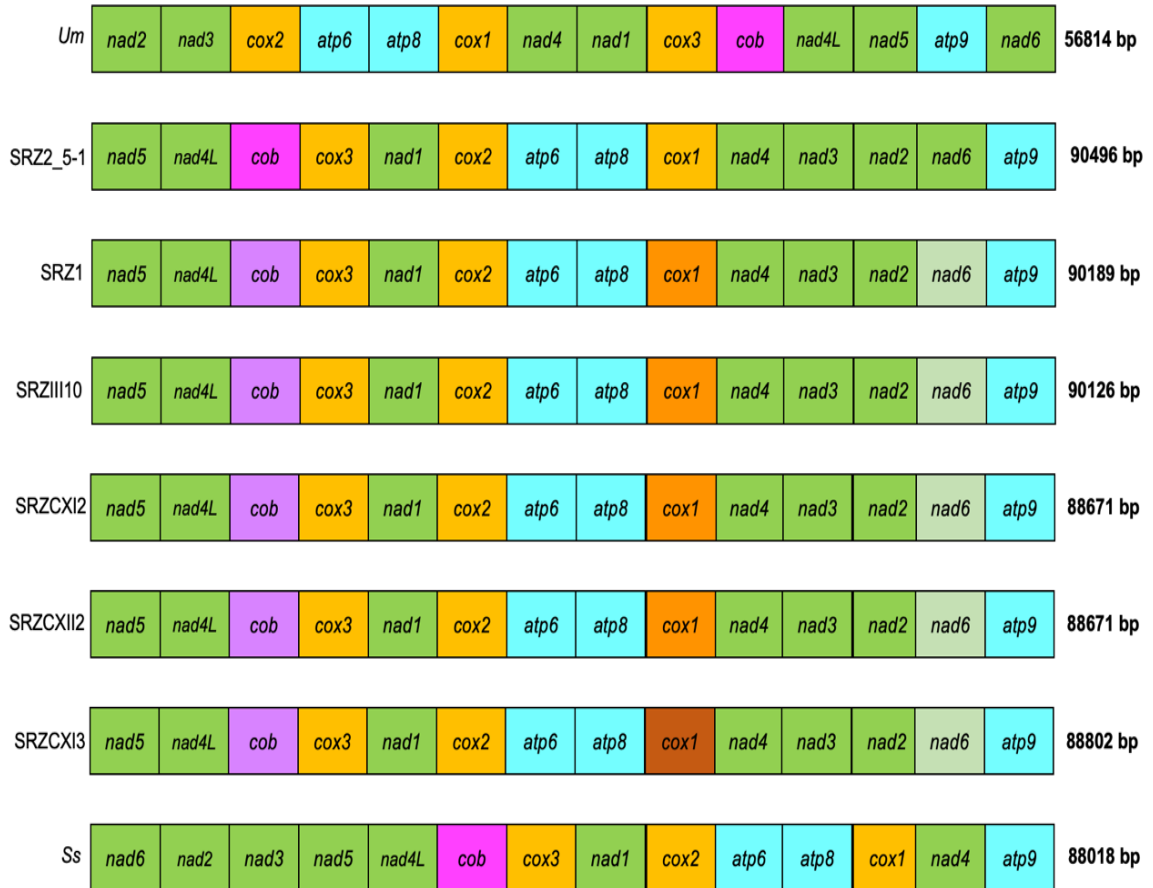


Figure 2.1 – Gene synteny analysis of SRZ strains. Concatenated alignments of 14 mitochondrial genes were made based on the raw WGS data and the annotated mitogenome of SRZ2 (NCBI Accession No. GCA_000230245.1). The mitogenomes of *U. maydis* (*Um*) and *S. scitamineum* (*Ss*) were included for comparison. The presence of unique polymorphisms in a single gene is indicated by color shade variation.

Table 2.3 – Summary of mutations detected in mitogenomes sequenced in reference to SRZ2. Colors indicate the type of mutation, with insertions represented in red, deletions represented in blue, and substitutions represented in green. Rows correspond to mutations detected within same region of mtDNA, although the numerical positions may vary otherwise due to the size disparities among mitogenomes. Shaded cells indicate that the mutation was not detected in the corresponding position. Legend: ins = insertion, del = deletion, delins = substitution.

SRZ1	SRZIII10	SRZCXI2	SRZCXII2	SRZCXI3
m.4966_4968insG	m.4966_4968insG	m.4966_4968insG	m.4966_4968insG	m.4966_4968insG
m.22393_22395insT	m.22393_22395insT	m.22393_22395insT	m.22393_22395insT	m.22393_22395insT
	m.39037del	m.39037del	m.39037del	m.39037del
m.(42869_42975)ins				
m.43211_43213insG	m.43103_43105insG	m.43103_43105insG	m.43103_43105insG	m.43103_43105insG
m.46772_46774insA	m.46664_46666insA	m.46664_46666insA	m.46664_46666insA	m.46664_46666insA
m.48456del	m.48456del	m.48456del	m.48456del	m.48456del
				m.(48944_49074)ins
		m.49207_50817del	m.49207_50817del	m.49207_50817del
m.50647del	m.50647del			
m.68067_68069insA	m.67959_67961insA	m.66480_66482insA	m.66480_66482insA	m.66611_66613insA
m.68492del	m.68492del	m.68492del	m.68492del	m.68492del
m.68390_68391delinsTT	m.68282_68283delinsTT	m.66803_66804delinsTT	m.66803_66804delinsTT	m.66934_66935delinsTT
m.84589del		m.84589_84590del	m.84589_84590del	m.84589_84590del
m.87332del	m.87332del	m.87332del	m.87332del	m.87332del
m.88146_88148insG	m.88013_88015insG	m.86558_86560insG	m.86558_86560insG	m.86689_86691insG

Confirmation of *nad6* deletion. The *nad6* gene corresponds to a single exon of 681 bp, predicted to encode a 24.4 kDa polypeptide of 226 amino acids.

Bioinformatic analysis revealed a single base-pair (m.633delG) deletion in *nad6*, at position 633, which causes a frameshift and would result in a polypeptide of only 220 amino acids. Verification of this mutation involved using the primer pair oHM121/122 to amplify a 1229 bp fragment containing *nad6* in its entirety (Figure 2.2A). The PCR fragment DNA was isolated and purified from agarose after gel

electrophoresis and sequencing was performed using primers oHM121 and oHM122, in separate reactions. All samples tested indeed had the single base-pair deletion previously detected by WGS. Surprisingly, this included SRZ2, which was used as control and should have been identical to the reference genome used for sequence alignment analysis (Figure 2.2B).

Further investigation of this mutation involved BLASTp of *nad6* obtained from the sequencing results against the annotated *nad6* amino acid sequence (NCBI Accession No. CBQ72567.1) to identify the corresponding alterations. The amino acid sequence of *nad6* in the related species *U. maydis* (NCBI Accession No. YP_762704.1) and *U. bromivora* (NCBI Accession No. SAM86553.1) were included for comparison. MUSCLE analysis revealed that the mutation truncates *nad6* at the C-terminus, producing a protein 220 amino acids long, as opposed to the 226 amino acid long polypeptide predicted by the annotated amino acid sequence (Supplemental Figure 1). Interestingly, the sequence of *U. maydis nad6* is highly similar to the annotated SRZ2 *nad6*, producing a polypeptide of the same length. When *U. bromivora nad6* was included, which corresponds to a larger polypeptide (291 amino acids), it is evident that the *S. reilianum* mutation in question significantly modifies the *nad6* polypeptide, as it is missing several amino acids that are shared across the species included in the analysis.

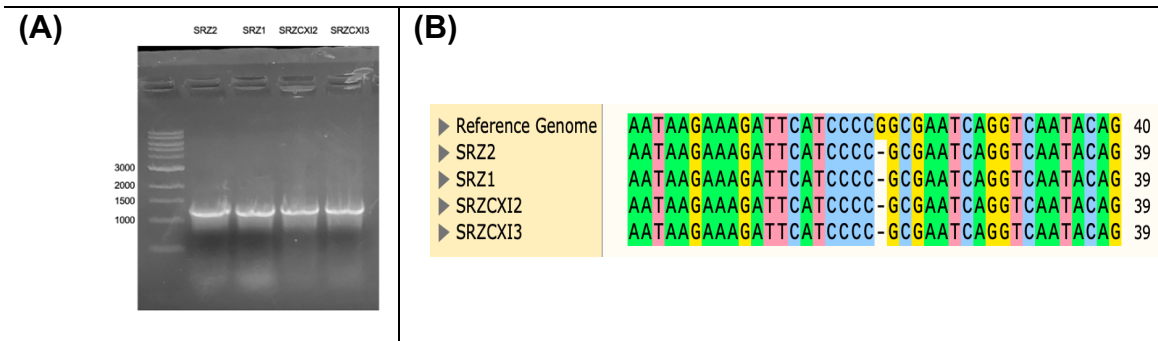


Figure 2.2 – Verification of *nad6* deletion via PCR and sequence alignment. (A) Agarose gel electrophoresis of PCR using the primer pair oHM121/122, which results in the amplification of a 1229 bp fragment containing the *nad6* (681 bp) sequence in its entirety. Resulting bands were isolated, purified and sequenced by a commercial facility (Eurofins, Louisville, KY). (B) Sequence alignment of samples tested against the reference genome of SRZ2 (NCBI Accession No. GCA_000230245.1).

Verification of *cox1* polymorphic region. The 1611 bp deletion detected in Chinese strains was used to perform diagnostic PCR with the primer pair oHM114/115, which bind outside of the region in which the deletion was originally detected. The resulting amplicon should be 2507 bp or 1158 bp in size for German and Chinese strains, respectively, and should be discernable after agarose gel electrophoresis. Surprisingly, all Chinese strains produced a band that was significantly larger in size (~4000 bp, Figure 2.3). Additional primer pairs oHM112/113 (expected amplicon: 1071 bp in German strains only) and oHM119/120 (expected amplicon: 4143 bp in German strains and 2795 bp in Chinese strains) were used to confirm this deviation of the Chinese strains from their expected amplicon sizes and these results are illustrated in Supplemental Figure 2.

The unexpected bands produced in the Chinese strains with the primer pairs oHM114/115 and oHM119/120, as well as the expected bands produced by the German strains, were isolated and purified for sequencing. A “Primer

Walking” approach was used, in which new sequencing primers (for both 5’ and 3’ ends) were designed as new DNA sequence was discovered, until results started to overlap in both sequencing directions (primers oHM133-139). This methodology confirmed that the sequence of the German DNA bands was in concordance with the reference mitogenome of SRZ2. Surprisingly, the DNA bands observed in the Chinese strains contained a 3356 bp fragment that did not match the SRZ2 reference mitogenome. BLASTn analysis of this unique fragment revealed high percent identity to *S. scitamineum* mtDNA (98.55%) and *U. bromivora* mtDNA (96.86%). The updated sequences of the Chinese strains corroborated what was observed in Figure 2.3, with the primer pair oHM114/115 generating an amplicon 4252 bp in size.

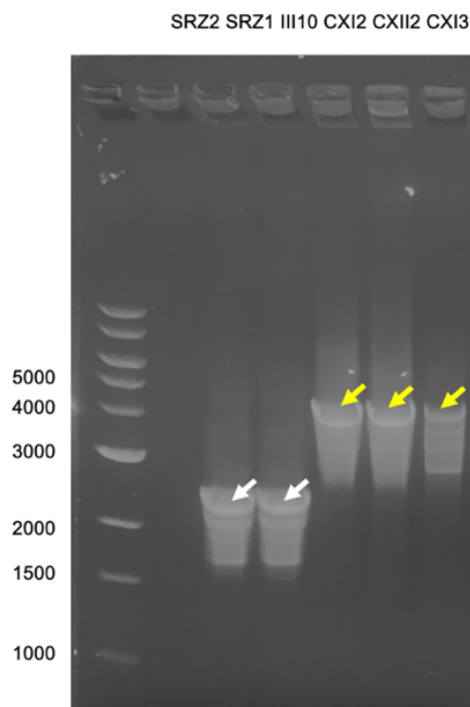


Figure 2.3 – Verification of *cox1* polymorphic region via PCR. PCR with the primer pair oHM114/115 was predicted to result in the amplification of a 2507 bp fragment for German strains (white arrows) and a 1158 bp fragment in Chinese strains. Unexpectedly, a band approximately 4000 bp in size was produced in the Chinese strains analyzed (yellow arrows). Resulting bands were isolated, purified and sent out for sequencing (Eurofins, Louisville, KY). Further analysis revealed unique sequence in Chinese strains 3356 bp in size, which was then used to update the mitogenomes of the Chinese strains. Correspondingly, the amplicon generated should be 4252 bp in size, which is consistent to the approximate sizes of the unexpected bands produced.

The polymorphic region detected in *cox1* is illustrated in Figure 2.4, where an obvious size difference between the German and Chinese versions of this gene (~1700 bp) is evident. Accordingly, the updated mitogenome sizes of Chinese strains are 91896 bp for SRZCXI2 and SRZCXII2, and 92158 bp for SRZCXI3. According to the annotated mitogenome of SRZ2 (NCBI Accession No. GCA_000230245.1), the predicted polypeptide of *cox1* consists of 9 exons to produce a polypeptide 528 amino acids in length. In Chinese strains, the unique sequence overlaps with exons 6 and 7 of the German *cox1* version.

Bioinformatic analysis of the unique region in the Chinese version of *cox1* was performed in reference to the *U. bromivora* mitogenome (NCBI Accession No. LT558140.1), as the *S. scitamineum* mitogenome is not fully annotated. BLASTn analysis revealed 5 regions of the unique sequence in the Chinese version of *cox1* with high percent identity to the mitogenome of *U. bromivora* (Supplemental Figure 3). These hits encompassed 2 intron-encoded LAGLIDAADG endonucleases and 3 exons of the *U. bromivora cox1*. Additionally, the complete amino acid sequences for *cox1* in *S. reilianum*, *U. bromivora* and *U. maydis* were compared by MUSCLE analysis, revealing high conservation in all three species (Supplemental Figure 3), suggesting that the putative exons identified in the unique region of *cox1* may in fact be part of a fully functional polypeptide that more closely resembles the *U. bromivora cox1* protein.

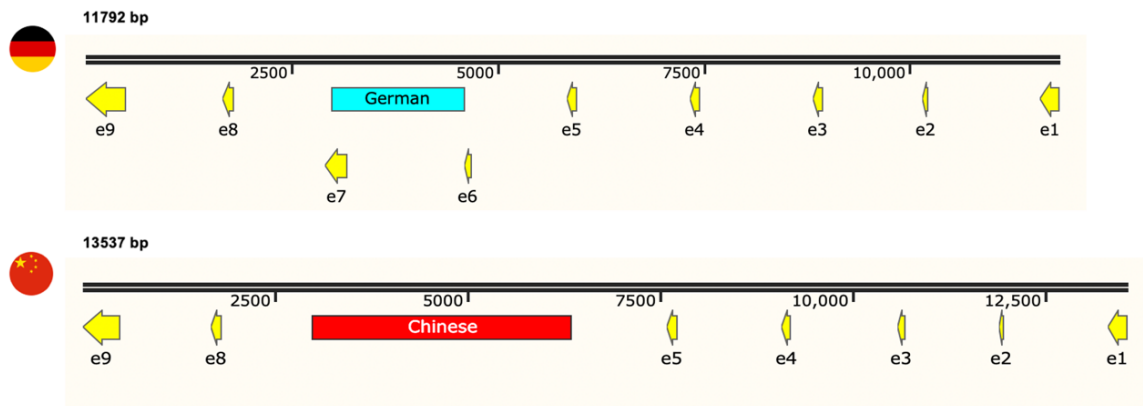


Figure 2.4 – Polymorphic region in the *cox1* of German and Chinese strains. The Primer Walking sequencing approach previously described revealed unique sequences in *cox1*, with a 1611 bp fragment in German strains matching SRZ2 mtDNA (blue block) and a 3356 bp fragment in Chinese strains matching *S. scitamineum* and *U. bromivora* mtDNA (red block). The updated gene sizes are indicated. Exons (“e”) are indicated as yellow arrows. Maps were created in SnapGene 5.3.2 (Insightful Science, LLC).

Development of diagnostic PCR for the determination of fungal mitotype.

The polymorphic region detected in *cox1* provides an auspicious opportunity to discern between German and Chinese mitotypes via PCR. The primers used in the characterization of this polymorphism can consequently be repurposed for the determination of offspring mitotype from specific crosses of SRZ strains to further explore mitochondrial inheritance patterns. Analysis of results will be based on gel electrophoresis, in which each mitotype will produce unique bands.

Discussion

The fungus *S. reilianum* provides the ideal setting from which to study mitochondrial inheritance. The degradation-mediated Lga2/Rga2 system first

identified and characterized in the related species, *U. maydis*, leads to attractive questions regarding preference of one mitochondrion over the other, and possibly emphasizing genomic conflicts and mitochondrial disorders associated with heteroplasmy and DNA incompatibilities. The studies previously carried out in *U. maydis* were solely based on data generated by restriction fragment length polymorphism (RFLP) analysis regarding a polymorphic region in the LSU rRNA gene of the mitochondrial genome (96). Contrastingly, the present study utilizes WGS data for the identification of potential polymorphisms among entire mtDNA molecules. After the initial WGS and analyses, this method ultimately proved to be less labor intensive and more cost-effective. Additionally, the SRZ strains included in this study were deliberately chosen due to their isolated geographic origins (German or Chinese), allowing for identification of distinctive diagnostic polymorphisms.

In a natural setting, the SRZ samples used in this study should never have encountered one another and consequently, their mtDNA populations would not have been subject to the bottleneck effect introduced by selective mitochondrial inheritance mechanisms. Notably, this resulted in the discovery of a distinct region of mtDNA among the Chinese samples that was initially undetected by WGS. This inaccuracy was most likely due to the reliance on the reference mitogenome used for WGS, SRZ2, which also has German origins. This finding was also quite perplexing, as the missing DNA sequence included protein-coding elements of *cox1*, which encodes one of the subunits of complex IV, an important component of the mitochondrial electron transport chain.

As revealed by the Primer Walking sequencing approach used in this study, the massive deletion initially detected by WGS in the Chinese samples was attributed to DNA sequence that was discordant with the SRZ2 annotated genome. BLASTn analysis of such sequence revealed high similarities to mtDNA of related species, including *S. scitamineum*, *U. bromivora*, *Melanopsichium pennsylvanicum* and *U. maydis*, but not SRZ2. This finding generates additional questions regarding the origin of novel mtDNA sequence in the Chinese samples. A possible explanation for this phenomenon lies in mtDNA recombination, which has been extensively reported in a variety of fungal systems (96,133-136). However, this theory is dubious when considering that the Chinese samples of SRZ would have to mate with the related species from which the novel DNA was acquired from (*i.e.*, *S. scitamineum* or *U. maydis*). Interspecific mating has been previously reported among the Ustilaginales, however, no published data have been generated regarding the viability of the potential hybrid offspring or the mitochondrial inheritance dynamics that may be involved. Nevertheless, it is possible that even aborted mating between species might lead to exchange of mitochondrial material between the transient partners.

Further bioinformatic analysis of the unique sequence discovered in the Chinese version of *cox1* involved BLASTn analysis against the *U. bromivora* mitochondrial genome. The analysis revealed 5 regions with high percent identity (>86%) that overlapped with intron-encoded LAGLIDAADG endonucleases, which are a group of homing endonucleases (HEs). These DNA elements behave as opportunistic selfish elements usually found in self-splicing introns that

recognize site-specific DNA targets to facilitate intron insertion (129). Intron homing has been extensively studied in *Saccharomyces cerevisiae*, with reported efficiencies close to 100% (137-139). However, the relevance of such mobile elements in sexual eukaryotes that have uniparental mitochondrial inheritance mechanisms that potentially purge these selfish elements remains unclear.

A recent study in *U. maydis* accidentally discovered the insertion of a mitochondrial HE-encoding gene in the telomeric region of the nuclear genome that is absent from the mitogenome, but resembles one found in the mitogenome of *S. reilianum* (140). The insertion caused the loss of the homing activity of the selfish gene, as well as the alteration of the function of the protein encoded in the insertion site, which would have led to its eventual elimination by natural selection. This astonishing discovery highlights the power of selfish elements like Hes to influence genetic diversity by the restructuring both nuclear and mitochondrial genomes.

The novel DNA sequence acquired by the Chinese SRZ strains may be the result of a combination of the presence of Hes in the mtDNA and potential horizontal gene transfer with other related species like *U. bromivora*, although such a theory has not yet been explored and requires additional experimental investigation. However, horizontal gene transfer has been extensively reported in plants (141-143) and, more recently, in *in vitro* co-cultures of human cells and, incredibly, in *in vivo* mouse tumor models (144). The region analyzed also included 3 exons of the *U. bromivora cox1*. Interestingly, the coding sequence of *cox1* in *U. bromivora* is made up of 14 exons, in contrast to the 9 exons that

make up the *S. reilianum cox1*. However, the resulting polypeptides are similar in size (524 and 528 amino acids, respectively). Accordingly, the exons present in the unique Chinese region of *cox1* may make up for the loss of the exons proper of the German version.

MUSCLE analysis of the amino acid sequences of *cox1* revealed high identity among *S. reilianum*, *U. bromivora* and *U. maydis*. Interestingly, the amino acid sequence of the *S. reilianum cox1* protein is more similar to that of *U. maydis*, both resulting in proteins 528 amino acids in length. Together, these last bioinformatic findings substantiate the hypothesis that the unique sequence in the Chinese version of *cox1* in *S. reilianum* contains exons highly similar to those found in *U. bromivora*, likely leading to production of a fully functional polypeptide. Additional studies are required to investigate the protein structure of *cox1* in *S. reilianum* to further to confirm normal function as a crucial component of the mitochondrial respiration machinery.

Analysis of the mitogenomic data was done by gene synteny analysis, based on a previous study that compared fungal mitogenomes among different families of fungi (136). Considering that this study found greater gene order variations among mitogenomes of different species, it was not surprising that the concatenated alignments of the fourteen classical mitochondrial genes of the samples sequenced in this study were identical. Nevertheless, this type of analysis provided the ideal framework to undertake the tedious and labor-intensive process of multiple sequence alignment.

Furthermore, the identification and subsequent verification of polymorphisms within different regions of the mitochondrial genes served a quality control purpose for the WGS approach, as some of these mutations occurred within protein-coding regions that can be expected to have serious effects on their predicted polypeptide sequences. These mutations needed to be verified individually, as their presence might have implied dysfunctional electron transport chain components. This was most obvious when examining the initially predicted 1611 bp deletion in *cox1* of the Chinese strains, which included an exon in its entirety and flanking intronic fragments. Sanger sequencing of this region proved to be crucial in uncovering sequence not detected during the production of contiguous sequences by WGS and may account for the apparent absence of an exon in *cox1*.

Standard PCR was an essential technique for this study, as the discovery of the 3356 bp fragment unique to the Chinese *cox1* would not have otherwise been possible. The unexpected band patterning produced by the Chinese strains when using primers associated with *cox1* was initially both a source of confusion, and later, encouragement for further exploration. Instead of redoing WGS or extensive bioinformatic analysis, Sanger sequencing was employed and quickly provided usable data. Moreover, the primers used for Primer Walking can be repurposed in different combinations to design diagnostic PCR experiments that allow the contrast between German and Chinese mitotypes.

Some of the polymorphisms detected in this study occur in protein-encoding regions of the mtDNA. Thus, the consequences on the corresponding predicted

polypeptide structure and function should be subject for further scrutiny. Notably, the SNP detected in *nad6*, a gene with no introns, results in a shorter predicted polypeptide of one of the subunits of the mitochondrial NADH dehydrogenase. Disruption of the structure and function of this crucial component of the mitochondrial electron transport chain could be detrimental for cell survival, thus increasing the need to confirm this type of mutation. The bioinformatic analysis of this mutation revealed a truncated polypeptide 220 amino acids long, when the predicted sequence should be 226 amino acids long according to the annotated SRZ2 mitogenome.

When compared against the protein sequences of *nad6* of related species, it is evident that the mutation truncates the polypeptide at the C-terminus, where it is missing several amino acids shared across all the species analyzed. Thus, the *nad6* deletion has the potential to alter the function of its predicted polypeptide, although further experimentation is needed to confirm this *in vitro*. This defect could be offset by the presence of alternative components of the mitochondrial electron transport chain, a topic that will be discussed in a later chapter.

The same is true for the polymorphisms detected in *cox1*, which cannot be situated with absolute certainty in the appropriate intronic or protein-encoding regions. The analyzed strains do not differ in growth or survival rates under standard laboratory conditions; thus, it can be assumed that these mutations may not have deleterious effects on their predicted polypeptides. Furthermore, BLASTn analysis of this region revealed the presence of putative exon sequences that show high homology to the ones found in *U. bromivora cox1*, potentially making up a

functional polypeptide that differs in genetic structure but not in function from the German version of *cox1*. However, specific respiratory assays should be considered to characterize the effectiveness of each of the mitochondrial respiration components in question.

CHAPTER III

CHARACTERIZATION OF THE Lga2/Rga2 MITOCHONDRIAL INHERITANCE SYSTEM IN *Sporisorium reilianum* f. sp. *zeae*

Chapter Overview

The mitochondrial inheritance mechanism of *Sporisorium reilianum* is predicted to be governed by a degradation-mediated mechanism previously identified in *Ustilago maydis*. Mating in *S. reilianum* may occur between three mating types, a1, a2 and a3, with the a2 housing the orthologous genes for the uniparental inheritance mechanism of mitochondria. Accordingly, a cross that includes the a2 partner is expected to result in offspring of the a2 mitotype. The following chapter centers around what will occur in a cross between the a1 and a3 partners, in which the mitochondrial inheritance mechanism is completely absent. Gene knockout experiments revealed that the Lga2/Rga2 system is dispensable in the overall maintenance of the cell, as illustrated by mating and stress tolerance assays. Preliminary pathogenicity assays revealed an apparent difference in disease severity and teliospore production, which need further investigation for more robust statistical analysis. Teliospores were collected from the test crosses used for the pathogenicity assays for further mitotype screening

using the diagnostic primers developed in Chapter 2. Absence of the Lga2/Rga2 system shifted mitochondrial inheritance patterns, further confirming its role in preventing heteroplasmy. This study also provides the framework to study the biparental inheritance of mitochondria, as offspring resulting from a1 x a3 crosses were successfully produced. Further experimentation with these teliospores is required to determine, in the context of heteroplasmy, their ability to germinate to produce viable cells requires for restarting the life cycle.

Introduction

The smut fungus *Ustilago maydis* serves as an excellent model to study sexual reproduction in higher eukaryotes. The life cycle of this pathogen of maize has been extensively characterized, depending on a tetrapolar mating type system that renders its life cycle dimorphic. The fungus can switch from yeast-like budding haploid sporidia that can enter a sexual lifestyle, governed by pheromone-pheromone receptor compatibility, to colonize and invade its host for the generation of diploid teliospores that can spread and germinate to restart the life cycle (94,145).

The components of the pheromone reaction are encoded in the *a* locus and are of two possible non-homologous variants, also referred to as idiotypes. Accordingly, sexual compatibility may only occur between different *a* mating types (a1 x a2). Further investigation of the *a* mating type locus revealed the existence of additional genes involved in mitochondrial inheritance. Notably, the

Lga2/Rga2 system, encoded exclusively in the a2 idiootype, controls a degradation-mediated uniparental mitochondrial inheritance mechanism, in which resulting offspring will be homoplasmic for the a2 mitotype (96,98). This mechanism has been previously described in higher eukaryotes, rendering mitochondrial inheritance predominantly “maternal”.

Sporisorium reilianum f. sp. zae (SRZ) is a close relative of *U. maydis*, also able to infect maize plants. The life cycles of these related species are for the most part analogous, mainly diverging in the pathogenic profiles caused on the plant host. Unlike *U. maydis*, SRZ causes systemic infection in maize, reflected as teliospore sori in fully mature male and female inflorescences. Moreover, investigation of the SRZ *a* mating type locus revealed the presence of *lga2* and *rga2* homologs in the a2 allele (123), hence suggesting a uniparental mode of inheritance of mitochondria in SRZ. More interestingly, the *a* locus of SRZ was found to have a third allelic variant, in which the genes for the Lga2/Rga2 system are absent.

Based on what was previously confirmed in *U. maydis*, it is expected that a cross involving the a2 partner will follow a uniparental inheritance pattern of mitochondria. However, what happens in a cross between the a1 and a3 partners remains unclear. Figure 3.1 summarizes mating in SRZ, proposing that in the absence of Lga2 and Rga2, mitochondrial inheritance will necessarily follow a biparental pattern, resulting in heteroplasmic offspring.

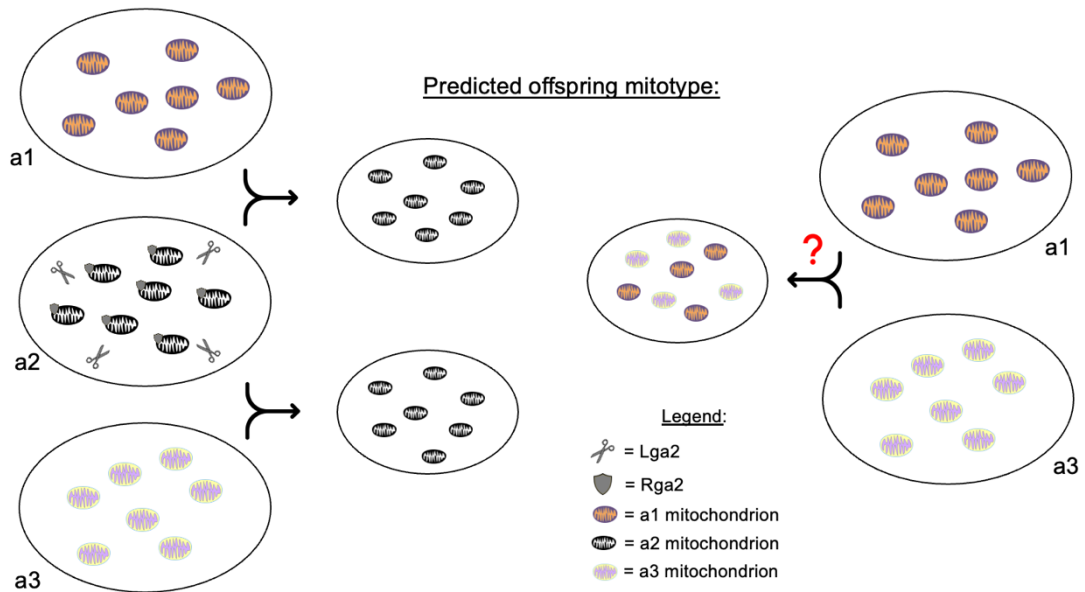
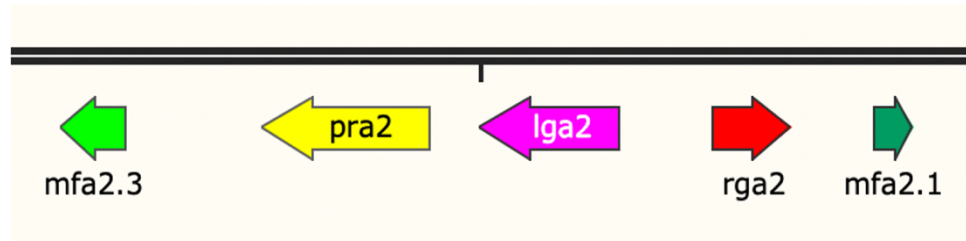


Figure 3.1 – Proposed mitochondrial inheritance patterns in SRZ. Compatible crosses involving the a2 partner (a1 x a2 or a2 x a3) will result in offspring of the a2 mitotype due to the presence of the Lga2/Rga2 uniparental inheritance system in the a2 partner. Based on the action of the Lga2/Rga2 system in the related species, *U. maydis*, a cross between a1 and a3, in which no inheritance control mechanisms have been identified, will most likely result in heteroplasmic offspring, in which mitochondrial material from both parental strains is inherited.

This chapter explores the mitochondrial inheritance mechanism in SRZ, based on loss of function experiments for Lga2 and Rga2. These two genes are located in the a2 locus of chromosome 20 of SRZ2 (Figure 3.2A), which also houses two genes encoding pheromones (*mfa2.1* and *mfa2.3*) that are compatible with the receptors of the a1 and a3 mating partners (*pra1* and *pra3*, respectively). The a2 locus also houses *pra2*, which encodes the pheromone receptor that recognizes the pheromones of a1 and a3 mating types (*mfa1.2* and *mfa3.2*, respectively). The a1, a2 and a3 loci are idiomorphs, with a2 exclusively housing *lga2* and *rga2*. Deletion constructs were designed by cloning the DNA regions upstream and downstream of the target gene flanking a resistance

cassette. This construct was then used to delete the target gene via homologous recombination (Figure 3.2B).

(A)



(B)

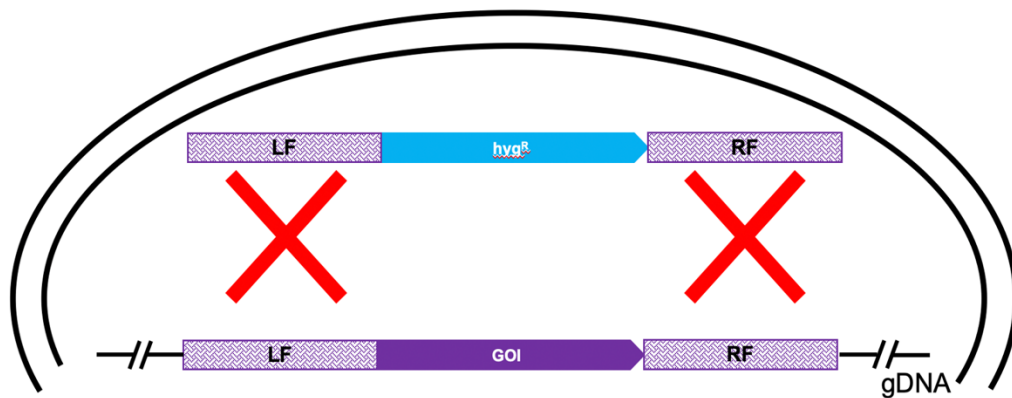


Figure 3.2 – Gene disruption in the *a2* locus by homologous recombination. (A) The *a2* locus of SRZ2 is ~11 kb in size and encodes pheromones *mfa2.3* and *mfa2.1* that can be recognized by the pheromone receptors found in *a3* (*pra3*) and *a1* (*pra1*), respectively. *pra2* codes for the pheromone receptor that is compatible with the pheromones synthesized by *a3* (*mf3.2*) and *a1* (*mfa1.2*). Additionally, the *a2* locus also has genes that encode Lga2 and Rga2, which are homologs to those found in *U. maydis*. (B) Gene deletions in SRZ are generated by cloning flanking regions (LF and RF) to the target gene, along with an antibiotic resistance cassette (*hyg^R*). The deletion constructs are then transformed into SRZ protoplasts, and the target gene is replaced by the deletion construct via homologous recombination, facilitated by the flanking regions.

As expected, the absence of Lga2 and/or Rga2 did not affect overall mating capabilities or overall cell integrity of SRZ. Accordingly, the deletion mutants were tested for their ability to cause disease in maize. Symptomatic profiles of plants infected with a compatible cross involving the deletion mutants

did not reveal an apparent effect on disease severity, although more technical and biological replicates are needed to generate more conclusive data.

Teliospores were produced in all plants infected, albeit at different rates, further emphasizing the need for a larger-scale pathogenicity assay involving *Lga2/Rga2* deletion mutants. Finally, teliospores were harvested and their mitotypes were determined based on the PCR-based diagnostic method developed in Chapter 2.

Materials and Methods

Strains and growth conditions. The SRZ strains used in this study are listed in Table 3.1 and some were kindly provided by Jan Schirawski's laboratory at the Matthias Schleiden Institute of Genetics at the Friedrich-Schiller University (Jena, Germany). Haploid strains were grown in potato dextrose (PD) broth on a rotary shaker at 200 rpm at 28°C or on solid PD agar at 28°C. Strains were maintained in PD glycerol (20%) medium at -80°C for long-term storage or on PD agar at 4°C for no longer than 7 days. Transgenic strains were selected by supplementing the PD medium with hygromycin at a final concentration of 200 µg/mL. The plasmids used in this study are listed in Table 3.2. For cloning purposes and plasmid maintenance, the transformed *Escherichia coli* DH5α strain (Thermo Fisher Scientific) was grown in Luria-Bertani (LB) broth on a rotary shaker at 200 rpm at 37°C or on solid LB agar at 37°C. Bacterial strains were maintained in LB glycerol (20%) medium at -80°C for long-term storage or on LB agar at 4°C for no longer than 7 days. Plasmid selection was achieved by

supplementing the LB medium with ampicillin at a final concentration of 200 µg/mL or gentamicin at a final concentration of 10 µg/mL.

Table 3.1 – SRZ strains used or generated in Chapter 3.

Strain	Genotype	Selectable marker	Source
SRZ1	a1b1	WT	(123)
SRZ2	a2b2	WT	(123)
SRZIII10	a1b2	WT	From SRZ1 x SRZ2
SRZCXI2	a3b3	WT	Unpublished
SRZCXII2	a3b1	WT	Unpublished
SRZCXI3	a2b3	WT	Unpublished
SRZ2Δlga2#12	a2b2Δlga2::hph	Hygromycin	This study
SRZ2Δrga2#7	a2b2Δrga2::hph	Hygromycin	This study
SRZ2Δlga2Δrga2#3	a2b2Δlga2Δrga2::hph	Hygromycin	This study

Table 3.2 – Plasmids used or generated in Chapter 3.

Plasmid	Insert of interest	Selectable marker for maintenance in <i>E. coli</i>	Source
pUM1507	<i>hph</i> (hygromycin B phosphotransferase)	Gentamicin	(146)
pUC19	<i>amp^r</i> (β-lactamase), <i>ori</i> (origin of replication cassette)	Ampicillin	New England Biolabs
pSra2L#1	Lga2 deletion construct	Ampicillin	This study
pSra2R#5	Rga2 deletion construct	Ampicillin	This study
pSra2LR#8	Lga2/Rga2 deletion construct	Ampicillin	This study

Table 3.3 – Primers used in Chapter 3.

Running #	Sequence (5'→3')	Amplicon
oHM21	CAGTACGTTAATTAATATTGAAAAAGGAAGAG	<i>amp^r</i> , <i>ori</i> for Lga2
oHM8	AATGAGAGATATCAAAAGGCCGCGTTGCTG	
oHM22	TGGGGTCAAGTGTGGAATTGTGAGCGGATA	<i>hph</i> for Lga2
oHM1	GGGTGATTGTTAAAACGACGGCCAGTGAAT	
oHM23	CAATCCACACTTGACCCACAACCACTTT	Downstream flanking region of Lga2
oHM24	TTCAATATTAATTAACGTACTGTTTTGCGGGAAT	
oHM3	GCCTTTTGATATCTCTCATTGCTGCTCAT	Upstream flanking region of Lga2
oHM4	CGTCGTTTTAACAAATCACCCATCCTTGCTC	
oHM17	CTTGCTCGATATCAAAAGGCCGCGTTGCTG	<i>amp^r</i> , <i>ori</i> for Rga2
oHM7	GGTTCGTTAATTAATATTGAAAAAGGAAGAG	
oHM20	CAACCACTTTAAAACGACGGCCAGTGAAT	<i>hph</i> for Rga2
oHM2	TCGAGGTGCTTGTGGAATTGTGAGCGGATA	
oHM5	CAATCCACAAGCACCTCGATACGACAAGC	Downstream flanking region of Rga2
oHM6	TTCAATATTAATTAACGACCCTGCTACGAAC	
oHM18	GCCTTTTGATATCGAGCAAGGATGGGTGATTGT	Upstream flanking region of Rga2
oHM19	CGTCGTTTTAAAAGTGTTGTGGGGTCAAG	
oYZ58	GGATTTTCATCGGCAACTCAC	<i>gapdh</i> for RT-qPCR
oYZ59	TACCACGAGACGAGCTTGAC	
oHM63	TCATTGCTCATCGCTAGTC	<i>lga2</i> for RT-qPCR
oHM64	TGGGCTGTAGGCGTTAATCT	
oHM65	AAATTGGATCGACCTTGTGG	<i>rga2</i> for RT-qPCR
oHM66	AAGGGTGCGTGCTCTTGAT	
oHM112	GCCGACGGTCTTTATACGAA	Diagnostic
oHM113	GCGCCTTCTTTTCTTGAATG	Diagnostic
oHM115	TAACGGAAAAATGCGAGGTC	Diagnostic
oHM119	TAGCTCGTTTTCGGCCTTTA	Diagnostic
oHM127	TCCCCTTTTATTAGCTGAGCA	Diagnostic
oHM128	TCAAGATTTTGGCAATTACAATG	Diagnostic
oHM131	CACCACAAATCCAATGACTGA	Diagnostic
oHM133	TGGGGACTCTATCTTCATCCA	Diagnostic
oHM136	AGGCTACACGCGAAACAAC	Diagnostic
oHM157	TCTGGGTAATCAGGGATTGCG	Diagnostic
oHM158	ACGCGGTAGTTCTGTTGACC	Diagnostic
oHM159	CAATAGCGGTTTGTCCATGA	Diagnostic
oHM160	TCATTGTATGTGCTAACGCTAGAT	Diagnostic
oHM161	AAAATGTTGCGGAAAAATG	Diagnostic
oHM162	TGCTATCAGATGCTTGATGA	Diagnostic
oHM163	TTCCGGTCTGTTAGTAGCATTG	Diagnostic
oHM164	GCATGTCCTTCTCCCCCTAT	Diagnostic

Molecular techniques. DNA isolation from SRZ sporidia and teliospores and transformation protocols were carried out as previously described for *U. maydis* (132). Primers used for the generation of the individual fragments of the deletion construct were designed using the open access Primer3 software (147) with complementary overlaps based on the Gibson Assembly cloning method (148). Primer sequences and respective amplicons are listed in Table 3.3.

The generation of individual pieces to make the *Lga2* deletion construct was achieved by using the primer pair oHM21/8 on pUC19 DNA for the ampicillin resistance cassette and origin of replication element, the primer oHM22/1 on pUMA1507 DNA for the hygromycin resistance cassette and the primer pairs oHM23/24 and oHM3/4 on SRZ2 gDNA for the downstream and upstream flanking regions, respectively, to *lga2*. The generation of the *Rga2* deletion construct was achieved by using the primer pair oHM17/7 on pUC19 DNA for the ampicillin resistance cassette and origin of replication element, the primer pair oHM20/2 on pUMA1507 DNA for the hygromycin resistance cassette and the primer pairs oHM5/6 and oHM18/19 on SRZ2 gDNA for the downstream and upstream flanking regions, respectively, to *rga2*. The generation of the deletion construct for the double mutant was achieved by using the primer pair oHM7/8 on pUC19 DNA for the ampicillin resistance cassette and origin of replication element, the primer pair oHM1/2 on pUMA1507 DNA for the hygromycin resistance cassette and the primer pairs oHM5/6 and oHM3/4 on SRZ2 gDNA for the downstream and upstream flanking regions, respectively, to *lga2* and *rga2*. These three fragment sets were ligated in separate Gibson reactions and

transformed into *E. coli* DH5 α . The final ligated plasmids containing the three deletion constructs are illustrated in Figure 3.3A-C, containing the Lga2, Rga2 and Lga2/Rga2 deletion constructs, respectively.

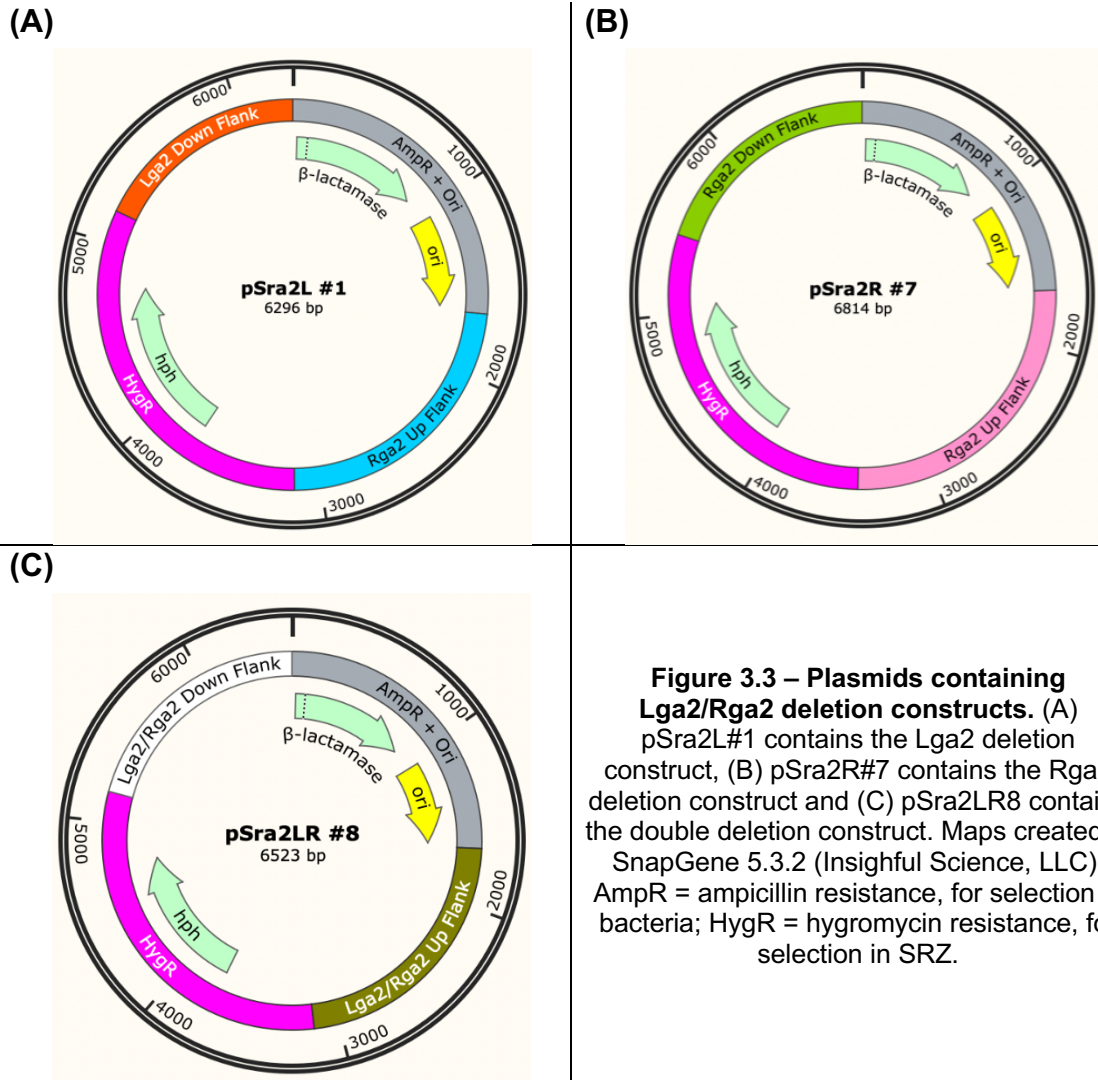


Figure 3.3 – Plasmids containing Lga2/Rga2 deletion constructs. (A) pSra2L#1 contains the Lga2 deletion construct, (B) pSra2R#7 contains the Rga2 deletion construct and (C) pSra2LR8 contains the double deletion construct. Maps created in SnapGene 5.3.2 (Insighful Science, LLC). AmpR = ampicillin resistance, for selection in bacteria; HygR = hygromycin resistance, for selection in SRZ.

For transformation of SRZ strains, each plasmid was first isolated from *E. coli* using a standard alkaline lysis protocol (149) and linearized with EcoRV (New England Biolabs). Subsequently, the deletion constructs for Lga2, Rga2 and Lga2/Rga2 were amplified with the primer pair oHM3/6. These last fragments, each made up of the upstream flanking region, followed by the

hygromycin cassette and the downstream flanking region, were used in the transformation of the different strains of SRZ, with genomic integration facilitated by homologous recombination. Preliminary verification of deletion mutants was achieved by polymerase chain reaction (PCR) using the primer pair oHM3/6, which resulted in the synthesis of 4622 bp, 5140 bp and 4849 bp fragments in Lga2, Rga2 and double deletion mutants, respectively. Wild type (WT) strains were simultaneously used as controls, in which synthesis of a 5768 bp fragment corresponded to the intact *lga2/rga2* locus. Additional verification of deletion mutants involved Southern blot hybridization (See Supplemental Protocol 1 and Supplemental Figure 4).

PCR was carried out in a T100 Thermal Cycler (Bio-Rad Laboratories) with Ex Taq Hot Start DNA Polymerase (TaKaRa Bio Usa, Inc), PrimeSTAR Max DNA Polymerase (TaKaRa Bio USA, Inc) or DreamTaq Hot Start PCR Master Mix (Thermo Fisher Scientific). PCR cycling conditions for Hot Start DNA polymerases involved an initial denaturation step at 94°C for 4 minutes, followed by 34 cycles of a three-step process (denaturation at 94°C for 30 seconds, annealing at primer 58-62°C for 30 seconds and extension at 72°C for 1 minute per 1 kb of anticipated product) and a final extension step at 72°C for 10 minutes. PCR cycling conditions for PrimeSTAR Max DNA Polymerase involved an initial denaturation step at 98°C for 2 minutes, followed by 34 cycles of a three-step process (denaturation at 98°C for 10 seconds, annealing at primer 58-62°C for 15 seconds and extension at 72°C for 30-45 seconds) and a final extension at 72°C for 5 minutes. In preparation for Gibson Assembly, all PCR products were

generated using PrimerSTAR Max DNA Polymerase. Gibson Assembly was carried out using the Gibson Assembly Master Mix kit (New England Biolabs) and according to the manufacturer's instructions.

Expression analysis. Two-step reverse transcription quantitative PCR (RT-qPCR) was used for the verification of gene deletions. Nucleic acids were isolated from SRZ by homogenization in a frozen mortar and pestle and treatment with TRIzol reagent (Invitrogen). Following cell disruption, RNA was isolated using the Direct-zol RNA Miniprep kit (Zymo). Subsequent cDNA synthesis was carried out using Super Script IV (Invitrogen) and followed the manufacturer's instructions. qPCR was carried out in a StepOne Real-Time PCR System (Applied Biosystems) using EvaGreen dye (Mango Biotechnology) according to the manufacturer's instructions. Cycling conditions involved an initial denaturation step at 95°C for 10 minutes, followed by 40 cycles of 95°C for 15 seconds and 60°C for 1 minute. Melting curve analysis was performed at the end of each cycle to ensure specificity of the reaction. Gene-specific primers were designed using the open access Primer3 software (147) and are included in Table 3.3.

The comparative Ct method was used to determine synthesized cDNA concentration, and values were normalized relative to the constitutively expressed housekeeping gene glyceraldehyde 3-phosphate dehydrogenase (*gapdh*, NCBI Accession No. sr109402). Ct values above 30 or not detectable were indicators of no gene expression. This analysis was done in technical triplicates to further confirm deletion of desired genes (data not shown).

Mating assays. Individual strains of SRZ were grown in 50 mL of PD broth on a rotary shaker at 200 rpm at 28°C until an absorbance at 600 nm (OD_{600}) of 1 was reached. Equal amounts of cells (5 mL) of the desired combinations were then mixed into 15 mL of fresh PD broth and were grown overnight on a rotary shaker at 28°C. Conjugation hyphae were scored by microscopic analysis. To confirm the production of dikaryotic filaments as a second indicator of successful mating, 15 μ L of each mating combination was spotted onto water-agar (2%) plates and incubated at 28°C for 48 hours. Dikaryotic hyphae formation was confirmed by microscopic observation as thin aerial projections on the colony surface.

Stress assays. Haploid strains were grown in 4 mL of PD broth on a rotary shaker at 200 rpm at 28°C until an OD_{600} of 1 was reached. Cells were harvested by centrifugation at 14,000 rpm, washed and resuspended in 1 mL of ddH₂O. Strains were further serially diluted in ddH₂O (from 1:10 to 1:100,000). Finally, 10 μ L of the diluted strains were spotted onto PD agar, supplemented with Congo red (CR, 100 μ M), sorbitol (1 M), NaCl (1 M) or H₂O₂ (1.5 mM). The plates were incubated for 48 hours at 28°C and photographed.

Pathogenicity assays and teliospore harvesting. Strains were grown in 50 mL of PD broth on a rotary shaker at 28°C until an OD_{600} of 0.5-0.8 was reached. Cells were harvested by centrifugation at 3500 rpm and resuspended in ddH₂O to a final OD_{600} of 2. The desired strain combinations were then mixed in a 1:1 ratio and used to inoculate 7-day old Tom Thumb maize (High Morning Organic Seeds) seedlings. Disease evaluation was performed 7-8 weeks post infection (wpi), in which plant height was recorded and symptoms were scored according

to preestablished criteria (Figure 3.4) for the calculation of disease severity indexes (150).

One-way ANOVA followed by Tukey's Multiple Comparison test was performed in GraphPad Prism 9.2.0 (GraphPad Software, LLC) to determine statistical significance, with $p \geq 0.05$ = not significant (ns), $p \leq 0.05$ = weakly significant (*), $p \leq 0.01$ = significant (**), $p \leq 0.001$ = very significant (***) and $p \leq 0.0001$ = extremely significant (****). Teliospores were harvested 7-8 wpi from infected ears of individual plants and were passed through a fine metal sieve to separate them from plant debris. Spores were incubated at 28°C for 72 hours for drying and were kept covered at room temperature.

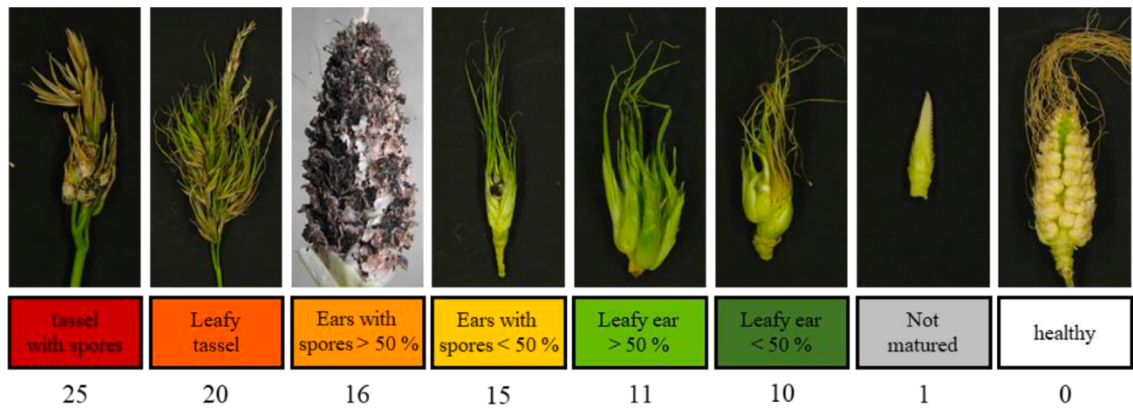


Figure 3.4 – Symptomatic profile of SRZ infection of maize. Symptoms were evaluated 7-8 wpi and were assigned a score based on a previously described methodology (151). Symptoms are visible in both male and female inflorescences and are assigned a numerical value to indicate degree of severity, ranging from healthy (score of 0) to the most severe (score of 25, “tassel with spores”).

Results

Lga2 and Rga2 are not essential components of the mating program, are not involved in overall cell viability and do not affect pathogenicity. Mating in SRZ follows the same compatibility rules previously described for *U. maydis* (152), making self vs. non-self-recognition a prerequisite for the formation of dikaryotic hyphae during the pathogenic stage of the fungus. Accordingly, successful mating will only occur between strains with different alleles for both *a* and *b* mating type loci. The absence of Lga2 and/or Rga2 did not affect mating capabilities, as indicated by successful formation of conjugation tubes between compatible sporidia and generation of aerial dikaryotic hyphae, producing ragged colony edges (see Supplemental Figure 5). Moreover, Lga2 and Rga2 are not essential for cell survival and development, as deletion mutants were able to grow normally under chemical stresses affecting cell wall integrity (CR), osmotic regulation (sorbitol), and ionic (NaCl) and oxidative (H₂O₂) equilibria (see Supplemental Figure 6).

To determine if Lga2 and Rga2 are involved in the pathogenic transition of SRZ, maize seedlings were infected with compatible combinations that included the SRZ2 deletion mutants and symptomatic profiles were analyzed 7-8 wpi. This preliminary infection assay suggests that the absence of Rga2 decreases overall disease severity (See Supplemental Figure 7). The same effect was observed in combinations involving the double mutant. These results are concordant with the individual symptom analysis that revealed that crosses involving the Lga2/Rga2

mutants produce less severe symptoms compared to the WT cross (See Supplemental Figure 7). Although these preliminary results may suggest an involvement of the Lga2/Rga2 system in the pathogenic stage of the fungus, they are inconclusive as the assay needs to include larger representative sample sizes and should be repeated to sharpen the power of statistical analysis.

Absence of Lga2 and Rga2 changes expected mitochondrial inheritance patterns. As previously mentioned, SRZ provides a mating type system that allows for the study of mitochondrial inheritance in the absence of a control mechanism that favors a uniparental model. The a2 partner of SRZ has orthologous sequences for *U. maydis lga2* and *rga2*. Accordingly, if following the *U. maydis* paradigm, any mating combination involving the SRZ a2 partner will most likely follow a uniparental inheritance pattern, resulting in offspring of the a2 mitotype. However, in addition to a1 and a2, the *a* mating type locus of SRZ can have a third allele, a3. To determine what ensues when a proper mitochondrial inheritance mechanism like the Lga2/Rga2 system is absent, infection assays were carried out to produce teliospores. Total DNA was then extracted from harvested teliospores and PCR was implemented based on the mtDNA polymorphisms identified in Chapter 2.

Samples were preliminarily tested for mtDNA integrity and suitability to use in PCR by amplification of the mitochondrially-encoded *nad6* gene (data not shown). A distinction among teliospores could be made based on which mtDNA was inherited (German or Chinese). Total DNA was also extracted from haploid sporidia and used as controls for the PCR experiments. Figure 3.5 summarizes

the findings, with the corresponding gel electrophoresis results illustrated in Supplemental Figure 8.

The primer pairs oHM127/131 and oHM119/115 were used for the initial screening of mtDNA from harvested teliospores, binding outside of the polymorphic region of *cox1* to produce discernable bands depending on the mitotype (oHM127/131: 2420 bp in German and 4165 bp in Chinese, oHM119/115: 3603 bp in German and 5347 bp in Chinese). Accordingly, the mitotypes of all haploid controls tested coincided with their predicted mitotypes (Figure 3.5A, SRZ1, SRZ2 and SRZIII10 are German isolates, and SRZCXI2, SRZCXII2 and SRZCXI3 are Chinese isolates).

For the teliospores tested, crosses in which the a2 partner was absent were predicted to follow a biparental inheritance pattern, thus resulting in the amplification of both bands within the same PCR reaction. A biparental pattern was also predicted for the *Lga2/Rga2* deletion mutants previously generated (note that the *SRZ2Δlga2* mutant was omitted due to low production of teliospores and poor total DNA quality). Unexpectedly, no amplification was detected for several crosses (Figure 3.5B, grey cells). Furthermore, a cross between SRZ2 and SRZCXI2, in which the resulting offspring should be of the German mitotype, resulted in the amplification of the Chinese band for the primer pair oHM127/131. The same pattern was observed in the analogous cross with the *Rga2* deletion mutant, with the Chinese band produced for both oHM127/131 and oHM119/115. These last findings were indeed surprising, as the predicted mitotypes were in complete disagreement with the observed band patterning.

A second PCR experiment was performed involving primers that work exclusively for German or Chinese mitotypes. Accordingly, the primer pairs oHM115/116 and oHM133/136 were used to detect the Chinese mitotype, producing bands 4154 bp and 3115 bp in size, respectively (Figure 3.5C, blue cells). The primer pairs oHM112/128 and oHM112/113 were used to detect the German mitotype, producing bands 1347 bp and 1071 bp in size, respectively (Figure 3.5C, yellow cells). The Chinese primer pairs resulted in the amplification of the corresponding bands for the crosses SRZ2 x SRZ2CXI2, SRZ2 Δ rga2 x SRZCXI2 and SRZ2 Δ lga2 Δ rga2 x SRZCXI2 (only for oHM115/116), diverging from the predicted patterns (Figure 3.5D). There was no amplification in the remaining crosses, which would suggest that they are of the German mitotype. However, this cannot be confirmed since no amplification was detected in the remaining crosses with the German primer pairs (Figure 3.5D).

The PCR experiments were only conclusive for teliospores produced in the cross between SRZ2 Δ rga2 and SRZCXI2, as PCR amplification was successful for all primer combinations used. This cross resulted in teliospores of the Chinese mitotype, which was unexpected, as absence of Rga2 would leave a2 mtDNA unprotected from the endonuclease activity of Lga2. In theory, absence of Rga2 would lead to the degradation of both a2 and a3 mtDNA upon plasmogamy. However, a biparental mitochondrial inheritance pattern was predicted in this cross since absence of any mitochondrial material would be lethal. The PCR results suggest that Chinese mtDNA persisted in teliospores resulting from this cross. The additional cross between SRZ2 and SRZCXI2

produced partially conclusive results, with successful amplification of the Chinese band for primer pairs oHM127/131, oHM115/116 and oHM133/136. Surprisingly, this result diverged from the expected mitotype, which should be governed by the a2 partner (SRZ2, German).

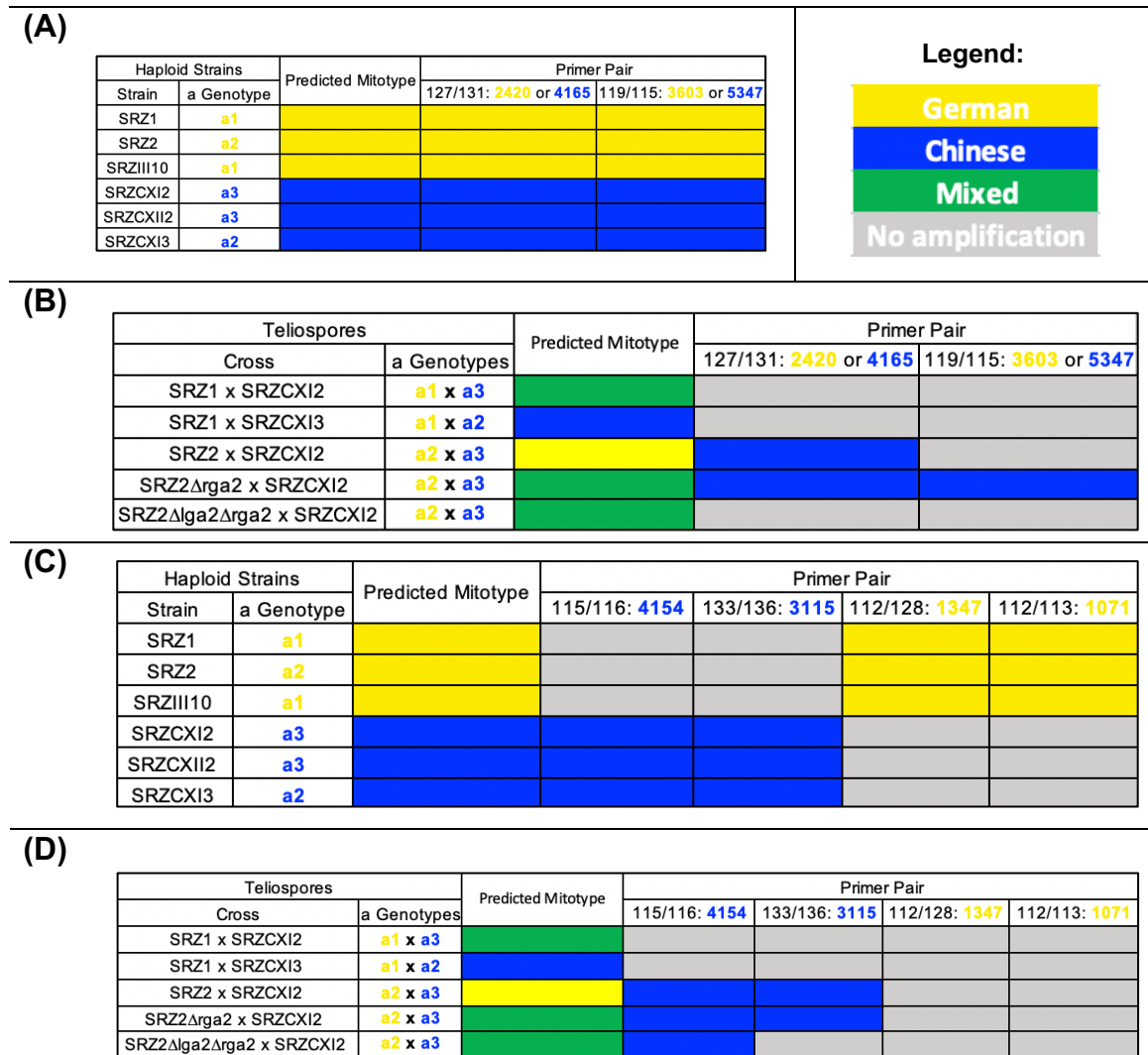


Figure 3.5 – Determination of teliospore mitotype. The primer pairs oHM127/131 and oHM119/115 produce distinct PCR bands in German and Chinese backgrounds and were tested in haploid cells (A) and teliospores (B). The primer pairs oHM115/116 and oHM133/136 produce a unique PCR band in Chinese strains only, while the primer pairs oHM112/128 and oHM112/113 produce a unique PCR band in German strains only. These last sets of primers were also tested in haploid cells (C) and teliospores (D). Note: resulting amplicon size (bp) is indicated next to each primer pair and is also color-coded to specify mtDNA template (German or Chinese).

Screening of *cox1* polymorphic region. Mitotype screening of teliospores resulting from different crosses between German and Chinese strains was mostly inconclusive, as several samples failed to produce any band patterning with all the primer combinations used. For this reason, further PCR screening around the *cox1* polymorphic region was performed to ensure the mtDNA integrity and uncover any signs of mtDNA rearrangement. Figure 3.6 illustrates the areas around the *cox1* polymorphic region investigated. The primers used in this study are included in Table 3.3 and should work in any SRZ strain, regardless of the mitotype. Corresponding gel electrophoresis results are illustrated in Supplemental Figure 9. Primers binding in the adjacent non-coding regions (oHM157/158 and oHM159/160) of *cox1* resulted in successful amplification of expected bands in all teliospore samples, except for SRZ1xCXI3 (very weak amplification was observed). Interestingly, PCR results were inconsistent, with primers binding in the immediate vicinity of the *cox1* polymorphic region (the primer pair oHM161/162 resulted in successful amplification in only 3 single replicates of 3 different crosses, while the primer pair oHM163/164 worked in all three replicates of 2 of the 5 crosses tested).

Additional PCR reactions were carried out by combining primers of the different regions screened. Correspondingly, the primer pairs oHM163/160 and oHM157/162 should result in the amplification of mtDNA fragments 8241 bp and 3992 bp in size, respectively. These primer combinations should also work for all strains regardless of the mitotype, as their binding sites are outside of the *cox1* polymorphic region. Amplification with the primer pair oHM163/160 was

inconsistent even for the controls. This experiment was repeated multiple times with the same result and may be due to the size of the predicted amplicon (8241 bp). On the other hand, successful amplification was observed with the primer pair oHM157/162. Interestingly, the pattern observed in Figure 3.5 was evident, with successful amplification observed in all replicates of SRZ2 x CXI2 and SRZ2 Δ *rga2* x SRZCXI2, and in one replicate of SRZ2 Δ *rga2* Δ *rga2* x SRZCXI2. A final PCR reaction was performed using the primer combination oHM161/164, which binds right outside of the *cox1* polymorphic region. Accordingly, the size of the predicted amplicon should be 5941 bp in German strains or 7686 bp in Chinese strains. Amplification with this last primer pair was inconsistent even with the controls tested. Successful amplification was evident in only one replicate of SRZ2 Δ *rga2* x SRZCXI2, which corresponded to the Chinese mitotype.

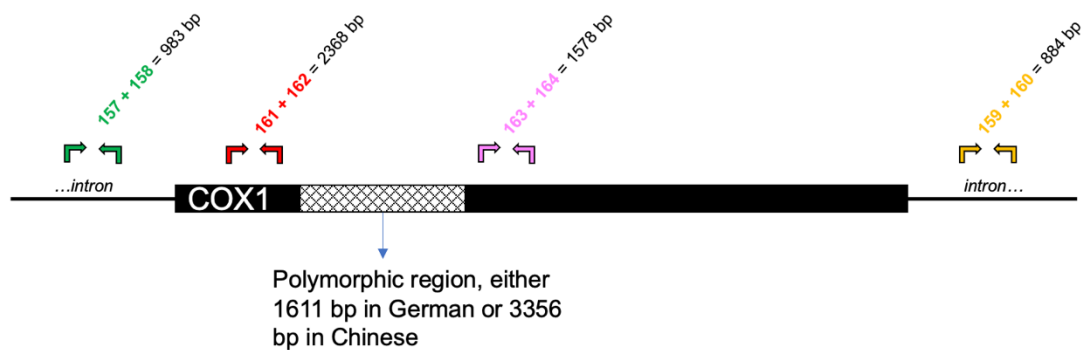


Figure 3.6 – Primer binding areas around the *cox1* polymorphic region. Primer pairs binding outside of the *cox1* polymorphic region were designed to inspect mtDNA integrity. These primer combinations should work in any SRZ strains, regardless of the mitotype. Predicted amplicon sizes are indicated. Gel electrophoresis results are illustrated in Supplemental Figure 9.

Discussion

The deletion of Lga2 and/or Rga2 did not have any effects in overall cell integrity or mating capabilities, as illustrated by the stress and mating assays. These results were not surprising, as previous experimentation involving the related species, *U. maydis*, also failed to identify a conspicuous phenotype associated with deletion of either Lga2 or Rga2 in haploid cells (96,98) . Moreover, here a clear effect on the pathogenicity of the fungus was not evident, as a larger study sample and the appropriate biological and technical replicates are required for more robust statistical analysis and inference. The pathogenicity assays performed in this study served the immediate purpose of producing teliospores from different crosses between German and Chinese strains. Total DNA isolation was performed on all teliospore samples and specific mtDNA primers were used to verify integrity of the extracted DNAs and PCR suitability. This was done to rule out any false-negative results that may be brought on by poor quality total DNA samples. This problem can be avoided in future studies by the improvement and implementation of mtDNA isolation protocols specific to this type of fungal system. The available procedures in the published literature are often too generalized (or too specific) and require costly and sophisticated equipment.

Mitotype screening of the teliospores produced in the pathogenicity assays was based on the polymorphic region detected in *cox1* in Chapter 2. The primers used for the characterization of this region were repurposed as

diagnostic primers that allowed mitotype discernment via PCR and subsequent gel electrophoresis. This methodology proved to be inexpensive and provided quick results. Nevertheless, the results of these PCR experiments were for the most part inconclusive, as some of the samples failed to produce the predicted amplicons with all primer combinations tested. Conclusive remarks can be made about teliospores resulting from the crosses between SRZ2 x SRZCX12 and SRZ2 Δ *rga2* x SRZCX12, which according to all the primer combinations tested, are of the Chinese mitotype. This was a surprising result, as the predicted mitotype for SRZ2 x SRZCX12 was German, since SRZ2 is the corresponding a2 partner equipped with the Lga2/Rga2 mitochondrial inheritance machinery. Absence of Rga2 did not seem to affect the observed pattern, as the mitotype of teliospores resulting from the cross between SRZ2 Δ *rga2* x SRZCX12 was persistently Chinese.

The region around the *cox1* polymorphic region was subjected to further scrutiny to ensure its integrity and with the hopes of uncovering any signals of mtDNA rearrangements that could explain the inconsistencies observed in the mitotype screening experiments. Accordingly, primers that bind in the proximal and distal adjacent areas of the *cox1* polymorphic region were designed. Successful amplification was observed with the primer pairs outside of the *cox1* gene, suggesting that this region is intact for all strains and that mtDNA quality is adequate for PCR. Results involving primer pairs that bind in the immediate vicinity of the *cox1* polymorphic region were inconsistent. Interestingly, one of these two primer pairs (oHM163/162) resulted in a similar pattern observed in the

initial mitotype screening of teliospore samples, in which successful amplification was evident for SRZ2 x SRZCXI2 and SRZ2 Δ *rga2* x SRZCXI2 only. This pattern was also evident in an additional primer combination tested (oHM157/162) that involved a forward primer binding outside of the *cox1* gene and a reverse primer binding right outside of the *cox1* polymorphic region.

Finally, the additional primer combination oHM161/164 was used to detect unique German and Chinese amplicons. However, amplification was successful only in one of the three replicates of SRZ2 Δ *rga2* x SRZCXI2, which corresponded to the Chinese mitotype. That result was consistent with what was previously found for this teliospore sample in the initial mitotyping experiments. Together, these PCR results suggest that mtDNA rearrangement or modification occurs in the downstream vicinity of the *cox1* gene may be a target site for genetic recombination, as all primer combinations with binding sites in that area failed to produce any DNA bands.

Further experimentation is required for this study, as most of the samples failed to produce any molecular pattern. Such investigations may include WGS of the teliospore mitogenomes and/or Sanger sequencing of the region in question to verify that it corresponds to the German or Chinese version of *cox1*. Additionally, if the *cox1* gene has been dramatically rearranged in the teliospores from crosses between German and Chinese strains, this would predict that such teliospores would be seriously impaired in germinations and/or that the resulting haploid cells after meiosis would be inviable. This argues the

need to further investigate these aspects of teliospores from the respective crosses.

CHAPTER IV

IDENTIFICATION AND FUNCTIONAL CHARACTERIZATION OF A PUTATIVE ALTERNATIVE OXIDASE (AOX) IN *Sporisorium reilianum* f. sp. *zeae*

Chapter Overview

The mitochondrial electron transport chain consists of the classical protein complexes (I-IV) that facilitate the flow of electrons and coupled oxidative phosphorylation to produce metabolic energy. The canonical route of electron transport may diverge by the presence of alternative components to the electron transport chain. The following chapter comprises the bioinformatic and functional characterization of a putative alternative oxidase in the smut fungus *Sporisorium reilianum*. This alternative component of the electron transport chain has been previously identified in other eukaryotes and is essential for alternative respiration as a response to environmental and chemical stressors, as well as for the developmental transitions during the life cycle of an organism. A growth inhibition assay, using specific mitochondrial inhibitors, functionally confirmed the presence of an antimycin resistant/SHAM sensitive alternative oxidase in the electron transport chain of *S. reilianum*. Gene knockout experiments revealed

that AOX is involved in the pathogenic stage of the fungus, with its absence effectively reducing overall disease severity in infected maize plants. Furthermore, gene expression analysis revealed that the alternative oxidase plays a prominent role in the morphological and metabolic switch of haploid sporidia to diploid teliospores, coinciding with previous studies in which alternative respiration is favored during quiescent stages of an organism's life cycle.

Introduction

Sporisorium reilianum is a phytopathogenic basidiomycete with two *formae speciales*, able to infect maize (SRZ) and sorghum (SRS). Much like its better known relative, *Ustilago maydis*, *S. reilianum* f. *sp. zaeae* displays a dimorphic lifestyle, existing as yeast-like haploid sporidia that reproduce asexually by budding (153). Sexual reproduction can take place and is dependent on a tetrapolar mating-type system that begins with a pheromone-pheromone receptor interaction and allows the fungus to enter its pathogenic stage, first as dikaryotic hyphae, and eventually, as diploid teliospores that can germinate under the right conditions and restart the life cycle (123). Unlike *U. maydis*, however, SRZ causes systemic infection on the plant host, emerging as teliospore sori on both male (tassel) and female (ear) inflorescences and causes additional developmental abnormalities, such as phyllody and irregular branching architecture (150,154).

The bioenergetics and intermediary metabolism of fungal systems are poorly understood, despite the relevance of mitochondria and the associated electron transport chain (ETC) as the main source of metabolic currency. Similar to the mammalian mitochondrion, the fungal “powerhouse” is comprised of the four classical protein complexes (I-IV) that function as proton pumps to help maintain the electrochemical gradient that drives ATP synthesis via oxidative phosphorylation. Pumping of protons is facilitated by the fixed movement of electrons through the protein complexes, from NADH as the initial donor to molecular oxygen as the final acceptor.

Alternative respiratory pathways have recently received special attention, in which additional components diverge electron movement from the classical cytochrome c pathway. For instance, plants have been known to deviate from the norm in response to specific metabolic needs, as is the case of the peanut plant, *Arachis hypogea*, whose embryos are deficient in cytochrome c, are insensitive to cyanide (KCN) and are able to use NADH and succinate as substrates for uncoupled respiration, with significantly reduced ATP production (155). Another notable alternative component of the ETC was discovered early in a variety of yeasts, which are among the only organisms devoid of complex I (156). Instead, yeasts have internal and external rotenone-insensitive NADH dehydrogenases that utilize matrix NADH as substrate.

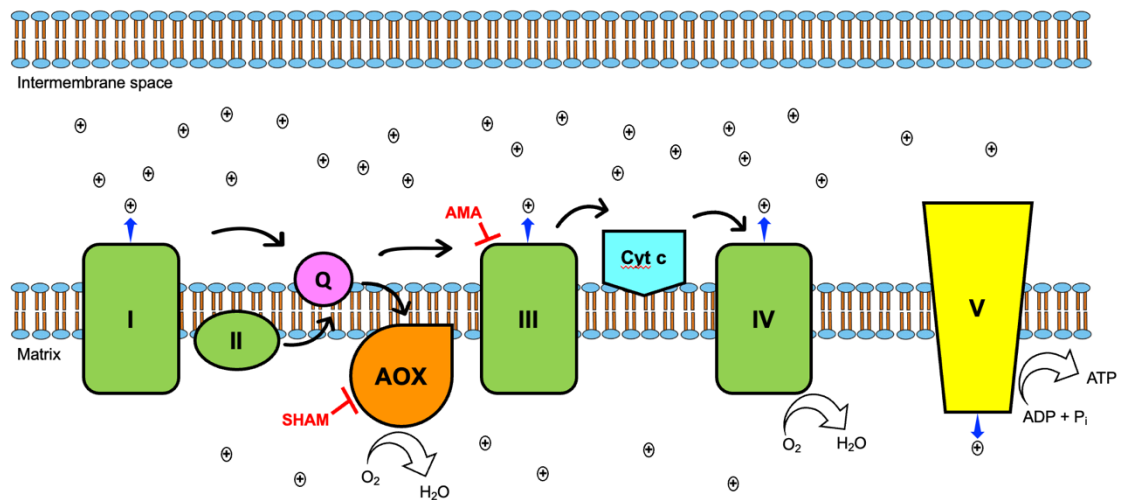


Figure 4.1 – AOX-mediated respiration. Thick black arrows indicate movement of electrons. The canonical cytochrome c pathway includes the classical protein complexes, depicted in green, with protons pumped into the intermembrane space by complexes I, III and IV. This pathway is coupled to ATP synthesis by contributing to the proton gradient in the intermembrane space that will drive ATP synthesis via ATP synthase (complex V, in yellow). Inhibiting complex III by drugs like antimycin A (AMA) halts the movement of electrons via the classical route. The SHAM-sensitive alternative oxidase functions as complex IV, reducing oxygen into water, thus providing an additional route to finish respiration. However, AOX does not function as a proton pump, effectively diminishing the proton gradient and, consequently, reducing ATP synthesis.

It is now known that the alternative respiratory component first identified in the peanut plant is a quinol oxidase, also known as alternative oxidase (AOX), which functions like complex IV and catalyzes the reduction of oxygen into water but is an inefficient proton pump (Figure 4.1) (157). In plants, deviation from the cytochrome c pathway has been associated with thermotolerance (158,159), chemical (160,161) and oxidative (162,163) stresses and as part of the immune response (164,165). AOX has also been identified in parasites like *Trypanosoma brucei* (TAO) (166), in which it is essential for the maintenance of the mammalian bloodstream forms and may prove a crucial target in the development of novel

drug therapies for the sleeping sickness (167,168), and in *Cryptosporidium parvum* (CpAOX), the causative agent of cryptosporidiosis that lacks membrane-bound organelles and is solely dependent on AOX-mediated respiration limited to mitochondrion-like compartments (mitosomes) (169,170).

In the case of fungi, AOX has been identified in most annotated genomes, including a variety of agriculturally relevant phytopathogens like *Botrytis cinerea* (171), *Magnaporthe grisea* (172), *Mycosphaerella graminicola* (173) and several *Aspergillus* species (174-176), making it an excellent fungicidal target for crop management approaches. AOX has also been suggested to be involved in developmental regulation, as is the case for the fungus *Blastocladiella emersonii*, in which respiratory capacity is higher in highly motile zoospores, compared to vegetative cells that favor AOX-mediated respiration due to their lower metabolic demands (177).

The aim of this study is the identification and functional characterization of a putative AOX in SRZ, based on previous studies involving the related species *U. maydis* (178-180), which found that AOX is dispensable for overall welfare of the fungus, but crucial during respiratory stress. SRZ differs from *U. maydis* in the way it infects maize, with symptoms appearing during the late stages of maturity of the plant. This peculiarity makes SRZ an excellent model to determine if AOX is involved in the long-term survival of the fungus in the plant tissue. Additionally, expression analysis of the distinct stages of the fungus was performed to investigate its involvement in developmental regulation.

Materials and Methods

Strains and growth conditions. The SRZ strains used in this study are listed in Table 4.1. Haploid strains were grown in potato dextrose broth (PD) broth on a rotary shaker at 200 rpm at 28°C or on solid PD agar at 28°C. Strains were maintained in PD glycerol (20%) medium at -80°C for long-term storage or on PD agar at 4°C for no longer than 7 days. Transgenic strains were selected by supplementing the PD medium with hygromycin at a final concentration of 200 µg/mL. The plasmids used in this study are listed in Table 4.2. For cloning purposes and plasmid maintenance, the transformed *Escherichia coli* DH5α strain (Thermo Fisher Scientific) was grown in Luria-Bertani (LB) broth on a rotary shaker at 200 rpm at 37°C or on solid LB agar at 37°C. Bacterial strains were maintained in LB glycerol (20%) medium at -80°C for long-term storage or on LB agar at 4°C for no longer than 7 days. Plasmid selection was achieved by supplementing the LB medium with ampicillin at a final concentration of 200 µg/mL or gentamicin at a final concentration of 10 µg/mL.

Table 4.1 – SRZ strains used or generated in Chapter 4.

Strain	Genotype	Selectable marker	Source
SRZ2	a2b2	WT	(123)
SRZ1	a1b1	WT	(123)
SRZCXI2	a3b3	WT	Unpublished, from teliospores collected in China
SRZ2Δa _{ox} #1	a2b2Δa _{ox} ::hph	Hygromycin	This study
SRZ1Δa _{ox} #2	a1b1Δa _{ox} ::hph	Hygromycin	This study
SRZCXI2Δa _{ox} #4	a3b3Δa _{ox} ::hph	Hygromycin	This study
SRZ2Δa _{oxc} #1	a2b2Δa _{ox} ::a _{ox} sdh	Carboxin	This study

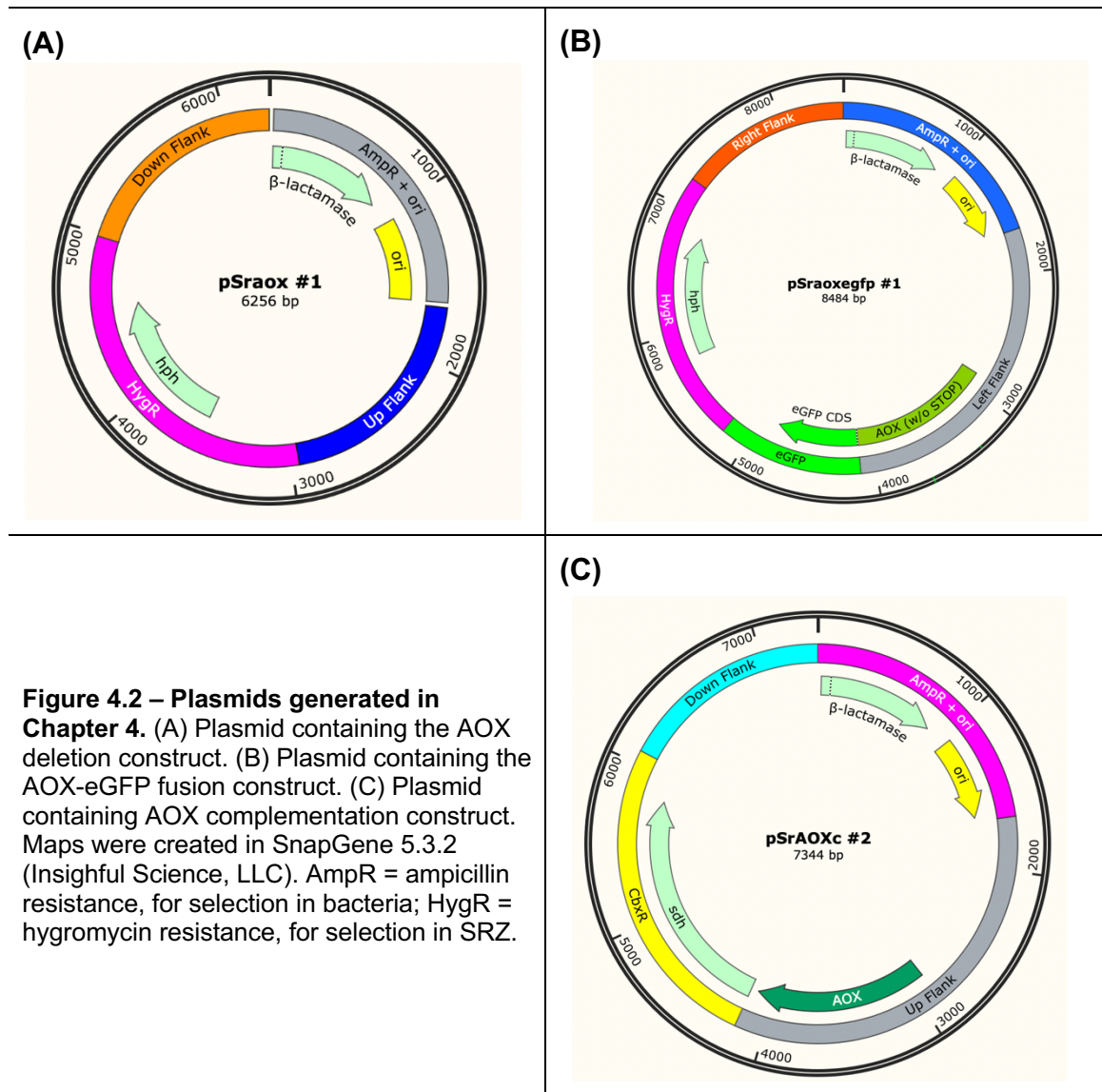
Table 4.2 – Plasmids used or generated in Chapter 4.

Plasmid	Insert of interest	Selectable marker in bacteria	Source
pUM1507	<i>hph</i> (hygromycin B phosphotransferase)	Gentamicin	(146)
pUC19	<i>amp^r</i> (β -lactamase), <i>ori</i> (origin of replication cassette)	Ampicillin	New England Biolabs
pMF4-1c	<i>eGFP</i> , <i>sdh</i> (succinate dehydrogenase)	Ampicillin	(181)
pSrAOX #1	AOX deletion construct	Ampicillin	This study
pSrAOXeGFP #1	AOX-eGFP fusion construct	Ampicillin	This study
pSrAOXc#2	AOX complementation construct	Carboxin	This study

Bioinformatics. The amino acid sequence of the *U. maydis aox1* (NCBI Accession No. UMAG_02774) was used in a BLASTp search against the genome of SRZ2 (NCBI Accession No. GCA_000230245.1). The resulting amino acid sequence was then used for Multiple Sequence Comparison by Log-Expectation (MUSCLE) in SnapGene 5.3.2 (Insightful Science, LLC).

Molecular techniques. DNA isolation from SRZ and transformation protocols were carried out as previously described for *U. maydis* (132). Primers used for the generation of the individual fragments of the AOX deletion construct were designed using the open access Primer3 software (147) with complementary overlaps based on the Gibson Assembly cloning method (148). Primer sequences and respective amplicons are listed in Table 4.3. Primer pair oHM33/34 was used to generate the hygromycin resistance cassette using pUMA1507 DNA as template. Primer pairs oHM35/36 and oHM37/38 were used

to generate upstream and downstream flanking regions, respectively, to *aox*, using SRZ2 gDNA as template. Primer pair oHM39/40 was used to generate a single fragment containing both the ampicillin resistance cassette and origin of replication element using pUC19 DNA as template. These fragments were ligated in a single Gibson reaction and the resulting fragment was used to transform *E. coli*.



The final plasmid, pSrAOX #1 (Figure 4.2A), was then isolated and linearized with EcoRV (New England Biolabs). Subsequently, the primer pair oHM36/38 was used to amplify the AOX deletion construct, made up of the flanking upstream region, followed by the hygromycin resistance cassette and the flanking downstream region (4582 bp). This last fragment was used in the transformation of the different strains of SRZ facilitated by homologous recombination. Preliminary verification of deletion mutants was achieved by polymerase chain reaction (PCR) using the primer pair oHM33/68, which resulted in the synthesis of a 4582 bp fragment in successful AOX deletion mutants. WT strains were simultaneously used as controls, in which synthesis of a 4005 bp fragment corresponded to the intact *aox* locus. Additional verification of deletion mutants used Southern blot hybridization (See Supplemental Protocol 1 and Supplemental Figure 4).

For the development of the AOX complementation construct, the primer pair oHM40/146 was used to generate a single fragment containing both the ampicillin resistance cassette and origin of replication element using pUC19 DNA as template. The primer pairs oHM147/148 and oHM39/155 were used to generate upstream and downstream flanking regions, respectively, to AOX using SRZ2 gDNA as template (the upstream region contains AOX in its entirety). The primer pair oHM149/156 was used to generate the carboxin resistance cassette fragment out of pMF4-1c. These fragments were then ligated in a single Gibson reaction and the resulting product was used to transform *E. coli*.

The final plasmid, pSrAOXc #2 (Figure 4.3C), was then isolated and linearized with EcoRV (New England Biolabs). Subsequently, the primer pair oHM30/147 was used to amplify the AOX complementation construct, made up of the flanking upstream region containing AOX in its entirety, followed by the carboxin resistance cassette and the downstream flanking region (5670 bp). This last fragment was used in the transformation of protoplasts of AOX deletion mutants. Preliminary verification of successful transformants was achieved by polymerase chain reaction (PCR) using the primer pair oHM147/156, which resulted in the production of a fragment 4400 bp in size (WT strains were used as negative controls).

For the investigation of mitochondrial localization of AOX, a fusion construct with a fluorescent protein was designed. The primer pair oHM39/40 was used to generate a single fragment containing both the ampicillin resistance cassette and origin of replication element using pUC19 DNA as template. The primer pairs oHM70/104 and oHM37/38 were used to generate upstream and downstream flanking regions, respectively, to *aox* using SRZ2 gDNA as template (the upstream region contains the AOX coding sequence without the STOP codon). The primer pair oHM102/103 was used to generate a fragment containing eGFP from pMF4-1c. The primer pair oHM34/105 was used to generate the hygromycin resistance cassette fragment out of pUMA1507. These fragments were then ligated in a single Gibson reaction and the resulting product was used to transform *E. coli*.

The final plasmid, pSrAOXeGFP #1 (Figure 4.2B), was then isolated and linearized with EcoRV (New England Biolabs). Subsequently, the primer pair oHM38/70 was used to amplify the AOX-eGFP construct, made up of the flanking upstream region containing the AOX coding sequence without the STOP codon, followed by the eGFP fragment, the hygromycin resistance cassette and the flanking downstream region (6835 bp). This last fragment was used in the transformation of the different strains of SRZ facilitated by homologous recombination. Preliminary verification of deletion mutants was achieved by PCR using the primer pair oHM34/102, which resulted in the synthesis of a 3101 bp fragment in successful transformants (WT strains were used as negative controls).

Polymerase chain reaction (PCR) was carried out in a T100 Thermal Cycler (Bio-Rad Laboratories) with Ex Taq Hot Start DNA Polymerase (TaKaRa Bio Usa, Inc), PrimeSTAR Max DNA Polymerase (TaKaRa Bio USA, Inc) or DreamTaq Hot Start PCR Master Mix (Thermo Fisher Scientific). PCR cycling conditions for Hot Start DNA polymerases involved an initial denaturation step at 94°C for 4 minutes, followed by 34 cycles of a three-step process (denaturation at 94°C for 30 seconds, annealing at primer 58-62°C for 30 seconds and extension at 72°C for 1 minute per 1 kb of anticipated product) and a final extension step at 72°C for 10 minutes. PCR cycling conditions for PrimeSTAR Max DNA Polymerase involved an initial denaturation step at 98°C for 2 minutes, followed by 34 cycles of a three-step process (denaturation at 98°C for 10 seconds, annealing at primer 58-62°C for 15 seconds and extension at 72°C for

30-45 seconds) and a final extension at 72°C for 5 minutes. In preparation for Gibson Assembly, all PCR products were generated using PrimeSTAR Max DNA Polymerase. Gibson Assembly was carried out using the Gibson Assembly Master Mix kit (New England Biolabs) and according to the manufacturer's instructions.

Table 4.3 – Primers used in Chapter 4.

Running #	Sequence (5'→3')	Amplicon
oHM33	ACCATCCCTCTAAAACGACGGCCAGTGAAT	<i>hph</i> (2027 bp)
oHM34	AGTTGATTCTGTGGAATTGTGAGCGGATA	
oHM35	CGTCGTTTTAGAGGGATGGTTGTGAAATGG	Upstream flanking region of <i>aox</i> (1285 bp)
oHM36	TTTTGATATCAAGCATGGTGACGAGGAGAT	
oHM37	CAATCCACAGAATCGAACTGGCGAATGTC	Downstream flanking region of <i>aox</i> (1270 bp)
oHM38	TTCAATATTAATTAAGGTGATGAAGGAACGAACG	
oHM39	CATGCTTGATATCAAAAGGCCGCGTTGCTG	<i>amp^r</i> , <i>ori</i> (1688 bp)
oHM40	ATCACCTTTAATTAATATTGAAAAAGGAAGAG	
oHM61	GAAAAGACCGTGGCTCTCC	<i>aox</i> for qRT-PCR
oHM62	GTGCTTCACTGGCATCGTC	
oHM70	TTTTGATATCCGACTTTTCGGGTGATTTTC	For AOX-eGFP fusion construct
oHM102	GAAGACCGCCATGGTGAGCAAGGGCGAG	
oHM103	CGTCGTTTTATTCTTGTGATTGCGGGACTC	
oHM104	TGCTCACCATGGCGGTCTTCTCAGCAGC	
oHM105	ATCACAAGAATAAAAACGACGGCCAGTGAAT	For AOX complementation construct
oHM146	CGAAAAGTCGGATATCAAAAGGCCGCGTTG	
oHM147	TTTTGATATCCGACTTTTCGGGTGATTTTC	
oHM148	GCTCGATATTGGTGGTAAGGGTATCGGACA	
oHM149	CCTTACCACCAATATCGAGCACGTTGATGG	
oHM155	CCACAATCGTGAATCGAACTGGCGAATGTC	
oHM156	AGTTGATTACGATTGTGGCGAATCGCGG	
oHM30	TTCAATATTAATTAAGGTATGCCTCAGCTCAAAGG	
oYZ58	GGATTCATCGGCAACTCAC	<i>gapdh</i> for qRT-PCR
oYZ59	TACCACGAGACGAGCTTGAC	

Mating assays. Individual strains of SRZ were grown in 50 mL of PD broth on a rotary shaker at 200 rpm at 28°C until an absorbance at 600 nm (OD_{600}) of 1 was reached. Equal amounts of cells (5 mL) of the desired combinations were then mixed into 15 mL of fresh PD broth and were grown overnight on a rotary shaker at 28°C. Conjugation hyphae were scored by microscopic analysis. To confirm the production of dikaryotic filaments as a second indicator of successful mating, 15 μ L of each mating combination was spotted onto water-agar (2%) plates and incubated at 28°C for 48 hours. Dikaryotic hyphae formation was confirmed by microscopic observation as thin aerial projections on the colony surface.

Stress assays. Haploid strains were grown in 4 mL of PD broth on a rotary shaker at 200 rpm at 28°C until an OD_{600} of 1 was reached. Cells were harvested by centrifugation at 14,000 rpm in a microcentrifuge, washed and resuspended in 1 mL of ddH₂O. Strains were further serially diluted in ddH₂O (from 1:10 to 1:100000). Finally, 10 μ L of the diluted strains were spotted onto PD agar, supplemented with Congo red (CR, 100 μ M), sorbitol (1 M), NaCl (1 M) or H₂O₂ (1.5 mM). The plates were incubated for 48 hours at 28°C and photographed.

Growth inhibition assays. Haploid strains were grown overnight in 4 mL of PD broth on a rotary shaker at 200 rpm at 28°C. Cells were harvested by centrifugation at 14,000 rpm, quantified using a hemocytometer and adjusted with fresh PD broth, supplemented with antimycin A (AMA, 50 μ M) and/or salicylhydroxamic acid (SHAM, 2 mM), to 10⁵ cells/mL. Control treatments

included PD broth supplemented with the respective respiratory inhibitor solvent (ethanol for AMA and DMSO for SHAM).

Cells were incubated overnight on a rotary shaker at 200 rpm at 28°C and subsequently sub-cultured onto PD agar for determination of total viable colonies (TVC) per mL of medium. One-way ANOVA followed by Tukey's Multiple Comparison test was performed in GraphPad Prism 9.2.0 (GraphPad Software, LLC) to determine statistical significance, with $p \geq 0.05$ = not significant (ns), $p \leq 0.05$ = weakly significant (*), $p \leq 0.01$ = significant (**), $p \leq 0.001$ = very significant (***) and $p \leq 0.0001$ = extremely significant (****).

Pathogenicity assays. Strains were grown in 50 mL of PD broth on a rotary shaker at 28°C until an OD₆₀₀ of 0.5-0.8 was reached. Cells were harvested by centrifugation at 3,500 rpm and resuspended in ddH₂O to a final OD₆₀₀ of 2. The desired strain combinations were then mixed in a 1:1 ratio and used to inoculate 7-day old Tom Thumb maize (High Morning Organic Seeds) seedlings. Disease evaluation was performed 7-8 weeks post infection (wpi), in which plant height was recorded and symptoms were scored (refer to Figure 3.4 in Chapter 3) for the calculation of disease severity indexes (150). One-way ANOVA followed by Tukey's Multiple Comparison test was performed in GraphPad Prism 9.2.0 (GraphPad Software, LLC) to determine statistical significance, with $p \geq 0.05$ = not significant (ns), $p \leq 0.05$ = weakly significant (*), $p \leq 0.01$ = significant (**), $p \leq 0.001$ = very significant (***) and $p \leq 0.0001$ = extremely significant (****).

Expression Studies. Two-step reverse transcription quantitative PCR (RT-qPCR) was used for the verification of gene deletions and differential gene

expression analysis. Nucleic acids were isolated from SRZ haploid sporidia, diploid teliospores and mated cells by homogenization in a frozen mortar and pestle and treatment with TRIzol reagent (Invitrogen). Following cell disruption, RNA was isolated using the Direct-zol RNA Miniprep kit (Zymo). Subsequent cDNA synthesis was carried out using Super Script IV (Invitrogen) and followed the manufacturer's instructions. qPCR was carried out in a StepOne Real-Time PCR System (Applied Biosystems) using EvaGreen dye (Mango Biotechnology) following to the manufacturer's instructions. Cycling conditions involved an initial denaturation step at 95°C for 10 minutes, followed by 40 cycles of 95°C for 15 seconds and 60°C for 1 minute.

Melting curve analysis was performed at the end of each cycle to ensure specificity of the reaction. Gene-specific primers were designed using the open access Primer3 software (147) and are included in Table 4.3. The glyceraldehyde 3-phosphate dehydrogenase (*gapdh*, NCBI Accession No. sr109402) was used as endogenous control for the calculation of relative expression levels using the $2^{-\Delta\Delta C_t}$ (Livak) method (182). Ct values above 30 or not detectable were indicators of no gene expression. The Student's t-test was performed in GraphPad Prism 9.2.0 (GraphPad Software, LLC) to determine statistical significance, with $p \geq 0.05$ = not significant (ns), $p \leq 0.05$ = weakly significant (*), $p \leq 0.01$ = significant (**), $p \leq 0.001$ = very significant (***) and $p \leq 0.0001$ = extremely significant (****).

Microscopy. Fluorescent images were acquired using a Nikon A1R confocal microscope. Transformed SRZ strains were grown overnight at 28°C in PDB to

an OD₆₀₀ of 1. Ten-fold dilutions of each culture were made and 500 µL were placed in the wells of 35-mm CELLview culture dishes (Greiner Bio-One). eGFP signal was acquired using a 488 line of an Argon laser. A transmitted light image was acquired during scanning for visualization of cell outline by grouping of the transmitted detector with the argon laser. For confirmation of localization, cells were treated with 100 µM MitoView Blue (Biotium) for 10 minutes. Blue fluorescence was acquired using the DAPI detection channel and overlapped with eGFP fluorescence.

Results

Identification of a putative alternative oxidase in SRZ. The amino acid sequence of the *U. maydis* AOX (*aox1*, NCBI Accession No. UMAG_02774) was used in a BLASTp search against the nuclear genome of SRZ (NCBI Accession No. GCA_000230245.1). The resulting sequence of 409 amino acids was then used for Multiple Sequence Comparison by Log Expectation (MUSCLE) analysis against known alternative oxidases in closely and distantly related species (Figure 4.3). Protein identities of the putative AOX of SRZ were 85.02% for *Sporisorium scitamineum*, 85.48% for *Sporisorium graminicola*, 67.06% for *Ustilago bromivora*, 70.91% for *Ustilago maydis* and 72.22% for *Pseudozyma hubeiensis*.

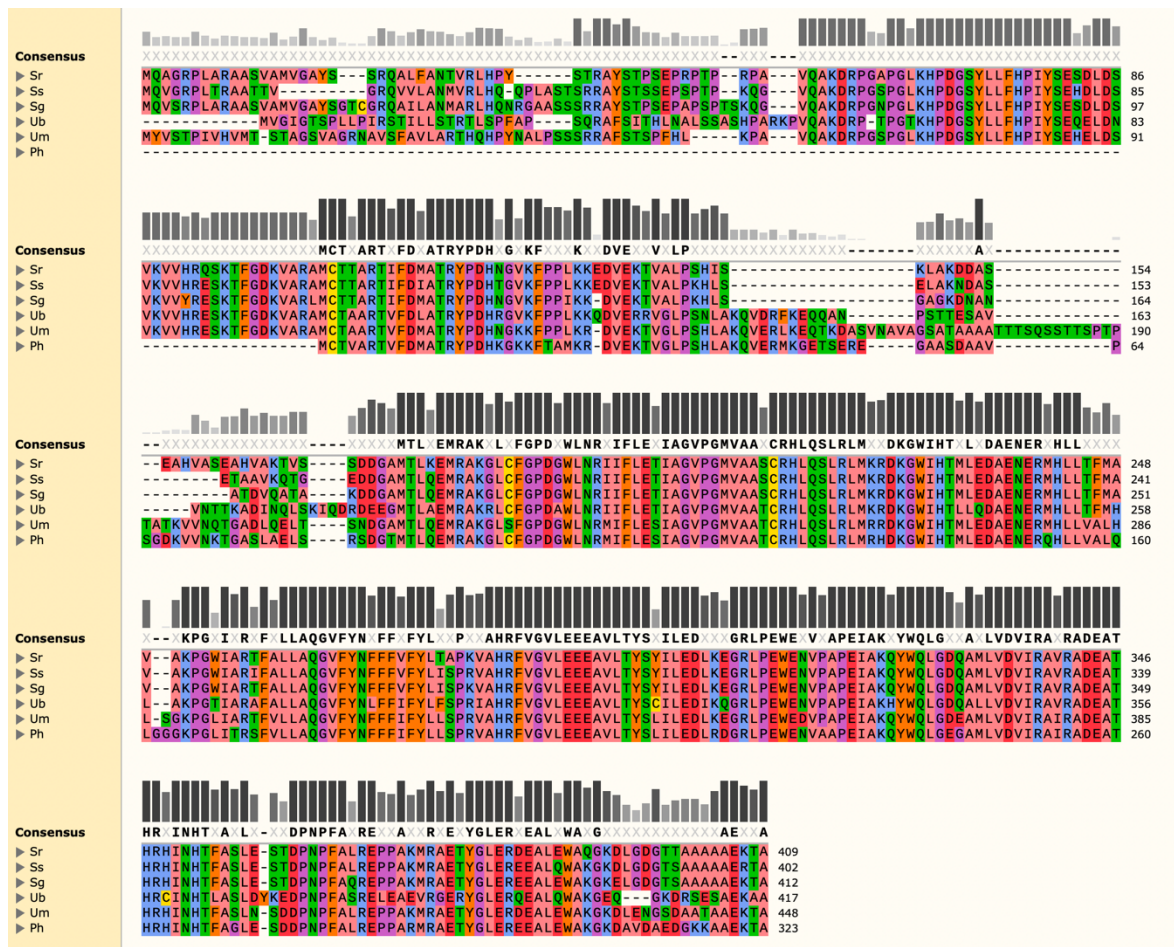


Figure 4.3 – MUSCLE analysis of amino acid sequence of putative SRZ AOX against known polypeptides. AOX amino acid sequences of the following organisms were used: *S. scitamineum* (CDU22616.1), *S. graminicola* (XP_029737873.1), *U. bromivora* (SAM82122.1), *U. maydis* (XP_011389130.1) and *Pseudozyma hubeiensis* (XP_012186999.1). Amino acids with similar physico-chemical properties are represented by the same color. Bars represent amino acid conservation across all sequences analyzed, with darker and taller bars corresponding to higher conservation indexes. Amino acids in bold make up the consensus sequence and represent 100% conservation in that position.

The highest amino acid identities were between the closest relatives of SRZ (*S. scitamineum* and *S. graminicola*) and were consistent with the size of their predicted polypeptides (402 and 412 amino acids, respectively). Greater size discrepancies were seen in *U. maydis* (448 amino acids), *U. bromivora* (417 amino acids) and, more notably, in the distantly related *P. hubeiensis* (323 amino

acids). Amino acid conservation was strongest in the carboxyl end of the aligned polypeptide sequences, coinciding with a ferritin-like diiron-binding domain (NCBI Accession No. cd01053, E-value = 2.43^{-85}) common in alternative oxidases of plants, fungi and protists. This preliminary bioinformatic evidence strongly suggests the presence of an AOX gene in SRZ, corresponding to a polypeptide of approximately 45 kDa and rich in alanine (13.45%).

Mating capability is not affected in the absence of AOX. Mating in SRZ follows the same compatibility rules previously described for *U. maydis* (152), making self vs. non-self-recognition a prerequisite for the formation of dikaryotic hyphae during the pathogenic stage of the fungus. Accordingly, successful mating will only occur between strains with different alleles for both *a* and *b* mating type loci. Mating in SRZ is characterized by the initial formation of conjugation tubes between compatible strains, seen as elongated hyphal projections protruding from the ovoid haploid sporidia, as seen in compatible crosses between WT strains (Figure 4.4B). Conjugation was not affected by the absence of AOX (Figure 4.4C).

As plasmogamy occurs, dikaryotic filaments are produced and can be distinguished when spotted on water-agar plates. Unmated strains and incompatible combinations can be distinguished by smooth colony surfaces (Figure 4.4D). Contrastingly, successful production of dikaryons can be seen as thin aerial filaments that give the colony surface an irregular and ragged appearance (Figure 4.4E). The absence of AOX did not affect dikaryon formation

in any of the crosses tested (Figure 4.4F). Supplemental Figure 10 includes all the combinations tested in all backgrounds of SRZ.

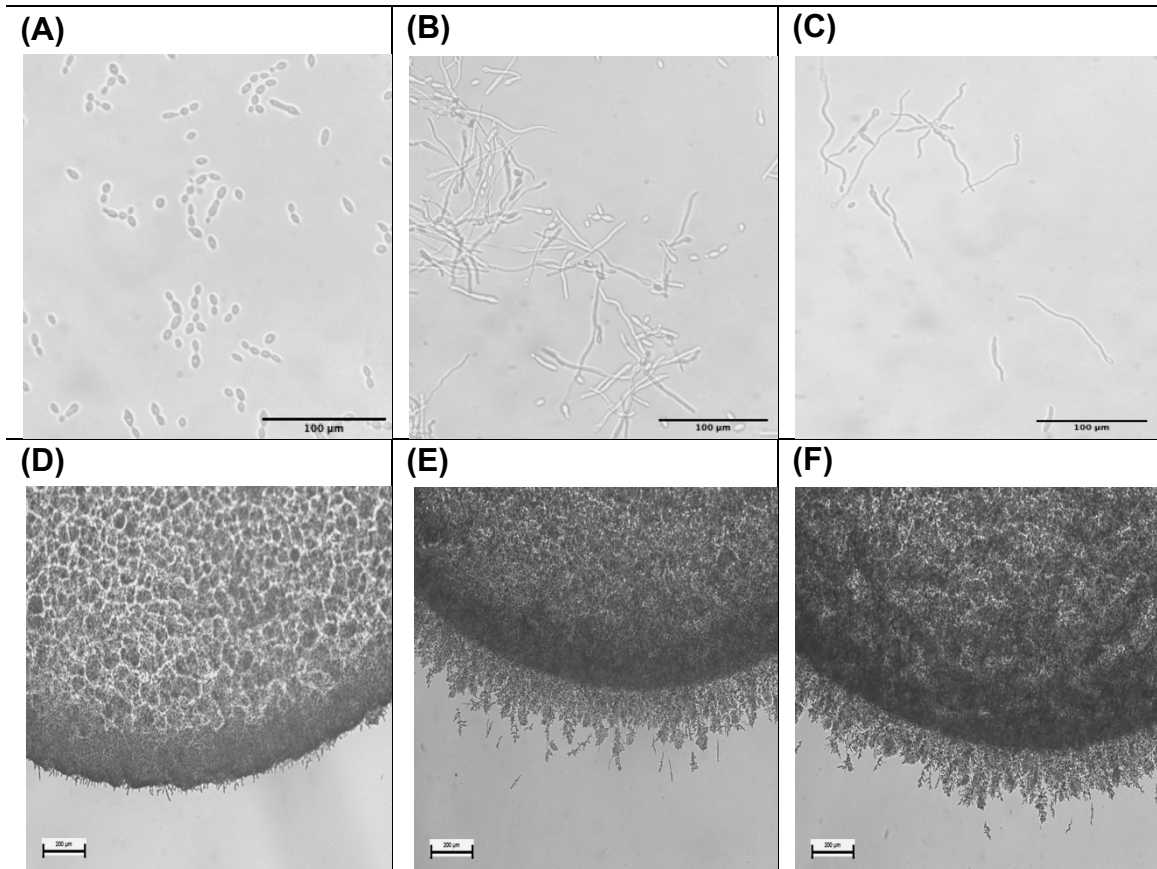
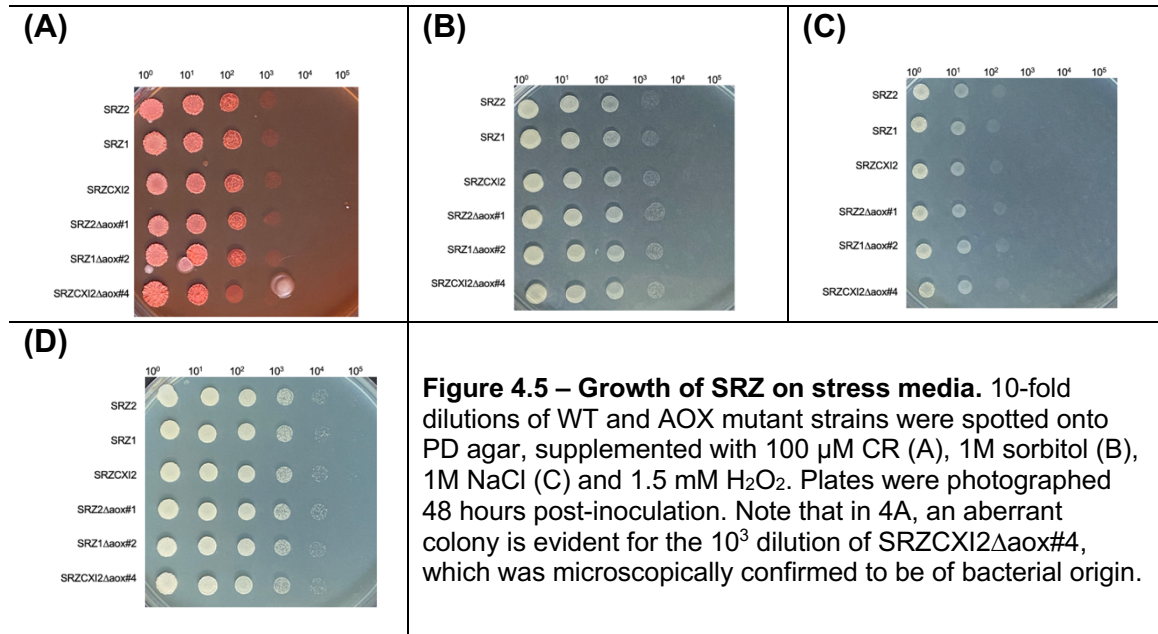


Figure 4.4 – Mating reactions of SRZ. Unmated strains or incompatible combinations did not produce conjugation hyphae (A: SRZ1) and had smooth colony surfaces (E: SRZ1), indicating that no dikaryotic hyphae were produced. The absence of AOX did not affect mating capability, as conjugation and formation of aerial filaments were comparable between WT strains (B and F: SRZ1 x SRZ2) and the deletion mutants (C and G: SRZ1 Δ aox x SRZ2 Δ aox). Additional crosses are included in Supplemental Figure 10.

AOX does not influence overall cell integrity and viability. Both mutant and WT strains of AOX were exposed to chemical stresses on PD agar supplemented with CR, sorbitol, NaCl and H₂O₂, which challenge cell wall integrity, osmotic regulation, ionic equilibrium, and tolerance to oxidative environments, respectively. There was no apparent difference in growth between AOX deletion mutants and their corresponding WT counterparts on any of the

stress media (Figure 4.5A-D). In Fig. 4.5A, the abnormal colony evident for the 10^3 dilution for SRZCXI2 Δ aox#4, which was later microscopically confirmed to be due to bacterial contamination.



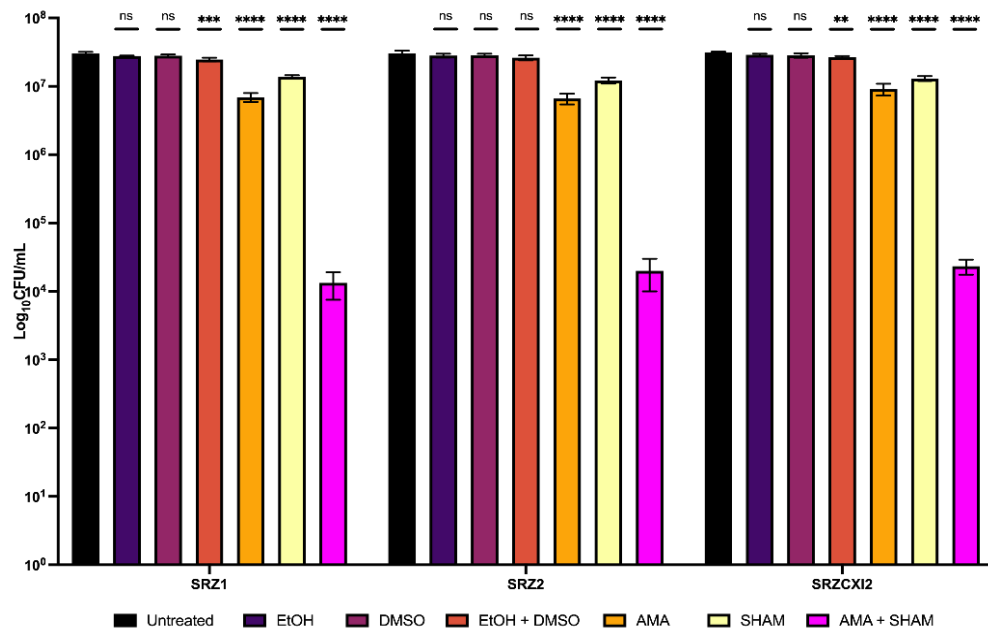
AOX provides an alternative route for the transport of electrons during oxidative phosphorylation. To functionally confirm the presence of an alternative oxidase in the ETC of SRZ, cells were grown in the presence of specific respiratory inhibitors. The classical cytochrome c pathway was blocked by inhibiting Q-cytochrome c oxidoreductase (complex III) using AMA. This bacterial secondary metabolite acts by binding to the Qi site of complex III, thereby displacing coenzyme Q (CoQ) and arresting the movement of electrons. Ultimately, this blockage leads to electron efflux, with the potential to become reactive and form highly toxic products, such as reactive oxygen species (ROS).

The presence of an alternative oxidase provides an alternate route for electron transport, receiving electrons directly from reduced ubiquinol to reduce

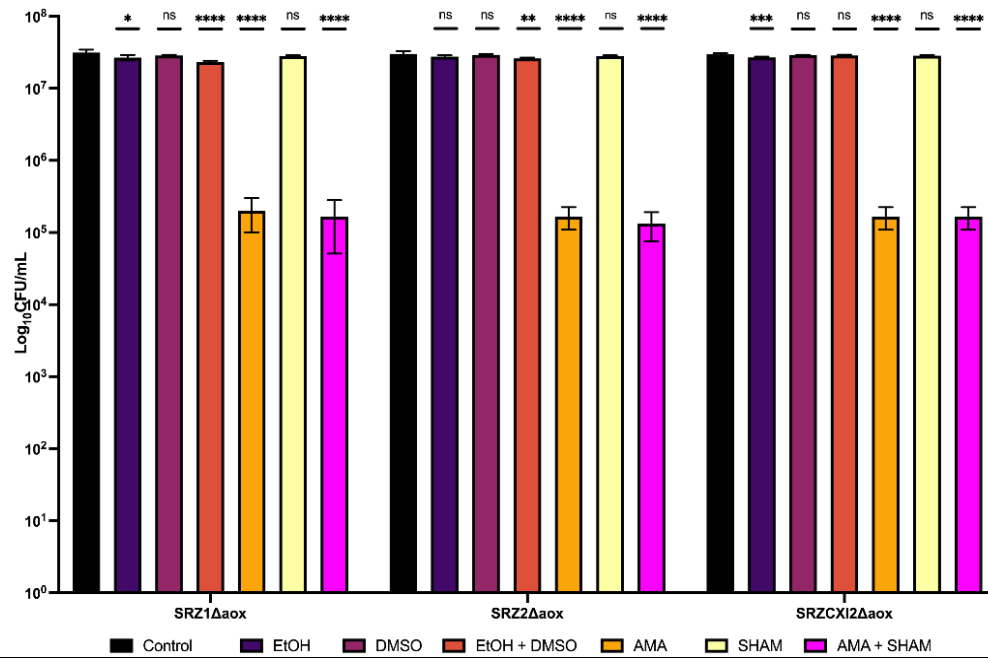
oxygen into water. This one-step process only depends on NADH oxidoreductase (complex I) as the sole contributor to the proton motive force (pmf) in the intermembrane space of the mitochondrion. An organism equipped with this diverging route for electron transport can dissipate the build-up of electrons caused by AMA and survive the inhibition of the classical cytochrome c pathway, albeit with a significant decrease in ATP synthesis. AOX is sensitive to the action of salicylhydroxamic acid (SHAM), a drug that acts as an irreversible inhibitor and prevents the final redox reaction from taking place.

Cells were treated with AMA, SHAM, or both to infer the predominant respiratory pathway as a function of cell survival. In addition to an untreated control group, cells were treated with the respective solvents used to prepare the respiratory inhibitors to account for their basal toxicity on SRZ cells. Treatment with AMA results in a reduced survival rate in all WT backgrounds, although it does not eliminate growth (Figure 4.6A, orange bars). Contrastingly, a higher number of cells is viable after treatment with SHAM (Figure 4.6A, yellow bars), and this number was significantly higher than that after treatment with AMA ($p < 0.0001$ not represented in Figure 4.6A). This suggests that SRZ is relatively sensitive to AMA and, to a lesser degree, to SHAM. Interestingly, treatment with both AMA and SHAM had a more pronounced effect on survival rate (Figure 4.6A, pink bars). This finding suggests that cells can survive despite the inhibitory action of AMA on the standard cytochrome c pathway by virtue of an alternative respiratory pathway promoted by AOX.

(A)



(B)



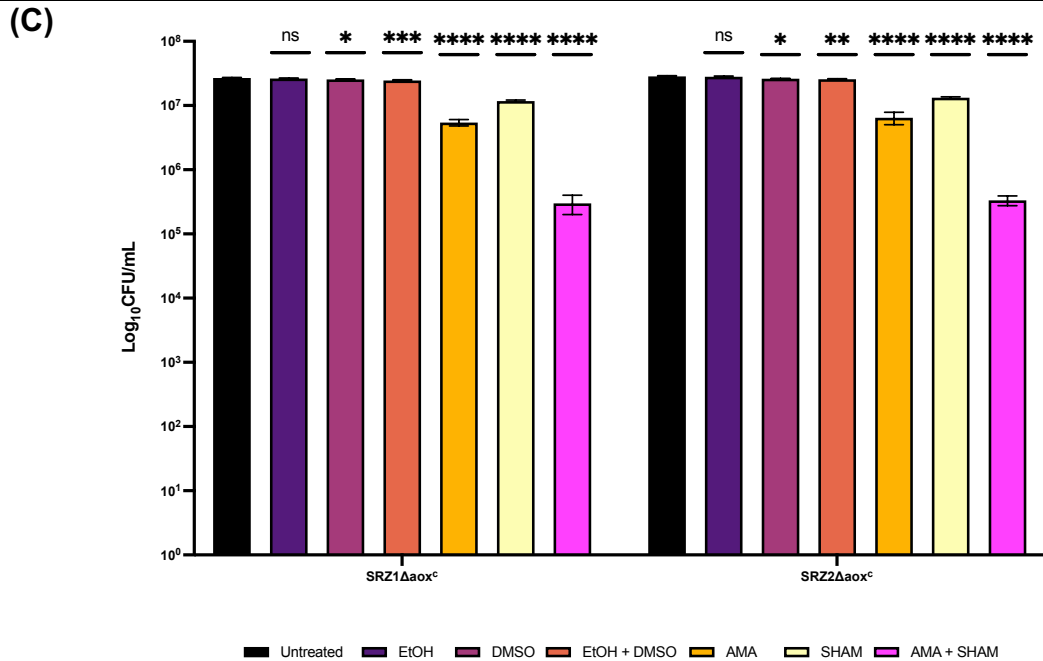


Figure 4.6 – Growth inhibition assay of SRZ. 10⁵ cells/mL were treated with 50 μM AMA and/or 2 mM SHAM at 28°C for 24 hours. Cultures were then plated onto PD agar to determine the number of surviving colonies. Bars represent averages of biological triplicates with standard errors indicated. One-way ANOVA followed by Tukey’s Multiple Comparison Test was performed in Graphpad 9.0. Treated samples in WT (A), AOX deletion mutants (B) and complemented mutant strains (C) were compared to their corresponding untreated controls and statistical significance is indicated on top of bars. All comparisons were made in reference to the untreated cultures (black bars), with p ≥ 0.05 = not significant (ns), p ≤ 0.05 = weakly significant (*), p ≤ 0.01 = significant (**), p ≤ 0.001 = very significant (***) and p ≤ 0.0001 = extremely significant (****)

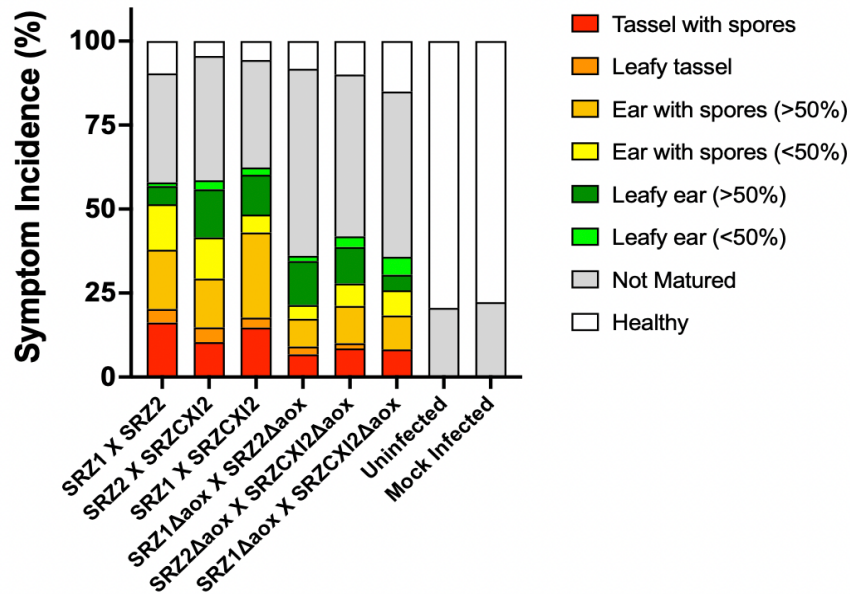
The AOX deletion mutants were subjected to the same inhibitory treatments as the WT strains (Figure 4.6B). AMA had a more serious effect on the mutants than it did on the WT strains (Figure 4.6B, orange bars, p < 0.0001 not represented). More importantly, this effect was comparable to that of both AMA and SHAM on the mutants (Figure 4.6B, p > 0.05 not represented). Interestingly, no effect was observed when the AOX mutants were treated with SHAM, suggesting that movement of electrons is unidirectional via the cytochrome c pathway, thus maximizing ATP synthesis and resulting in healthier

cultures. These results suggest that AOX is a functioning alternative component of the ETC of SRZ, rendering respiration resistant to the action of AMA.

Lastly, complementation of the deleted AOX gene was achieved by transformation of protoplasts of the deletion mutant strains with the complementation construct. This construct incorporated the AOX gene in its entirety as part of the upstream flank, in addition to the extra DNA sequence flanking the insertion target site. Successful homologous recombination resulted in the replacement of the hygromycin resistance cassette used to disrupt AOX by a carboxin resistance cassette and the AOX gene in its native state. The resulting complemented strains were subjected to the same inhibitory treatment as the WT strains. Complementation successfully restored respiratory capacity, as the same WT trends with AMA and SHAM are evident (Figure 4.6C).

Secondary respiration is involved in pathogenicity of SRZ. To determine if AOX is a crucial component of SRZ during its pathogenic stage, maize seedlings were infected with compatible combinations of both WT and AOX mutant strains. Symptomatic profiles were analyzed once plants were fully matured (7-8 wpi) and are illustrated in Figure 4.7A. Interestingly, all symptoms were present in plants infected by both WT and mutant strains. However, plants infected with the AOX deletion mutants displayed a reduction in serious symptoms (tassel with spores, leafy tassel and ear with spores) compared to plants infected with the WT strains.

(A)



(B)

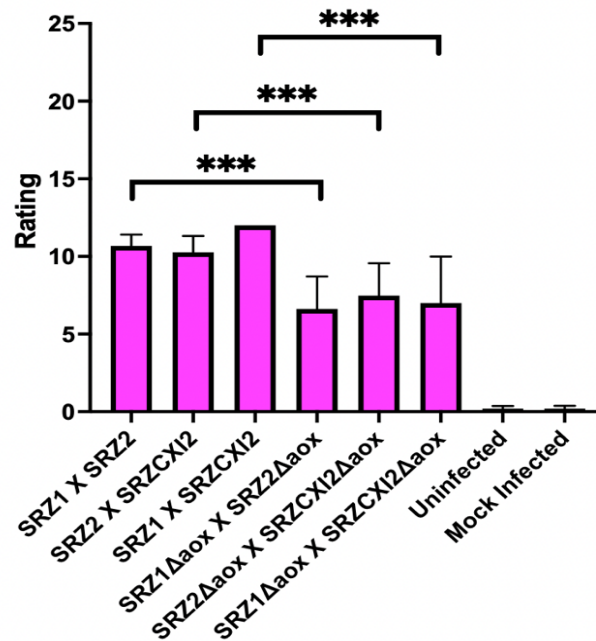
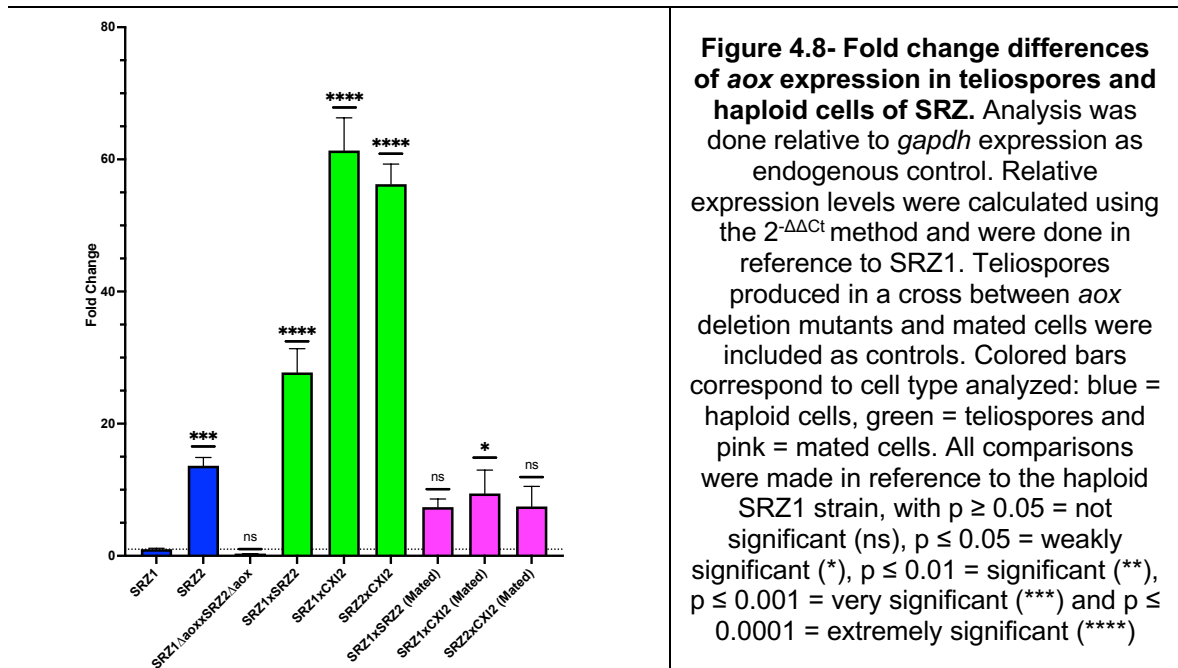


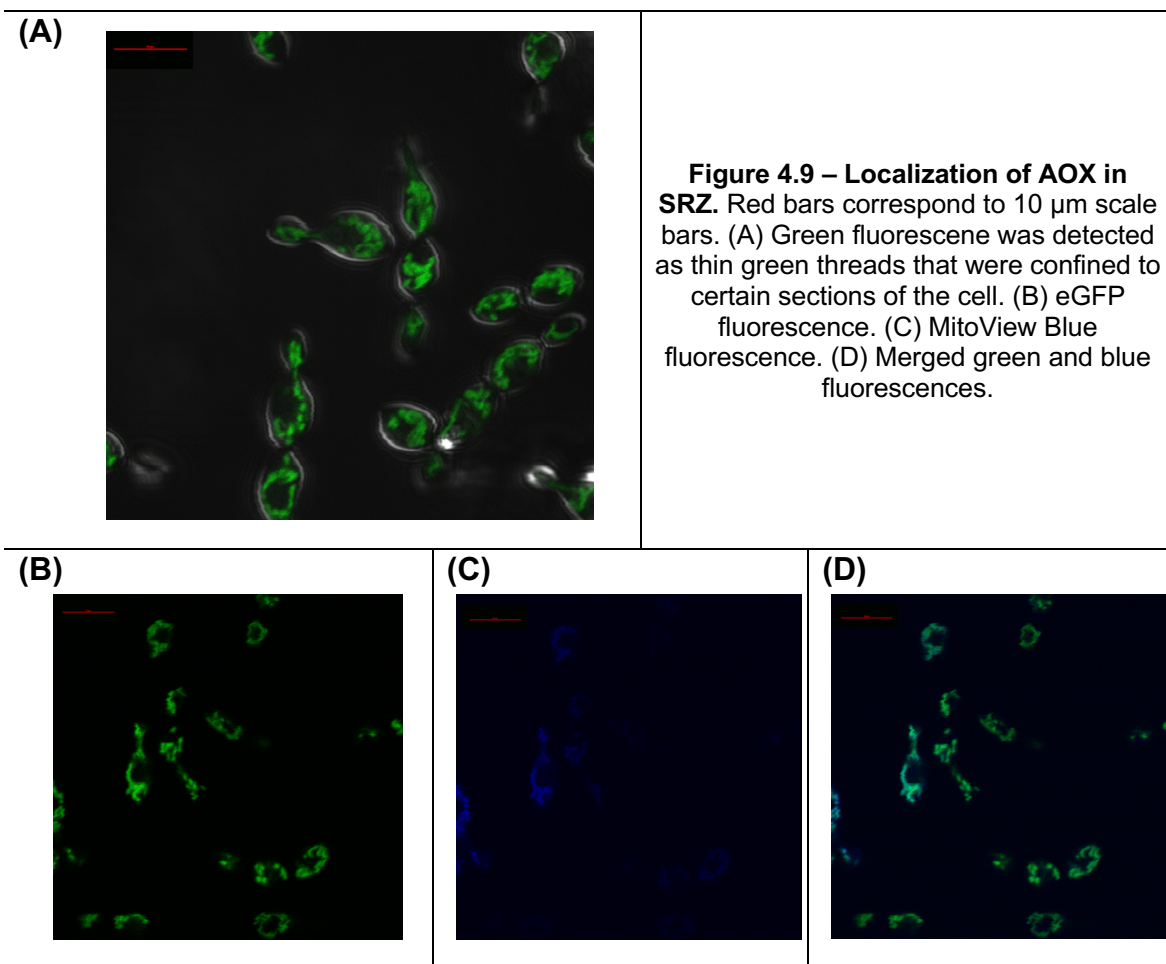
Figure 4.7 – Assessment of pathogenicity of SRZ on maize. (A) Mutant and WT strains of SRZ were used to infect maize seedlings. Infections were done in triplicate, with 20 plants per replicate (N=60). Symptoms were scored 7-8 wpi according to the ranking score illustrated in Figure 3. (B) Mean disease severity indexes were calculated based on the individual symptoms ranking. Bars represent averages of biological triplicates, with standard errors indicated. Comparisons were made between WT crosses and their corresponding AOX deletion mutant crosses, with statistical significance indicated on top of bars. For comparisons, $p \geq 0.05$ = not significant (ns), $p \leq 0.05$ = weakly significant (*), $p \leq 0.01$ = significant (**), $p \leq 0.001$ = very significant (***) and $p \leq 0.0001$ = extremely significant (****)

This last finding was discernable in the overall disease severity analysis, in which individual symptoms were taken into consideration to ascribe single ratings to the different symptomatic profiles generated. Along these lines, mating combinations of the WT strains were responsible for significantly higher disease severity indexes than those caused by combinations of the AOX mutants (Figure 4.7B). The mutants' reduced disease severity without fully disrupting the fungal life cycle may indicate that AOX is acting synergistically with other cellular components during the pathogenic stage of SRZ.

AOX expression is upregulated during the teliospore stage of the fungal life cycle. To determine if AOX is involved in developmental regulation, gene expression analysis was implemented. Accordingly, AOX expression was compared via qRT-PCR during the teliospore (diploid), mated (beginning of dikaryon phase) and sporidium (haploid) stages of SRZ. Relative expression analysis of AOX in teliospores was done separately in reference to SRZ1 (Figure 4.8) and SRZ2 (Supplemental Figure 11) sporidia. As controls, teliospores resulting from a compatible cross between AOX deletion mutants, as well as mated cells resulting from combining compatible haploid sporidia, were included. AOX was found to be upregulated, albeit at different magnitudes, in teliospores regardless of the reference strain. These preliminary results suggest AOX-mediated respiration is favored during teliospore development and maintenance, consistent with the lower metabolic demands of a quiescent lifestyle.



SRZ AOX localizes to the mitochondrial membrane. Previous studies in *U. maydis* confirmed localization of AOX to the inner mitochondrial membrane using protein purification assays. To determine if the SRZ AOX ortholog identified bioinformatically corresponds to a mitochondrial protein, a fluorescent fusion AOX protein was designed with eGFP. The SRZ transformants generated with this construct were then analyzed using confocal microscopy. Fluorescence was detected as thin threads that spread out throughout the cell, and even extended to budding daughter cells (Figure 4.9A). Treatment of cells with a mitochondrial fluorogenic dye confirmed that the green fluorescence coincided with mitochondrial structures.



Discussion

Identification and characterization of alternative components of the ETC has recently received special attention across different fungal families, linking them to thermotolerance, pathogenicity and the overall cellular welfare in the face of chemical and environmental stresses. In some cases, however, the benefit of secondary respiration remains unclear. For instance, studies in *U. maydis* were

inconclusive regarding when the fungus switches respiratory routes at different stages of its life cycle. Accordingly, the current study focused on identifying an AOX homolog in the related species SRZ, as it provides some peculiarities during its life cycle that may shed light on the advantages of AOX-mediated respiration.

The bioinformatic analysis used for the identification of AOX in SRZ revealed high amino acid identity to that encoded by the *U. maydis* homolog, *aox1*. The analysis also included AOX amino acid sequences of species closely and distantly related to SRZ, providing further support for the identification of a putative AOX in SRZ. Despite some polypeptide size differences between the predicted AOX polypeptide of SRZ and that of distantly related species, amino acid identity was relatively high across all species. More importantly, the analysis revealed the presence of an iron binding domain in all sequences, as previously characterized in other organisms. Additionally, localization of AOX to the mitochondrial membrane was confirmed via fluorescence studies.

Due to what was previously found in *U. maydis*, it was not surprising to find that loss of AOX did not affect in vitro life cycle processes shared with SRZ, as demonstrated by the assessment of mating capability and stress tolerance. However, there were notable differences during the infection assays of maize. Although WT and mutant crosses of SRZ successfully colonized, invaded and induced symptoms in the plant, they did so at significantly different frequencies and severity. This effect was not found in *U. maydis*, as it only produces local infection and symptoms are scored as early as 2 wpi. SRZ infection provides the

ability for long-term evaluation of the phytopathogen, as disease evaluation requires fully mature maize plants. Accordingly, AOX may be involved in the endurance of the fungus once inside of the host plant. It is also worth mentioning that the controlled nature of the infection experiments might have contributed to the survival of the deletion mutants in the plant tissue, as a natural population of maize is constantly challenged by environmental insults. More importantly, smut fungi possess unique pathogenic determinants, also known as effectors, that may compensate for the loss of AOX and ensure completion of the fungal life cycle. Further experimentation is required and should take into consideration environmental factors that may affect both the fungus and the host plant, such as extreme temperatures, as well as the effector armament of the pathogen, to uncover additional aspects of the involvement of AOX in pathogenicity.

Expression analysis of different stages of the life cycle of SRZ revealed that AOX is upregulated in teliospores, in contrast with haploid sporidia and even mated cells. The analysis was done in reference to different haploid strains, as these behaved differently in preliminary qRT-PCR experiments. However, AOX transcript levels of teliospores remained significantly higher regardless of the reference strain used. This finding is consistent with what was found in other organisms, in which specific life cycle stages favor secondary respiration in response to different metabolic demands. Correspondingly, it can be deduced that respiration in SRZ teliospores is predominantly AOX-mediated, as these specialized structures remain relatively quiescent until they disseminate and are able to germinate under favorable conditions. In contrast, requirement for haploid

sporidia to constantly divide and eventually grow by filamentation when successful mating occurs requires maximized production of ATP, provided by the canonical cytochrome c pathway of the ETC. Further experiments should include expression analysis of the classical components of the ETC in both teliospores and sporidia to confirm the switch in respiratory pathways. The presence of AOX in plants contributes additional complexities to studies of this nature, as the evolutionary history of host-pathogen interactions should not be ignored. Quite surprisingly, the AOX of *Zea mays* (Aox1a, NCBI Accession No. LOC100273671) was identified and extensively characterized early, and it has been linked to thermotolerance and osmotic and oxidative regulation (183-185). Along these lines, many arguments could be made regarding the biological interactions between SRZ and maize throughout their evolutionary history and if AOX emerged in the plant as a response to fungal infection or if the fungus acquired AOX to assimilate and survive inside the plant tissue.

CHAPTER V

CONCLUSIONS

Sexual reproduction is coupled with distinct mechanisms of inheritance of organelles. In anisogamous organisms like plants and mammals, production of morphologically distinct sex cells promotes the inheritance of organelle genetic material from a single parent. This uniparental pattern is reinforced by different molecular mechanisms that may target organelle genetic material for eventual degradation or exclusion. A selective advantage of uniparental inheritance of organelles is the prevention of horizontal transfer of “selfish” genes that may have adverse effects on offspring development. This hypothesis, however, is mostly theoretical, as selfish organelle genes have not been investigated extensively. Contrastingly, other theories argue that uniparental inheritance of organelles imposes a selective disadvantage by weakening the effects of natural selection on beneficial mutations in organelle genetic material, thus compromising an organism’s ability to adapt to changing environments.

Sporisorium reilianum f. sp. zaeae (SRZ) is the causative agent of head smut in maize, distinguished by the production of black teliospore sori in male and female inflorescences of the plant host. This biotrophic pathogen displays a

dimorphic lifestyle, being able to switch from an asexual stage, in which reproduction is achieved through budding of yeast-like haploid spordia, to a sexual stage, controlled by mating type loci that regulate a pheromone reaction between compatible partners and subsequent development of specialized structures that facilitate colonization and infiltration of plant tissue. The sexual stage of this fungus is of high interest, as it may also involve appropriate segregation of mitochondria via a degradation-mediated molecular mechanism. More importantly, SRZ provides a biological system in which the uniparental inheritance pattern can be subject of further scrutiny, as mating may also occur between compatible partners that are not under the influence of a uniparental control system. Accordingly, heteroplasmy can be explored in the context of its effects on fitness of the resulting offspring.

In this work, the Lga2/Rga2 mitochondrial inheritance mechanism of SRZ was investigated. The molecular machinery of this system was previously characterized in the related species, *Ustilago maydis*, and it was found to be involved in a degradation-mediated mechanism, in which genetic material of the mitochondria of one parent is shielded by Rga2 from the endonuclease activity of Lga2, which is upregulated during plasmogamy, thus promoting the generation of homoplasmic offspring. The findings in *U. maydis* were facilitated by using classical molecular genetic approaches that can be costly and tedious. As a result, the first objective of this study involved the bioinformatic analysis of whole genome sequencing (WGS) data for the identification of polymorphisms in the mitochondrial DNA (mtDNA) of different strains of SRZ.

Analysis of the mitogenomes in this study revealed an assortment of polymorphisms that were subsequently verified by polymerase chain reaction (PCR) and Sanger sequencing approaches. This initial screening proved to be essential, as WGS may yield inaccurate results or results that are challenging to use for full determination of mitochondrial genomes. Notably, sequence alignment of the mtDNA samples initially suggested a massive deletion in *cox1*, a gene that encodes one of the subunits that make up complex IV of the mitochondrial electron transport chain (ETC). Interestingly, this polymorphic region was only detected in strains originally collected in China, providing a genetic hot spot for mitotype screening. However, further exploration of this region uncovered unique mtDNA sequence that matched other closely related species and not the reference genome. A PCR-based diagnostic method was designed around this polymorphic region that allowed distinguishing between German and Chinese mitotypes.

The characterization of the *Lga2/Rga2* uniparental inheritance system involved a loss-of-function (LOF) approach, in which single and double mutants for *lga2* and *rga2* were generated and subjected to standard assays to determine their role in overall cell viability and integrity. Absence of *Lga2/Rga2* did not affect mating ability of SRZ and did not compromise growth in the face of chemical stressors. These findings were not surprising, as similar results were previously reported in *U. maydis*. Moreover, the pathogenicity assays did not provide a clear pattern in disease severity between wild type and mutant strains, but a difference in the production of teliospores was noted. These last results, however, are not

conclusive, as additional larger sample sizes and additional biological replicates need to be included in the study for more robust statistical inference.

The third objective of this study involved the harvesting and subsequent screening of teliospores produced in the different crosses of SRZ strains. This analysis was facilitated by standard PCR and Sanger sequencing methods, which proved to be a more cost-effective approach than what was previously done in *U. maydis*. The PCR and sequencing results were compared to the theoretical outcomes of the different crosses of SRZ strains. Accordingly, a cross involving the a2 partner, equipped with the Lga2/Rga2 machinery, would be predicted to be subject to the uniparental inheritance pattern of mitochondria. Contrastingly, a cross between strains of the a1 and a3 mating types might be expected to result in a biparental inheritance pattern, resulting in heteroplasmic offspring. The screening process was also centered around the polymorphic region detected in *cox1*, thus allowing for the discrimination between Chinese and/or German mitotypes.

The results of the mitotyping studies were, for the most part, inconclusive, as most of the samples screened failed to produce the expected amplicons for all primer combinations tested. A more conclusive statement can be made for teliospores resulting from the cross between SRZ2 x SRZCX12 and SRZ2 Δ *rga2* x SRZCX12, which consistently produced Chinese bands with all the primer combinations tested. This was an unexpected finding, as the mitotype of the offspring of SRZ2 and SRZCX12 should be determined by the a2 partner (SRZ2) and be of German origin, if *S. reilianum* follows the paradigm of *U. maydis*.

Moreover, absence of Rga2 did not affect the pattern observed, as teliospores resulting from the cross between SRZ2 Δ rga2 and SRZCXI2 were of the Chinese mitotype. Further exploration of the *cox1* polymorphic region involved additional PCR experiments that examined the integrity and intactness of the *cox1* gene and its environs. These last experiments revealed that the immediate vicinities of the *cox1* polymorphic region may, in fact, be modified since successful amplification was evident only in SRZ2 x SRZCXI2 and SRZ2 Δ rga2 x SRZCXI2. Additionally, this finding may suggest that the teliospores from the crosses that did not produce any PCR results could be physiologically compromised, as *cox1* has been subjected to further modifications that may have altered its function in the mitochondrial respiratory chain. These teliospores should be subject to further experimentation to determine whether their germination is impaired and the viability of the resulting sporidia, including respiratory assays.

The last goal of this study involved further exploration of mitochondrial metabolism of SRZ. Based on previous studies in *U. maydis*, a putative alternative oxidase (AOX) was identified in SRZ. This alternative component of the mitochondrial ETC has been linked to alternative respiration, in which the flow of electrons diverges from the classical cytochrome c pathway and decreases the production of metabolic energy. This alternate route of the ETC has been extensively characterized in other organisms and has been associated with chemical and environmental stress tolerance and developmental transition. Functional characterization of AOX was achieved by using specific mitochondrial inhibitors and their effect on the growth of wild type and deletion mutant strains.

These experiments demonstrated that disruption of the classical cytochrome c pathway of the mitochondrial ETC of SRZ does not have a significant effect on growth. Rather, cells succumbed when an additional mitochondrial inhibitor specific to AOX was added.

Furthermore, absence of AOX in SRZ did not affect mating capabilities nor chemical stress tolerance. However, a significant reduction in disease severity was detected in the deletion mutants. It is important to note that although pathogenicity was compromised, the fungus was still able to complete its life cycle (*i.e.*, generation of teliospores). This may prove crucial when considering that the pathogenicity assays were performed in a highly controlled environment, potentially blurring the importance of AOX and alternative respiration in natural conditions in which plant development may be compromised by additional environmental factors (*e.g.*, extreme temperatures, limited rainfall, predators).

REFERENCES

1. Vartak, R., Porras, C. A., and Bai, Y. (2013) Respiratory supercomplexes: structure, function and assembly. *Protein Cell* **4**, 582-590
2. Hernandez, M. E., and Newman, D. K. (2001) Extracellular electron transfer. *Cell Mol Life Sci* **58**, 1562-1571
3. Ramsay, R. R. (2019) Electron carriers and energy conservation in mitochondrial respiration. *ChemTexts* **5**
4. Bonner, W. D., & Voss, D. O. (1961) Some Characteristics of Mitochondria Extracted from Higher Plants. *Nature* **191**, 682-884
5. Ohnishi, T., Kawaguchi, K., Hagihara, B. (1966) Preparation and some properties of yeast mitochondria. *Journal of Biological Chemistry* **241**, 1797-1806
6. Weiss, H., von Jagow, G., Klingenberg, M., and Bucher, T. (1970) Characterization of *Neurospora crassa* mitochondria prepared with a grind-mill. *Eur J Biochem* **14**, 75-82
7. Buschges, R., Bahrenberg, G., Zimmermann, M., and Wolf, K. (1994) NADH: ubiquinone oxidoreductase in obligate aerobic yeasts. *Yeast* **10**, 475-479
8. Martins Vde, P., Dinamarco, T. M., Curti, C., and Uyemura, S. A. (2011) Classical and alternative components of the mitochondrial respiratory chain in pathogenic fungi as potential therapeutic targets. *J Bioenerg Biomembr* **43**, 81-88
9. Chinnery, P. F. (1993) Mitochondrial Disorders Overview. in *GeneReviews((R))* (Adam, M. P., Ardinger, H. H., Pagon, R. A., Wallace, S. E., Bean, L. J. H., Stephens, K., and Amemiya, A. eds.), Seattle (WA). pp
10. Li, H., Slone, J., Fei, L., and Huang, T. (2019) Mitochondrial DNA Variants and Common Diseases: A Mathematical Model for the Diversity of Age-Related mtDNA Mutations. *Cells* **8**
11. Wallace, D. C., and Chalkia, D. (2013) Mitochondrial DNA genetics and the heteroplasmy conundrum in evolution and disease. *Cold Spring Harb Perspect Biol* **5**, a021220
12. Ye, K., Lu, J., Ma, F., Keinan, A., and Gu, Z. (2014) Extensive pathogenicity of mitochondrial heteroplasmy in healthy human individuals. *Proc Natl Acad Sci U S A* **111**, 10654-10659
13. Stefano, G. B., and Kream, R. M. (2015) Cancer: Mitochondrial Origins. *Med Sci Monit* **21**, 3736-3739
14. Stefano, G. B., and Kream, R. M. (2016) Mitochondrial DNA heteroplasmy in human health and disease. *Biomed Rep* **4**, 259-262

15. Stefano, G. B., and Kream, R. M. (2017) Aging Reversal and Healthy Longevity is in Reach: Dependence on Mitochondrial DNA Heteroplasmy as a Key Molecular Target. *Med Sci Monit* **23**, 2732-2735
16. Schon, E. A., Bonilla, E., and DiMauro, S. (1997) Mitochondrial DNA mutations and pathogenesis. *J Bioenerg Biomembr* **29**, 131-149
17. Macmillan, C., Lach, B., and Shoubridge, E. A. (1993) Variable distribution of mutant mitochondrial DNAs (tRNA(Leu[3243])) in tissues of symptomatic relatives with MELAS: the role of mitotic segregation. *Neurology* **43**, 1586-1590
18. Li, W., Qi, Y., Cui, X., Sun, Y., Huo, Q., Yang, Y., Wen, X., Tan, M., Du, S., Zhang, H., Zhang, M., Liu, C., and Kong, Q. (2017) Heteroplasmy and Copy Number Variations of Mitochondria in 88 Hepatocellular Carcinoma Individuals. *J Cancer* **8**, 4011-4017
19. Verma, M., and Kumar, D. (2007) Application of mitochondrial genome information in cancer epidemiology. *Clin Chim Acta* **383**, 41-50
20. Goldring, E. S., Grossman, L. I., and Marmur, J. (1971) Petite mutation in yeast. II. Isolation of mutants containing mitochondrial deoxyribonucleic acid of reduced size. *J Bacteriol* **107**, 377-381
21. Sagan, L. (1967) On the origin of mitosing cells. *J Theor Biol* **14**, 255-274
22. Thrash, J. C., Boyd, A., Huggett, M. J., Grote, J., Carini, P., Yoder, R. J., Robbertse, B., Spatafora, J. W., Rappe, M. S., and Giovannoni, S. J. (2011) Phylogenomic evidence for a common ancestor of mitochondria and the SAR11 clade. *Sci Rep* **1**, 13
23. Wang, Z., and Wu, M. (2015) An integrated phylogenomic approach toward pinpointing the origin of mitochondria. *Sci Rep* **5**, 7949
24. The Genetic Codes.
25. Gabaldon, T., and Huynen, M. A. (2007) From endosymbiont to host-controlled organelle: the hijacking of mitochondrial protein synthesis and metabolism. *PLoS Comput Biol* **3**, e219
26. Sasser, D., Lo, N., Epis, S., D'Auria, G., Montagna, M., Comandatore, F., Horner, D., Pereto, J., Luciano, A. M., Franciosi, F., Ferri, E., Crotti, E., Bazzocchi, C., Daffonchio, D., Sacchi, L., Moya, A., Latorre, A., and Bandi, C. (2011) Phylogenomic evidence for the presence of a flagellum and cbb(3) oxidase in the free-living mitochondrial ancestor. *Mol Biol Evol* **28**, 3285-3296
27. Wang, Z., and Wu, M. (2014) Phylogenomic reconstruction indicates mitochondrial ancestor was an energy parasite. *PLoS One* **9**, e110685
28. Tyagi, S., Pande, V., and Das, A. (2014) Whole mitochondrial genome sequence of an Indian Plasmodium falciparum field isolate. *Korean J Parasitol* **52**, 99-103
29. Wu, Z., Cuthbert, J. M., Taylor, D. R., and Sloan, D. B. (2015) The massive mitochondrial genome of the angiosperm *Silene noctiflora* is evolving by gain or loss of entire chromosomes. *Proc Natl Acad Sci U S A* **112**, 10185-10191
30. Karnkowska, A., Vacek, V., Zubacova, Z., Treitli, S. C., Petrzalkova, R., Eme, L., Novak, L., Zarsky, V., Barlow, L. D., Herman, E. K., Soukal, P.,

- Hroudova, M., Dolezal, P., Stairs, C. W., Roger, A. J., Elias, M., Dacks, J. B., Vlcek, C., and Hampl, V. (2016) A Eukaryote without a Mitochondrial Organelle. *Curr Biol* **26**, 1274-1284
31. Haig, D. (2016) Intracellular evolution of mitochondrial DNA (mtDNA) and the tragedy of the cytoplasmic commons. *Bioessays* **38**, 549-555
 32. Hirose, M., Schilf, P., Gupta, Y., Zarse, K., Kunstner, A., Fahrnich, A., Busch, H., Yin, J., Wright, M. N., Ziegler, A., Vallier, M., Belheouane, M., Baines, J. F., Tautz, D., Johann, K., Oelkrug, R., Mittag, J., Lehnert, H., Othman, A., Johren, O., Schwaninger, M., Prehn, C., Adamski, J., Shima, K., Rupp, J., Hasler, R., Fuellen, G., Kohling, R., Ristow, M., and Ibrahim, S. M. (2018) Low-level mitochondrial heteroplasmy modulates DNA replication, glucose metabolism and lifespan in mice. *Sci Rep* **8**, 5872
 33. James, A. C., and Ballard, J. W. (2003) Mitochondrial genotype affects fitness in *Drosophila simulans*. *Genetics* **164**, 187-194
 34. Smigrodzki, R. M., and Khan, S. M. (2005) Mitochondrial microheteroplasmy and a theory of aging and age-related disease. *Rejuvenation Res* **8**, 172-198
 35. Yahalomi, D., Atkinson, S. D., Neuhof, M., Chang, E. S., Philippe, H., Cartwright, P., Bartholomew, J. L., and Huchon, D. (2020) A cnidarian parasite of salmon (Myxozoa: Henneguya) lacks a mitochondrial genome. *Proc Natl Acad Sci U S A* **117**, 5358-5363
 36. Cole, L. W. (2016) The Evolution of Per-cell Organelle Number. *Front Cell Dev Biol* **4**, 85
 37. Lackner, L. L. (2014) Shaping the dynamic mitochondrial network. *BMC Biol* **12**, 35
 38. Bui, H. T., Karren, M. A., Bhar, D., and Shaw, J. M. (2012) A novel motif in the yeast mitochondrial dynamin Dnm1 is essential for adaptor binding and membrane recruitment. *J Cell Biol* **199**, 613-622
 39. Mears, J. A., Lackner, L. L., Fang, S., Ingerman, E., Nunnari, J., and Hinshaw, J. E. (2011) Conformational changes in Dnm1 support a contractile mechanism for mitochondrial fission. *Nat Struct Mol Biol* **18**, 20-26
 40. Lackner, L. L., Horner, J. S., and Nunnari, J. (2009) Mechanistic analysis of a dynamin effector. *Science* **325**, 874-877
 41. Tieu, Q., Okreglak, V., Naylor, K., and Nunnari, J. (2002) The WD repeat protein, Mdv1p, functions as a molecular adaptor by interacting with Dnm1p and Fis1p during mitochondrial fission. *J Cell Biol* **158**, 445-452
 42. Koirala, S., Bui, H. T., Schubert, H. L., Eckert, D. M., Hill, C. P., Kay, M. S., and Shaw, J. M. (2010) Molecular architecture of a dynamin adaptor: implications for assembly of mitochondrial fission complexes. *J Cell Biol* **191**, 1127-1139
 43. Cervený, K. L., Studer, S. L., Jensen, R. E., and Sesaki, H. (2007) Yeast mitochondrial division and distribution require the cortical num1 protein. *Dev Cell* **12**, 363-375

44. Hammermeister, M., Schodel, K., and Westermann, B. (2010) Mdm36 is a mitochondrial fission-promoting protein in *Saccharomyces cerevisiae*. *Mol Biol Cell* **21**, 2443-2452
45. Otera, H., Wang, C., Cleland, M. M., Setoguchi, K., Yokota, S., Youle, R. J., and Mihara, K. (2010) Mff is an essential factor for mitochondrial recruitment of Drp1 during mitochondrial fission in mammalian cells. *J Cell Biol* **191**, 1141-1158
46. Yu, R., Jin, S. B., Lendahl, U., Nister, M., and Zhao, J. (2019) Human Fis1 regulates mitochondrial dynamics through inhibition of the fusion machinery. *EMBO J* **38**
47. Dorn, G. W., 2nd. (2020) Mitofusins as mitochondrial anchors and tethers. *J Mol Cell Cardiol*
48. Del Dotto, V., Fogazza, M., Carelli, V., Rugolo, M., and Zanna, C. (2018) Eight human OPA1 isoforms, long and short: What are they for? *Biochim Biophys Acta Bioenerg* **1859**, 263-269
49. Mitra, S., and Elliott, S. J. (2009) Oxidative disassembly of the [2Fe-2S] cluster of human Grx2 and redox regulation in the mitochondria. *Biochemistry* **48**, 3813-3815
50. Gerstenberger, J. P., Occhipinti, P., and Gladfelter, A. S. (2012) Heterogeneity in mitochondrial morphology and membrane potential is independent of the nuclear division cycle in multinucleate fungal cells. *Eukaryot Cell* **11**, 353-367
51. Boldogh, I. R., and Pon, L. A. (2006) Interactions of mitochondria with the actin cytoskeleton. *Biochim Biophys Acta* **1763**, 450-462
52. Yang, H. C., Palazzo, A., Swayne, T. C., and Pon, L. A. (1999) A retention mechanism for distribution of mitochondria during cell division in budding yeast. *Curr Biol* **9**, 1111-1114
53. Rafelski, S. M., Viana, M. P., Zhang, Y., Chan, Y. H., Thorn, K. S., Yam, P., Fung, J. C., Li, H., Costa Lda, F., and Marshall, W. F. (2012) Mitochondrial network size scaling in budding yeast. *Science* **338**, 822-824
54. Longo, V. D., Shadel, G. S., Kaerberlein, M., and Kennedy, B. (2012) Replicative and chronological aging in *Saccharomyces cerevisiae*. *Cell Metab* **16**, 18-31
55. McFaline-Figueroa, J. R., Vevea, J., Swayne, T. C., Zhou, C., Liu, C., Leung, G., Boldogh, I. R., and Pon, L. A. (2011) Mitochondrial quality control during inheritance is associated with lifespan and mother-daughter age asymmetry in budding yeast. *Aging Cell* **10**, 885-895
56. Lawrence, E. J., Boucher, E., and Mandato, C. A. (2016) Mitochondria-cytoskeleton associations in mammalian cytokinesis. *Cell Div* **11**, 3
57. Lackner, L. L. (2019) The Expanding and Unexpected Functions of Mitochondria Contact Sites. *Trends Cell Biol* **29**, 580-590
58. Mishra, P., and Chan, D. C. (2014) Mitochondrial dynamics and inheritance during cell division, development and disease. *Nat Rev Mol Cell Biol* **15**, 634-646
59. Kanki, T., and Klionsky, D. J. (2008) Mitophagy in yeast occurs through a selective mechanism. *J Biol Chem* **283**, 32386-32393

60. Koehler, C. M., Lindberg, G. L., Brown, D. R., Beitz, D. C., Freeman, A. E., Mayfield, J. E., and Myers, A. M. (1991) Replacement of bovine mitochondrial DNA by a sequence variant within one generation. *Genetics* **129**, 247-255
61. Krasich, R., and Copeland, W. C. (2017) DNA polymerases in the mitochondria: A critical review of the evidence. *Front Biosci (Landmark Ed)* **22**, 692-709
62. Falkenberg, M. (2018) Mitochondrial DNA replication in mammalian cells: overview of the pathway. *Essays Biochem* **62**, 287-296
63. Macao, B., Uhler, J. P., Siibak, T., Zhu, X., Shi, Y., Sheng, W., Olsson, M., Stewart, J. B., Gustafsson, C. M., and Falkenberg, M. (2015) The exonuclease activity of DNA polymerase gamma is required for ligation during mitochondrial DNA replication. *Nat Commun* **6**, 7303
64. Nicholls, T. J., Nadalutti, C. A., Motori, E., Sommerville, E. W., Gorman, G. S., Basu, S., Hoberg, E., Turnbull, D. M., Chinnery, P. F., Larsson, N. G., Larsson, E., Falkenberg, M., Taylor, R. W., Griffith, J. D., and Gustafsson, C. M. (2018) Topoisomerase 3alpha Is Required for Decatenation and Segregation of Human mtDNA. *Mol Cell* **69**, 9-23 e26
65. Chen, X. J., and Clark-Walker, G. D. (2018) Unveiling the mystery of mitochondrial DNA replication in yeasts. *Mitochondrion* **38**, 17-22
66. Kukat, C., Wurm, C. A., Spahr, H., Falkenberg, M., Larsson, N. G., and Jakobs, S. (2011) Super-resolution microscopy reveals that mammalian mitochondrial nucleoids have a uniform size and frequently contain a single copy of mtDNA. *Proc Natl Acad Sci U S A* **108**, 13534-13539
67. Kukat, C., Davies, K. M., Wurm, C. A., Spahr, H., Bonekamp, N. A., Kuhl, I., Joos, F., Polosa, P. L., Park, C. B., Posse, V., Falkenberg, M., Jakobs, S., Kuhlbrandt, W., and Larsson, N. G. (2015) Cross-strand binding of TFAM to a single mtDNA molecule forms the mitochondrial nucleoid. *Proc Natl Acad Sci U S A* **112**, 11288-11293
68. Lewis, S. C., Uchiyama, L. F., and Nunnari, J. (2016) ER-mitochondria contacts couple mtDNA synthesis with mitochondrial division in human cells. *Science* **353**, aaf5549
69. Longley, M. J., Nguyen, D., Kunkel, T. A., and Copeland, W. C. (2001) The fidelity of human DNA polymerase gamma with and without exonucleolytic proofreading and the p55 accessory subunit. *J Biol Chem* **276**, 38555-38562
70. Torriani, S. F., Penselin, D., Knogge, W., Felder, M., Taudien, S., Platzer, M., McDonald, B. A., and Brunner, P. C. (2014) Comparative analysis of mitochondrial genomes from closely related *Rhynchosporium* species reveals extensive intron invasion. *Fungal Genet Biol* **62**, 34-42
71. Nissanka, N., and Moraes, C. T. (2018) Mitochondrial DNA damage and reactive oxygen species in neurodegenerative disease. *FEBS Lett* **592**, 728-742
72. Fan, W., Waymire, K. G., Narula, N., Li, P., Rocher, C., Coskun, P. E., Vannan, M. A., Narula, J., Macgregor, G. R., and Wallace, D. C. (2008) A

- mouse model of mitochondrial disease reveals germline selection against severe mtDNA mutations. *Science* **319**, 958-962
73. Rossignol, R., Faustin, B., Rocher, C., Malgat, M., Mazat, J. P., and Letellier, T. (2003) Mitochondrial threshold effects. *Biochem J* **370**, 751-762
 74. Radzvilavicius, A. L., Lane, N., and Pomiankowski, A. (2017) Sexual conflict explains the extraordinary diversity of mechanisms regulating mitochondrial inheritance. *BMC Biol* **15**, 94
 75. Burr, S. P., Pezet, M., and Chinnery, P. F. (2018) Mitochondrial DNA Heteroplasmy and Purifying Selection in the Mammalian Female Germ Line. *Dev Growth Differ* **60**, 21-32
 76. Luo, S., Valencia, C. A., Zhang, J., Lee, N. C., Slone, J., Gui, B., Wang, X., Li, Z., Dell, S., Brown, J., Chen, S. M., Chien, Y. H., Hwu, W. L., Fan, P. C., Wong, L. J., Atwal, P. S., and Huang, T. (2018) Biparental Inheritance of Mitochondrial DNA in Humans. *Proc Natl Acad Sci U S A* **115**, 13039-13044
 77. Crow, J. F. (1992) An advantage of sexual reproduction in a rapidly changing environment. *J Hered* **83**, 169-173
 78. Hagemann, R. (2010) The foundation of extranuclear inheritance: plastid and mitochondrial genetics. *Mol Genet Genomics* **283**, 199-209
 79. Zhang, Q., Liu, Y., and Sodmergen. (2003) Examination of the cytoplasmic DNA in male reproductive cells to determine the potential for cytoplasmic inheritance in 295 angiosperm species. *Plant Cell Physiol* **44**, 941-951
 80. Neale, D. B., Marshall, K. A., and Sederoff, R. R. (1989) Chloroplast and mitochondrial DNA are paternally inherited in *Sequoia sempervirens* D. Don Endl. *Proc Natl Acad Sci U S A* **86**, 9347-9349
 81. Bell, G. (1978) The evolution of anisogamy. *J Theor Biol* **73**, 247-270
 82. DeLuca, S. Z., and O'Farrell, P. H. (2012) Barriers to male transmission of mitochondrial DNA in sperm development. *Dev Cell* **22**, 660-668
 83. Nishimura, Y., Yoshinari, T., Naruse, K., Yamada, T., Sumi, K., Mitani, H., Higashiyama, T., and Kuroiwa, T. (2006) Active digestion of sperm mitochondrial DNA in single living sperm revealed by optical tweezers. *Proc Natl Acad Sci U S A* **103**, 1382-1387
 84. Luo, S. M., Ge, Z. J., Wang, Z. W., Jiang, Z. Z., Wang, Z. B., Ouyang, Y. C., Hou, Y., Schatten, H., and Sun, Q. Y. (2013) Unique insights into maternal mitochondrial inheritance in mice. *Proc Natl Acad Sci U S A* **110**, 13038-13043
 85. Andereg, R. J., Betz, R., Carr, S. A., Crabb, J. W., and Duntze, W. (1988) Structure of *Saccharomyces cerevisiae* mating hormone a-factor. Identification of S-farnesyl cysteine as a structural component. *J Biol Chem* **263**, 18236-18240
 86. Hagen, D. C., Bruhn, L., Westby, C. A., and Sprague, G. F., Jr. (1993) Transcription of alpha-specific genes in *Saccharomyces cerevisiae*: DNA sequence requirements for activity of the coregulator alpha 1. *Mol Cell Biol* **13**, 6866-6875
 87. Hanson, S. J., and Wolfe, K. H. (2017) An Evolutionary Perspective on Yeast Mating-Type Switching. *Genetics* **206**, 9-32

88. Maddox, P., Chin, E., Mallavarapu, A., Yeh, E., Salmon, E. D., and Bloom, K. (1999) Microtubule dynamics from mating through the first zygotic division in the budding yeast *Saccharomyces cerevisiae*. *J Cell Biol* **144**, 977-987
89. Rine, J., Sprague, G. F., Jr., and Herskowitz, I. (1981) *rme1* Mutation of *Saccharomyces cerevisiae*: map position and bypass of mating type locus control of sporulation. *Mol Cell Biol* **1**, 958-960
90. Strausberg, R. L., and Perlman, P. S. (1978) The effect of zygotic bud position on the transmission of mitochondrial genes in *Saccharomyces cerevisiae*. *Mol Gen Genet* **163**, 131-144
91. Wilson, A. J. X., J. (2012) Mitochondrial inheritance: diverse patterns and mechanisms with an emphasis on fungi. *Mycology* **3**, 158-166
92. Hewitt, S. K., Duangrattanalert, K., Burgis, T., Zeef, L. A. H., and Delneri, D. (2018) Plasticity of Mitochondrial DNA Inheritance and its Impact on Nuclear Gene Transcription in Yeast Hybrids. *bioRxiv*, 394858
93. Van Dyck, E., and Clayton, D. A. (1998) Transcription-dependent DNA transactions in the mitochondrial genome of a yeast hypersuppressive petite mutant. *Mol Cell Biol* **18**, 2976-2985
94. Gillissen, B., Bergemann, J., Sandmann, C., Schroeer, B., Bolker, M., and Kahmann, R. (1992) A two-component regulatory system for self/non-self recognition in *Ustilago maydis*. *Cell* **68**, 647-657
95. Kronstad, J. W., and Leong, S. A. (1990) The *b* mating-type locus of *Ustilago maydis* contains variable and constant regions. *Genes Dev* **4**, 1384-1395
96. Fedler, M., Luh, K. S., Stelter, K., Nieto-Jacobo, F., and Basse, C. W. (2009) The *a2* mating-type locus genes *Iga2* and *rga2* direct uniparental mitochondrial DNA (mtDNA) inheritance and constrain mtDNA recombination during sexual development of *Ustilago maydis*. *Genetics* **181**, 847-860
97. Urban, M., Kahmann, R., and Bolker, M. (1996) The biallelic *a* mating type locus of *Ustilago maydis*: remnants of an additional pheromone gene indicate evolution from a multiallelic ancestor. *Mol Gen Genet* **250**, 414-420
98. Mahlert, M., Vogler, C., Stelter, K., Hause, G., and Basse, C. W. (2009) The *a2* mating-type-locus gene *Iga2* of *Ustilago maydis* interferes with mitochondrial dynamics and fusion, partially in dependence on a Dnm1-like fission component. *J Cell Sci* **122**, 2402-2412
99. Barr, C. M., Neiman, M., and Taylor, D. R. (2005) Inheritance and recombination of mitochondrial genomes in plants, fungi and animals. *New Phytol* **168**, 39-50
100. Chen, C., and Sathananthan, A. H. (1986) Early penetration of human sperm through the vestments of human eggs in vitro. *Arch Androl* **16**, 183-197
101. Shalgi, R., Magnus, A., Jones, R., and Phillips, D. M. (1994) Fate of sperm organelles during early embryogenesis in the rat. *Mol Reprod Dev* **37**, 264-271

102. Kaneda, H., Hayashi, J., Takahama, S., Taya, C., Lindahl, K. F., and Yonekawa, H. (1995) Elimination of paternal mitochondrial DNA in intraspecific crosses during early mouse embryogenesis. *Proc Natl Acad Sci U S A* **92**, 4542-4546
103. Al Rawi, S., Louvet-Vallee, S., Djeddi, A., Sachse, M., Culetto, E., Hajjar, C., Boyd, L., Legouis, R., and Galy, V. (2011) Postfertilization autophagy of sperm organelles prevents paternal mitochondrial DNA transmission. *Science* **334**, 1144-1147
104. Kemler, M., Goker, M., Oberwinkler, F., and Begerow, D. (2006) Implications of molecular characters for the phylogeny of the Microbotryaceae (Basidiomycota: Urediniomycetes). *BMC Evol Biol* **6**, 35
105. Yockteng, R., Marthey, S., Chiapello, H., Gendrault, A., Hood, M. E., Rodolphe, F., Devier, B., Wincker, P., Dossat, C., and Giraud, T. (2007) Expressed sequences tags of the anther smut fungus, *Microbotryum violaceum*, identify mating and pathogenicity genes. *BMC Genomics* **8**, 272
106. Xu, L., Petit, E., and Hood, M. E. (2016) Variation in mate-recognition pheromones of the fungal genus *Microbotryum*. *Heredity (Edinb)* **116**, 44-51
107. Wilch, G., Ward, S., and Castle, A. (1992) Transmission of mitochondrial DNA in *Ustilago violacea*. *Curr Genet* **22**, 135-140
108. Soroka, M. (2008) Doubly uniparental inheritance of mitochondrial DNA in the freshwater bivalve *Anodonta woodiana* (Bivalvia: Unionidae). *Folia Biol (Krakow)* **56**, 91-95
109. Milani, L., Ghiselli, F., Maurizii, M. G., and Passamonti, M. (2011) Doubly uniparental inheritance of mitochondria as a model system for studying germ line formation. *PLoS One* **6**, e28194
110. Kwon-Chung, K. J. (1976) A new species of *Filobasidiella*, the sexual state of *Cryptococcus neoformans* B and C serotypes. *Mycologia* **68**, 943-946
111. Lengeler, K. B., Fox, D. S., Fraser, J. A., Allen, A., Forrester, K., Dietrich, F. S., and Heitman, J. (2002) Mating-type locus of *Cryptococcus neoformans*: a step in the evolution of sex chromosomes. *Eukaryot Cell* **1**, 704-718
112. Hull, C. M., Boily, M. J., and Heitman, J. (2005) Sex-specific homeodomain proteins Sxi1alpha and Sxi2a coordinately regulate sexual development in *Cryptococcus neoformans*. *Eukaryot Cell* **4**, 526-535
113. Yan, Z., and Xu, J. (2003) Mitochondria are inherited from the MATa parent in crosses of the basidiomycete fungus *Cryptococcus neoformans*. *Genetics* **163**, 1315-1325
114. Yan, Z., Hull, C. M., Sun, S., Heitman, J., and Xu, J. (2007) The mating type-specific homeodomain genes SXI1 alpha and SXI2a coordinately control uniparental mitochondrial inheritance in *Cryptococcus neoformans*. *Curr Genet* **51**, 187-195
115. Hsueh, Y. P., Fraser, J. A., and Heitman, J. (2008) Transitions in sexuality: recapitulation of an ancestral tri- and tetrapolar mating system in *Cryptococcus neoformans*. *Eukaryot Cell* **7**, 1847-1855

116. Gyawali, R., and Lin, X. (2013) Prezygotic and postzygotic control of uniparental mitochondrial DNA inheritance in *Cryptococcus neoformans*. *mBio* **4**, e00112-00113
117. Wang, L., Zhai, B., and Lin, X. (2012) The link between morphotype transition and virulence in *Cryptococcus neoformans*. *PLoS Pathog* **8**, e1002765
118. Sun, S., Fu, C., Ianiri, G., and Heitman, J. (2020) The Pheromone and Pheromone Receptor Mating-Type Locus Is Involved in Controlling Uniparental Mitochondrial Inheritance in *Cryptococcus*. *Genetics* **214**, 703-717
119. Hintz, W., Anderson, J. B., and Horgen, P. A. (1988) Nuclear migration and mitochondrial inheritance in the mushroom *agaricus bitorquis*. *Genetics* **119**, 35-41
120. May, G., and Taylor, J. W. (1988) Patterns of mating and mitochondrial DNA inheritance in the agaric Basidiomycete *Coprinus cinereus*. *Genetics* **118**, 213-220
121. Yan, Z., Li, Z., Yan, L., Yu, Y., Cheng, Y., Chen, J., Liu, Y., Gao, C., Zeng, L., Sun, X., Guo, L., and Xu, J. (2018) Deletion of the sex-determining gene *SX11alpha* enhances the spread of mitochondrial introns in *Cryptococcus neoformans*. *Mob DNA* **9**, 24
122. Poloni, A., and Schirawski, J. (2016) Host specificity in *Sporisorium reilianum* is determined by distinct mechanisms in maize and sorghum. *Mol Plant Pathol* **17**, 741-754
123. Schirawski, J., Heinze, B., Wagenknecht, M., and Kahmann, R. (2005) Mating type loci of *Sporisorium reilianum*: novel pattern with three a and multiple b specificities. *Eukaryot Cell* **4**, 1317-1327
124. Burger, G., Gray, M. W., and Lang, B. F. (2003) Mitochondrial genomes: anything goes. *Trends Genet* **19**, 709-716
125. Rodley, C. D., Grand, R. S., Gehlen, L. R., Greyling, G., Jones, M. B., and O'Sullivan, J. M. (2012) Mitochondrial-nuclear DNA interactions contribute to the regulation of nuclear transcript levels as part of the inter-organelle communication system. *PLoS One* **7**, e30943
126. Fetterman, J. L., and Ballinger, S. W. (2019) Mitochondrial genetics regulate nuclear gene expression through metabolites. *Proc Natl Acad Sci U S A* **116**, 15763-15765
127. Bullerwell, C. E., and Gray, M. W. (2004) Evolution of the mitochondrial genome: protist connections to animals, fungi and plants. *Curr Opin Microbiol* **7**, 528-534
128. Kolesnikov, A. A., and Gerasimov, E. S. (2012) Diversity of mitochondrial genome organization. *Biochemistry (Mosc)* **77**, 1424-1435
129. Megarioti, A. H., and Kouvelis, V. N. (2020) The Coevolution of Fungal Mitochondrial Introns and Their Homing Endonucleases (*GIY-YIG* and *LAGLIDADG*). *Genome Biol Evol* **12**, 1337-1354
130. Cedergren, R., and Lang, B. F. (1985) Probing fungal mitochondrial evolution with tRNA. *Biosystems* **18**, 263-267

131. Jimenez-Becerril, M. F., Hernandez-Delgado, S., Solis-Oba, M., and Gonzalez Prieto, J. M. (2018) Analysis of mitochondrial genetic diversity of *Ustilago maydis* in Mexico. *Mitochondrial DNA A DNA Mapp Seq Anal* **29**, 1-8
132. Schulz, B., Banuett, F., Dahl, M., Schlesinger, R., Schafer, W., Martin, T., Herskowitz, I., and Kahmann, R. (1990) The b alleles of *U. maydis*, whose combinations program pathogenic development, code for polypeptides containing a homeodomain-related motif. *Cell* **60**, 295-306
133. Fritsch, E. S., Chabbert, C. D., Klaus, B., and Steinmetz, L. M. (2014) A genome-wide map of mitochondrial DNA recombination in yeast. *Genetics* **198**, 755-771
134. Wang, P., Sha, T., Zhang, Y., Cao, Y., Mi, F., Liu, C., Yang, D., Tang, X., He, X., Dong, J., Wu, J., Yoell, S., Yoell, L., Zhang, K. Q., Zhang, Y., and Xu, J. (2017) Frequent heteroplasmy and recombination in the mitochondrial genomes of the basidiomycete mushroom *Thelephora ganbajun*. *Sci Rep* **7**, 1626
135. Zhang, Y., Yang, G., Fang, M., Deng, C., Zhang, K. Q., Yu, Z., and Xu, J. (2020) Comparative Analyses of Mitochondrial Genomes Provide Evolutionary Insights Into Nematode-Trapping Fungi. *Front Microbiol* **11**, 617
136. Aguilera, G., de Vienne, D. M., Ross, O. N., Hood, M. E., Giraud, T., Petit, E., and Gabaldon, T. (2014) High variability of mitochondrial gene order among fungi. *Genome Biol Evol* **6**, 451-465
137. Lazowska, J., Meunier, B., and Macadre, C. (1994) Homing of a group II intron in yeast mitochondrial DNA is accompanied by unidirectional co-conversion of upstream-located markers. *EMBO J* **13**, 4963-4972
138. Eskes, R., Liu, L., Ma, H., Chao, M. Y., Dickson, L., Lambowitz, A. M., and Perlman, P. S. (2000) Multiple homing pathways used by yeast mitochondrial group II introns. *Mol Cell Biol* **20**, 8432-8446
139. Dickson, L., Huang, H. R., Liu, L., Matsuura, M., Lambowitz, A. M., and Perlman, P. S. (2001) Retrotransposition of a yeast group II intron occurs by reverse splicing directly into ectopic DNA sites. *Proc Natl Acad Sci U S A* **98**, 13207-13212
140. Dutheil, J. Y., Munch, K., Schotanus, K., Stukenbrock, E. H., and Kahmann, R. (2020) The insertion of a mitochondrial selfish element into the nuclear genome and its consequences. *Ecol Evol* **10**, 11117-11132
141. Vaughn, J. C., Mason, M. T., Sper-Whitis, G. L., Kuhlman, P., and Palmer, J. D. (1995) Fungal origin by horizontal transfer of a plant mitochondrial group I intron in the chimeric *CoxI* gene of *Peperomia*. *J Mol Evol* **41**, 563-572
142. Bergthorsson, U., Adams, K. L., Thomason, B., and Palmer, J. D. (2003) Widespread horizontal transfer of mitochondrial genes in flowering plants. *Nature* **424**, 197-201
143. Quispe-Huamanquispe, D. G., Gheysen, G., and Kreuze, J. F. (2017) Horizontal Gene Transfer Contributes to Plant Evolution: The Case of *Agrobacterium* T-DNAs. *Front Plant Sci* **8**, 2015

144. Berridge, M. V., McConnell, M. J., Grasso, C., Bajzikova, M., Kovarova, J., and Neuzil, J. (2016) Horizontal transfer of mitochondria between mammalian cells: beyond co-culture approaches. *Curr Opin Genet Dev* **38**, 75-82
145. Bolker, M., Urban, M., and Kahmann, R. (1992) The a mating type locus of *U. maydis* specifies cell signaling components. *Cell* **68**, 441-450
146. Terfruchte, M., Joehnk, B., Fajardo-Somera, R., Braus, G. H., Riquelme, M., Schipper, K., and Feldbrugge, M. (2014) Establishing a versatile Golden Gate cloning system for genetic engineering in fungi. *Fungal Genet Biol* **62**, 1-10
147. Untergasser, A., Cutcutache, I., Koressaar, T., Ye, J., Faircloth, B. C., Remm, M., and Rozen, S. G. (2012) Primer3--new capabilities and interfaces. *Nucleic Acids Res* **40**, e115
148. Gibson, D. G., Young, L., Chuang, R. Y., Venter, J. C., Hutchison, C. A., 3rd, and Smith, H. O. (2009) Enzymatic assembly of DNA molecules up to several hundred kilobases. *Nat Methods* **6**, 343-345
149. Sambrook, J., Fritsch, E.F., Maniatis, T. (1989) *Molecular Cloning: A Laboratory Manual*, 2nd Edition ed., Cold Spring Harbor Laboratory, NY
150. Ghareeb, H., Zhao, Y., and Schirawski, J. (2019) *Sporisorium reilianum* possesses a pool of effector proteins that modulate virulence on maize. *Mol Plant Pathol* **20**, 124-136
151. Temme, I. J. (2019) *Identification of a histone methyltransferase influencing cell morphology in Sporisorium reilianum f. sp. zaeae*. Master's Thesis, RWTH Aachen University
152. Bakkeren, G., and Kronstad, J. W. (1994) Linkage of mating-type loci distinguishes bipolar from tetrapolar mating in basidiomycetous smut fungi. *Proc Natl Acad Sci U S A* **91**, 7085-7089
153. Martinez, C., Roux, C., Jauneau, A., and Dargent, R. (2002) The biological cycle of *Sporisorium reilianum* f.sp. zaeae: an overview using microscopy. *Mycologia* **94**, 505-514
154. Ghareeb, H., Becker, A., Iven, T., Feussner, I., and Schirawski, J. (2011) *Sporisorium reilianum* infection changes inflorescence and branching architectures of maize. *Plant Physiol* **156**, 2037-2052
155. Wilson, S. B., and Bonner, W. D. (1971) Studies of electron transport in dry and imbibed peanut embryos. *Plant Physiol* **48**, 340-344
156. Nosek, J., and Fukuhara, H. (1994) NADH dehydrogenase subunit genes in the mitochondrial DNA of yeasts. *J Bacteriol* **176**, 5622-5630
157. Moore, A. L., and Siedow, J. N. (1991) The regulation and nature of the cyanide-resistant alternative oxidase of plant mitochondria. *Biochim Biophys Acta* **1059**, 121-140
158. Erdal, S., Genisel, M., Turk, H., Dumlupinar, R., and Demir, Y. (2015) Modulation of alternative oxidase to enhance tolerance against cold stress of chickpea by chemical treatments. *J Plant Physiol* **175**, 95-101
159. Grabelnych, O. I., Borovik, O. A., Tauson, E. L., Pobezhimova, T. P., Katyshev, A. I., Pavlovskaya, N. S., Koroleva, N. A., Lyubushkina, I. V., Bashmakov, V. Y., Popov, V. N., Borovskii, G. B., and Voinikov, V. K. (2014)

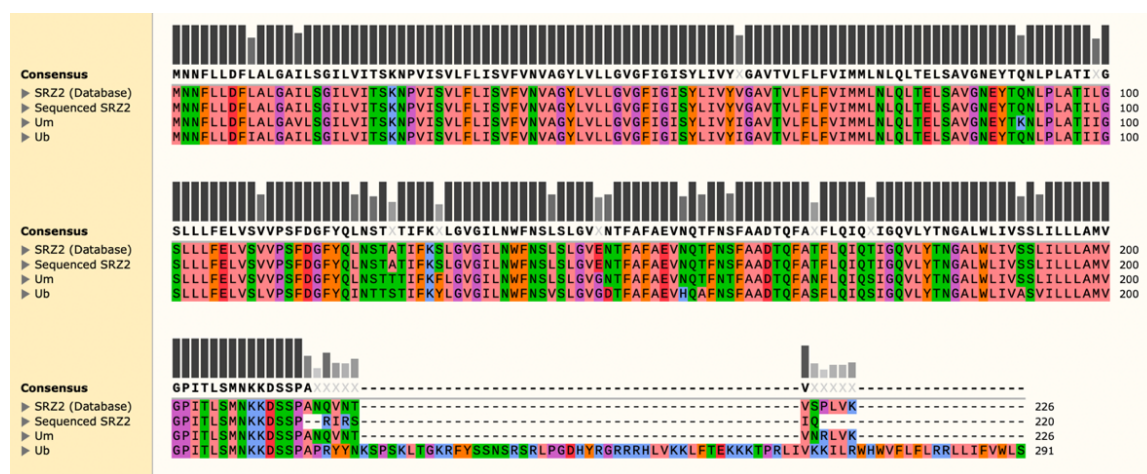
- Mitochondrial energy-dissipating systems (alternative oxidase, uncoupling proteins, and external NADH dehydrogenase) are involved in development of frost-resistance of winter wheat seedlings. *Biochemistry (Mosc)* **79**, 506-519
160. Smith, C. A., Melino, V. J., Sweetman, C., and Soole, K. L. (2009) Manipulation of alternative oxidase can influence salt tolerance in *Arabidopsis thaliana*. *Physiol Plant* **137**, 459-472
 161. Wu, G., Li, S., Li, X., Liu, Y., Zhao, S., Liu, B., Zhou, H., and Lin, H. (2019) A Functional Alternative Oxidase Modulates Plant Salt Tolerance in *Physcomitrella patens*. *Plant Cell Physiol* **60**, 1829-1841
 162. Mhadhbi, H., Fotopoulos, V., Mylona, P. V., Jebara, M., Aouani, M. E., and Polidoros, A. N. (2013) Alternative oxidase 1 (Aox1) gene expression in roots of *Medicago truncatula* is a genotype-specific component of salt stress tolerance. *J Plant Physiol* **170**, 111-114
 163. Dinakar, C., Vishwakarma, A., Raghavendra, A. S., and Padmasree, K. (2016) Alternative Oxidase Pathway Optimizes Photosynthesis During Osmotic and Temperature Stress by Regulating Cellular ROS, Malate Valve and Antioxidative Systems. *Front Plant Sci* **7**, 68
 164. Zhang, L., Oh, Y., Li, H., Baldwin, I. T., and Galis, I. (2012) Alternative oxidase in resistance to biotic stresses: *Nicotiana attenuata* AOX contributes to resistance to a pathogen and a piercing-sucking insect but not *Manduca sexta* larvae. *Plant Physiol* **160**, 1453-1467
 165. Liao, Y., Cui, R., Xu, X., Cheng, Q., and Li, X. (2021) Jasmonic Acid- and Ethylene-Induced Mitochondrial Alternative Oxidase Stimulates *Marssonina brunnea* Defense in Poplar. *Plant Cell Physiol* **61**, 2031-2042
 166. Chaudhuri, M., Ajayi, W., and Hill, G. C. (1998) Biochemical and molecular properties of the *Trypanosoma brucei* alternative oxidase. *Mol Biochem Parasitol* **95**, 53-68
 167. Ott, R., Chibale, K., Anderson, S., Chipeleme, A., Chaudhuri, M., Guerrah, A., Colowick, N., and Hill, G. C. (2006) Novel inhibitors of the trypanosome alternative oxidase inhibit *Trypanosoma brucei* growth and respiration. *Acta Trop* **100**, 172-184
 168. Nakamura, K., Fujioka, S., Fukumoto, S., Inoue, N., Sakamoto, K., Hirata, H., Kido, Y., Yabu, Y., Suzuki, T., Watanabe, Y., Saimoto, H., Akiyama, H., and Kita, K. (2010) Trypanosome alternative oxidase, a potential therapeutic target for sleeping sickness, is conserved among *Trypanosoma brucei* subspecies. *Parasitol Int* **59**, 560-564
 169. Roberts, C. W., Roberts, F., Henriquez, F. L., Akiyoshi, D., Samuel, B. U., Richards, T. A., Milhous, W., Kyle, D., McIntosh, L., Hill, G. C., Chaudhuri, M., Tzipori, S., and McLeod, R. (2004) Evidence for mitochondrial-derived alternative oxidase in the apicomplexan parasite *Cryptosporidium parvum*: a potential anti-microbial agent target. *Int J Parasitol* **34**, 297-308
 170. Liu, S., Roellig, D. M., Guo, Y., Li, N., Frace, M. A., Tang, K., Zhang, L., Feng, Y., and Xiao, L. (2016) Evolution of mitosome metabolism and invasion-related proteins in *Cryptosporidium*. *BMC Genomics* **17**, 1006

171. Lin, Z., Wu, J., Jamieson, P. A., and Zhang, C. (2019) Alternative Oxidase Is Involved in the Pathogenicity, Development, and Oxygen Stress Response of *Botrytis cinerea*. *Phytopathology* **109**, 1679-1688
172. Yukioka, H., Inagaki, S., Tanaka, R., Katoh, K., Miki, N., Mizutani, A., and Masuko, M. (1998) Transcriptional activation of the alternative oxidase gene of the fungus *Magnaporthe grisea* by a respiratory-inhibiting fungicide and hydrogen peroxide. *Biochim Biophys Acta* **1442**, 161-169
173. Miguez, M., Reeve, C., Wood, P. M., and Hollomon, D. W. (2004) Alternative oxidase reduces the sensitivity of *Mycosphaerella graminicola* to QOI fungicides. *Pest Manag Sci* **60**, 3-7
174. Magnani, T., Soriani, F. M., Martins Vde, P., Policarpo, A. C., Sorgi, C. A., Faccioli, L. H., Curti, C., and Uyemura, S. A. (2008) Silencing of mitochondrial alternative oxidase gene of *Aspergillus fumigatus* enhances reactive oxygen species production and killing of the fungus by macrophages. *J Bioenerg Biomembr* **40**, 631-636
175. Hou, L., Liu, L., Zhang, H., Zhang, L., Zhang, L., Zhang, J., Gao, Q., and Wang, D. (2018) Functional analysis of the mitochondrial alternative oxidase gene (*aox1*) from *Aspergillus niger* CGMCC 10142 and its effects on citric acid production. *Appl Microbiol Biotechnol* **102**, 7981-7995
176. Tian, F., Lee, S. Y., Woo, S. Y., and Chun, H. S. (2020) Alternative Oxidase: A Potential Target for Controlling Aflatoxin Contamination and Propagation of *Aspergillus flavus*. *Front Microbiol* **11**, 419
177. Luevano-Martinez, L. A., Caldeira da Silva, C. C., Nicastro, G. G., Schumacher, R. I., Kowaltowski, A. J., and Gomes, S. L. (2019) Mitochondrial alternative oxidase is determinant for growth and sporulation in the early diverging fungus *Blastocladiella emersonii*. *Fungal Biol* **123**, 59-65
178. Juarez, O., Guerra, G., Martinez, F., and Pardo, J. P. (2004) The mitochondrial respiratory chain of *Ustilago maydis*. *Biochim Biophys Acta* **1658**, 244-251
179. Juarez, O., Guerra, G., Velazquez, I., Flores-Herrera, O., Rivera-Perez, R. E., and Pardo, J. P. (2006) The physiologic role of alternative oxidase in *Ustilago maydis*. *FEBS J* **273**, 4603-4615
180. Cardenas-Monroy, C. A., Pohlmann, T., Pinon-Zarate, G., Matus-Ortega, G., Guerra, G., Feldbrugge, M., and Pardo, J. P. (2017) The mitochondrial alternative oxidase *Aox1* is needed to cope with respiratory stress but dispensable for pathogenic development in *Ustilago maydis*. *PLoS One* **12**, e0173389
181. Brachmann, A., Konig, J., Julius, C., and Feldbrugge, M. (2004) A reverse genetic approach for generating gene replacement mutants in *Ustilago maydis*. *Mol Genet Genomics* **272**, 216-226
182. Livak, K. J., and Schmittgen, T. D. (2001) Analysis of relative gene expression data using real-time quantitative PCR and the 2⁻(Delta Delta C(T)) Method. *Methods* **25**, 402-408

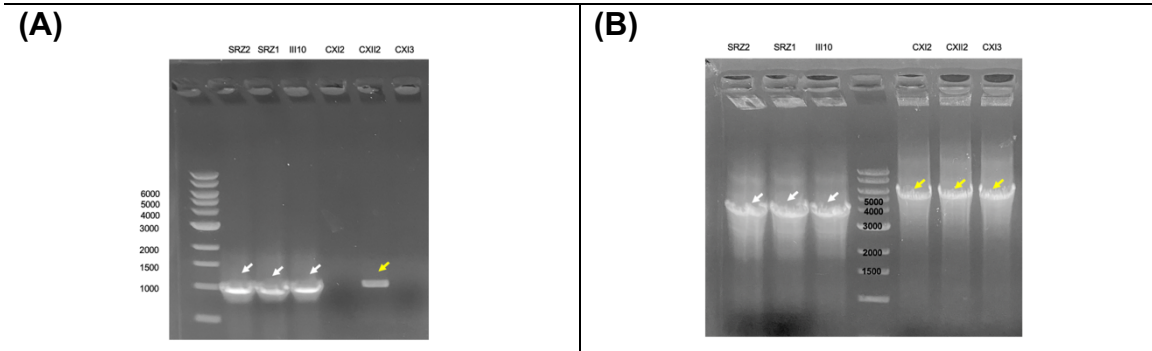
183. Stewart, C. R., Martin, B. A., Reding, L., and Cerwick, S. (1990) Seedling growth, mitochondrial characteristics, and alternative respiratory capacity of corn genotypes differing in cold tolerance. *Plant Physiol* **92**, 761-766
184. Stewart, C. R., Martin, B. A., Reding, L., and Cerwick, S. (1990) Respiration and Alternative Oxidase in Corn Seedling Tissues during Germination at Different Temperatures. *Plant Physiol* **92**, 755-760
185. Polidoros, A. N., Mylona, P. V., Pasentsis, K., Scandalios, J. G., and Tsiftaris, A. S. (2005) The maize alternative oxidase 1a (Aox1a) gene is regulated by signals related to oxidative stress. *Redox Rep* **10**, 71-78

APPENDIX

SUPPLEMENTAL MATERIAL



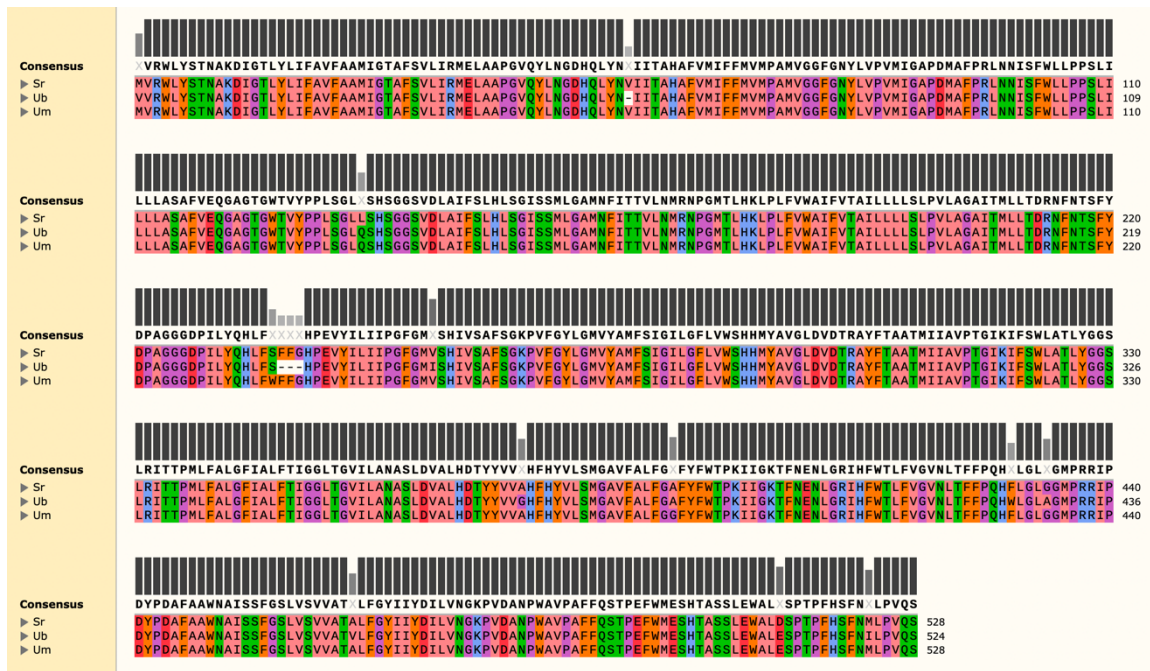
Supplemental Figure 1 - MUSCLE analysis of amino acid sequence of *nad6* against known polypeptides. Protein sequences for *nad6* of the following organisms were used: *S. reilianum* (NCBI Accession No. CBQ72567.1), *U. maydis* (Um, NCBI Accession No. YP_762704.1) and *U. bromivora* (Ub, NCBI Accession No. SAM86553.1). Amino acids with similar physico-chemical properties are represented by the same color. Bars represent amino acid conservation across all sequences analyzed, with darker and taller bars corresponding to higher conservation indexes. Amino acids in bold make up the consensus sequence and represent 100% conservation in that position.



Supplemental Figure 2 – Agarose gel electrophoresis of PCR using primers around the 1611 bp deletion initially detected in Chinese strains. (A) The use of the primer pair oHM112/113 results in the amplification of a 1071 bp fragment in German strains only (white arrows), as these primers have no binding site on Chinese mtDNA. A band was detected in the strain SRZCXI2 (yellow arrow) but was very faint and appeared larger than the expected amplicon. (B) The use of the primer pair oHM119/120 results in the amplification of a 4143 bp fragment in German strains (white arrows) and a 2795 bp fragment in Chinese strains. Surprisingly, the Chinese strains produced a fragment significantly larger (~6000 bp). The updated sequences of the Chinese strains that include the novel DNA fragment discovered through Primer Walking sequencing confirm that this primer pair should result in the amplification of a fragment 5889 bp in size.



(B)



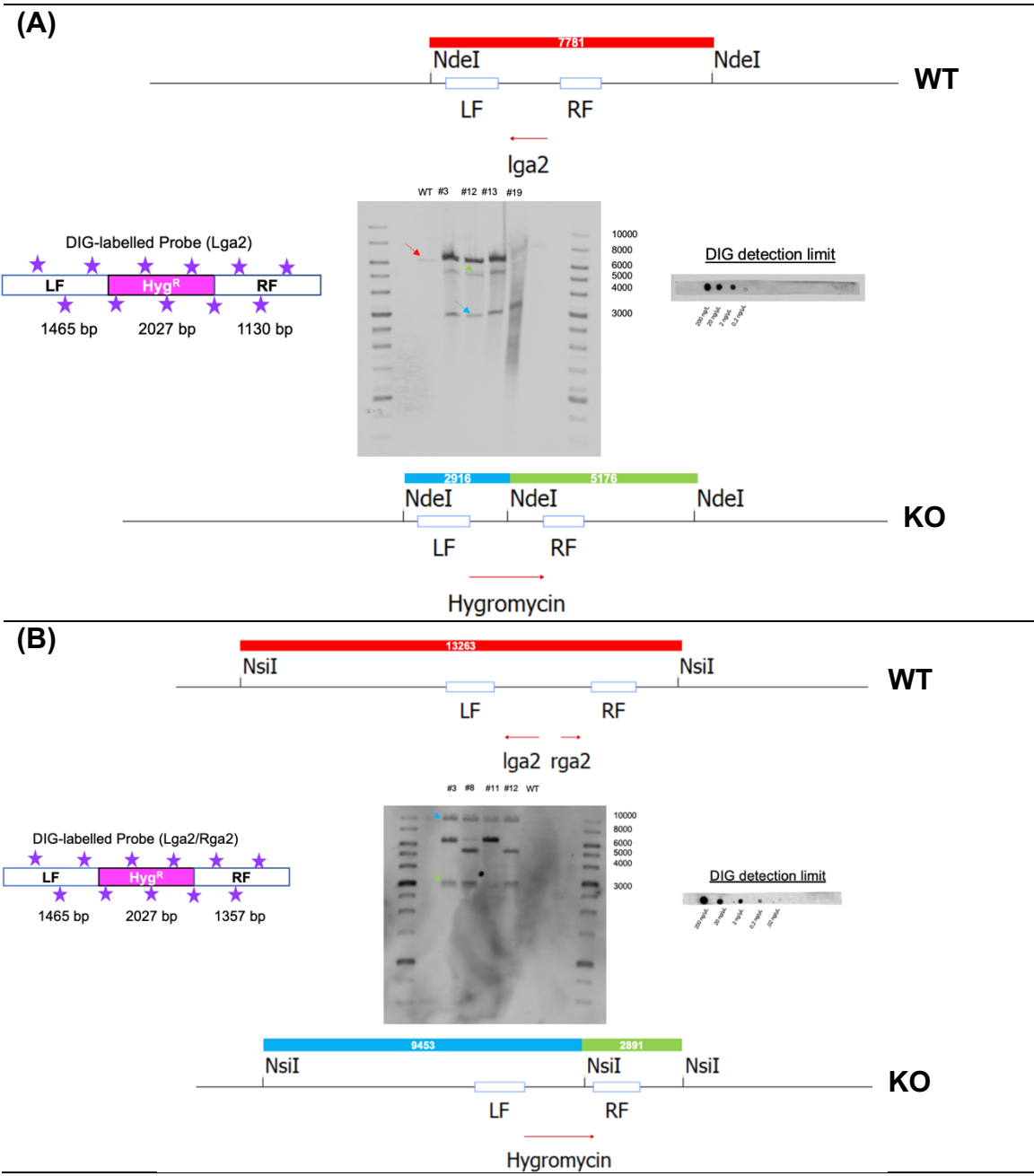
Supplemental Figure 3 – Bioinformatic analysis of *cox1*. (A) Graphical representation of BLASTn analysis of unique region of *cox1* in Chinese strains against the mitogenome of *U. bromivora*. Five regions of high percent identity were identified and are depicted as grey boxes with red lines indicating single-base mismatches. These 5 regions overlapped 2 intron-encoded LAGLIDAADG endonucleases (NCBI Accession No. UBRO_21211 and SAM86524.1) and exons 9, 10 and 11 corresponding to the coding sequence of the *U. bromivora cox1* (NCBI Accession No. SAM86522.1). (B) MUSCLE analysis of amino acid sequence of *aox1* against known polypeptides. Protein sequences for *cox1* of the following organisms were used: *S. reilianum* (Sr, NCBI Accession No. CBQ72556.1), *U. bromivora* (Ub, NCBI Accession No. SAM86522.1) and *U. maydis* (Um, NCBI Accession No. AAZ67011.1). Amino acids with similar physico-chemical properties are represented by the same color. Bars represent amino acid conservation across all sequences analyzed, with darker and taller bars corresponding to higher conservation indexes. Amino acids in bold make up the consensus sequence and represent 100% conservation in that position.

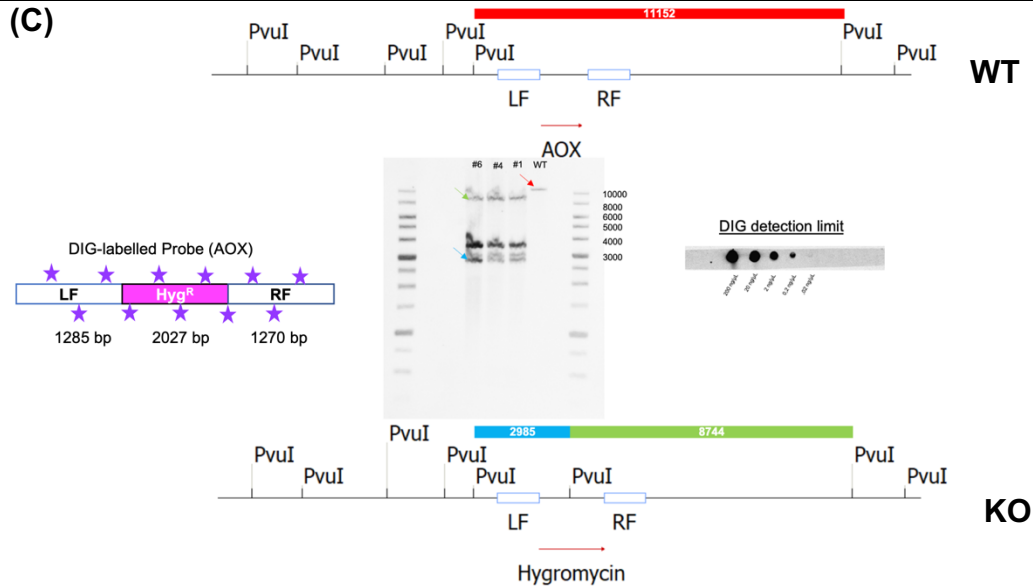
Supplemental Protocol 1: southern blots

Southern blot analysis was performed to verify the deletion mutants generated in Chapters 3 and 4. For this, the deletion constructs for Lga2, Lga2/Rga2, and AOX were used as hybridization probes by PCR amplification using Q5 High-Fidelity DNA Polymerase (New England Biolabs) and subsequent digoxigenin labelling using DIG-High Prime DNA Labelling Mix (Roche AG). The fully synthesized probe was stored at -20°C.

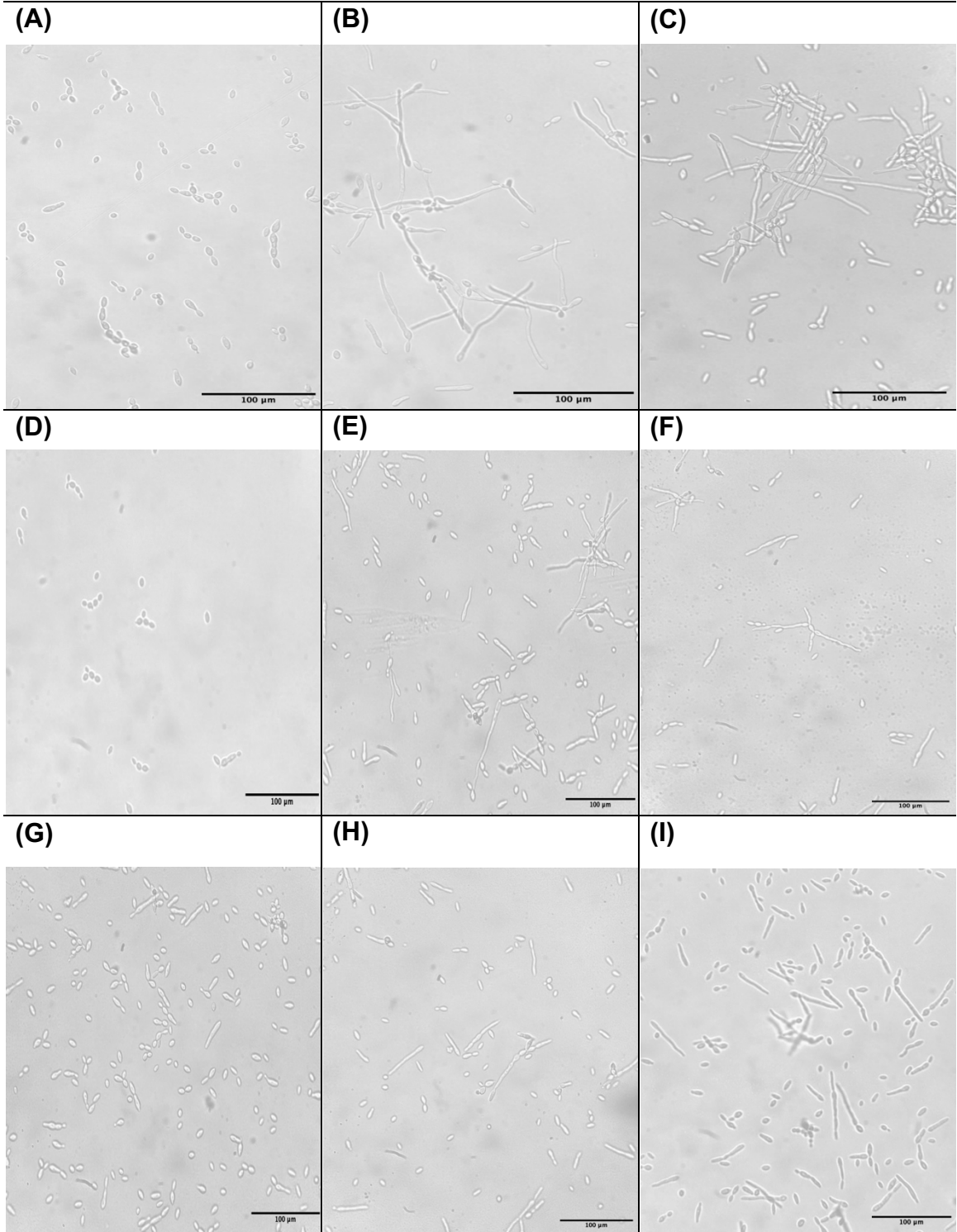
Genomic DNA (gDNA) from the mutant and WT strains was digested with the appropriate restriction enzymes (New England Biolabs) and used as controls. The digested gDNA was transferred from TAE agarose gel electrophoresis to a nylon membrane using a capillary blot in 0.25M HCl and subsequent neutralization in 0.4M NaOH. The transferred DNA was auto crosslinked to the membrane via exposure to UV light at 120 mJ/cm² for 5 minutes.

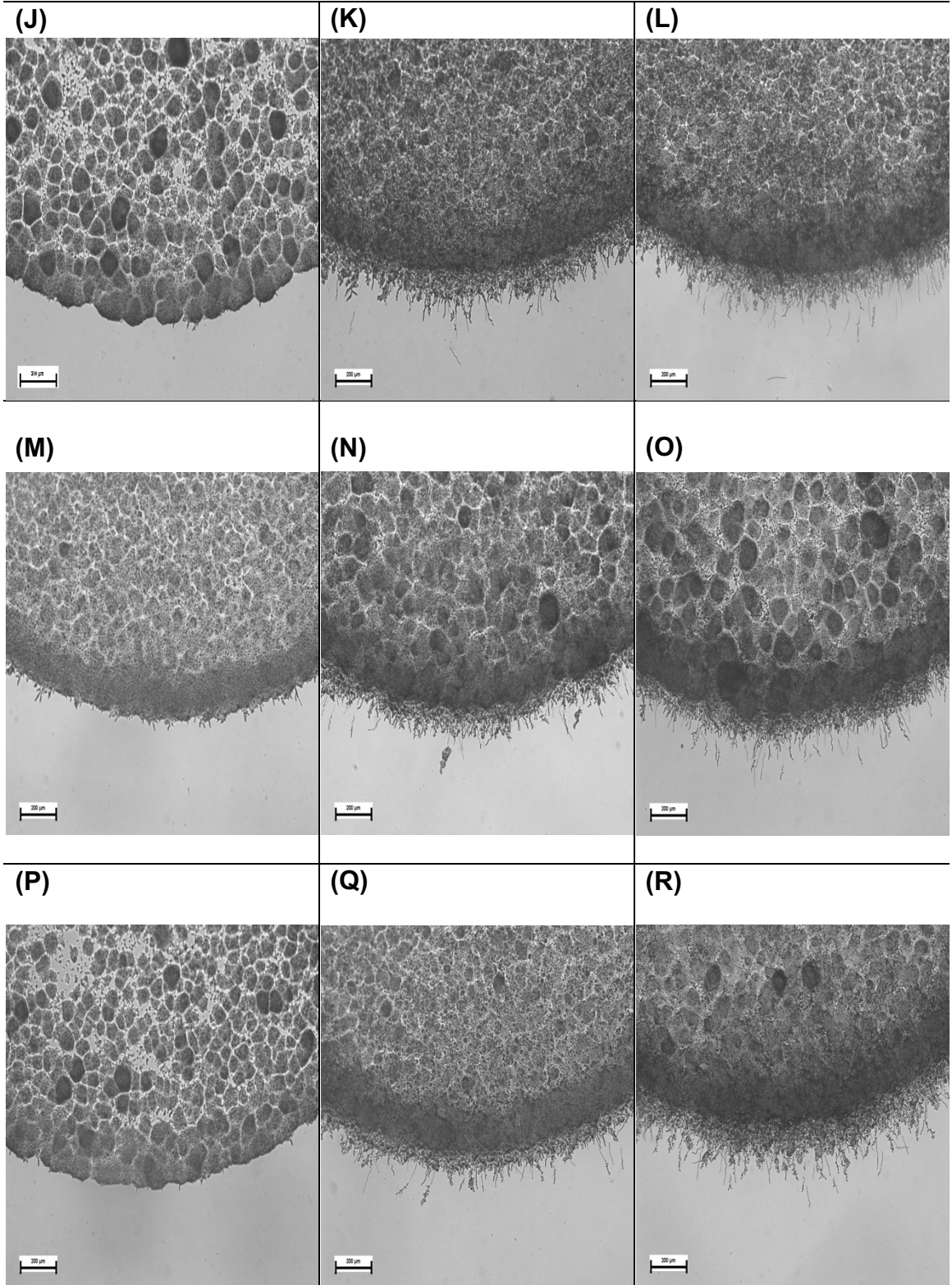
Hybridization of the involved incubation of the membrane with Southern hybridization buffer (SHB) at 65°C for 1 hour with simultaneous denaturation of the probes resuspended in 30 mL of SHB at 99°C for 10 minutes. The hybridization SHB was then replaced by the SHB-probe solution and incubated overnight at 65°C. Prior to signal detection, membranes were washed twice with Southern was buffer (SWB) at 65°C for 15 minutes. The SWB was then replaced by DIG wash buffer (DIG) and incubated at room temperature for 10 minutes. The DWB was replaced by the DIG II buffer and incubated at room temperature for an additional 30 minutes. The DIG II buffer was replaced anti-digoxigenin antibody solution (Roche AG) and incubated at room temperature for 30 minutes. The membrane was then washed twice with DWB at room temperature for 15 minutes and then treated with DIG III buffer at room temperature for 5 minutes. Finally, the DIG III buffer was replaced by CDP-Star solution (Roche AG) and incubated at 37°C for 5 minutes. Once the CDP-Start solution was removed, the membrane was incubated in the dark at 37°C for 15 minutes. Imaging was performed using a chemiluminescence-sensitive gel imaging system (ChemiDoc™ XRS) with exposure times varying between 30-240 seconds.



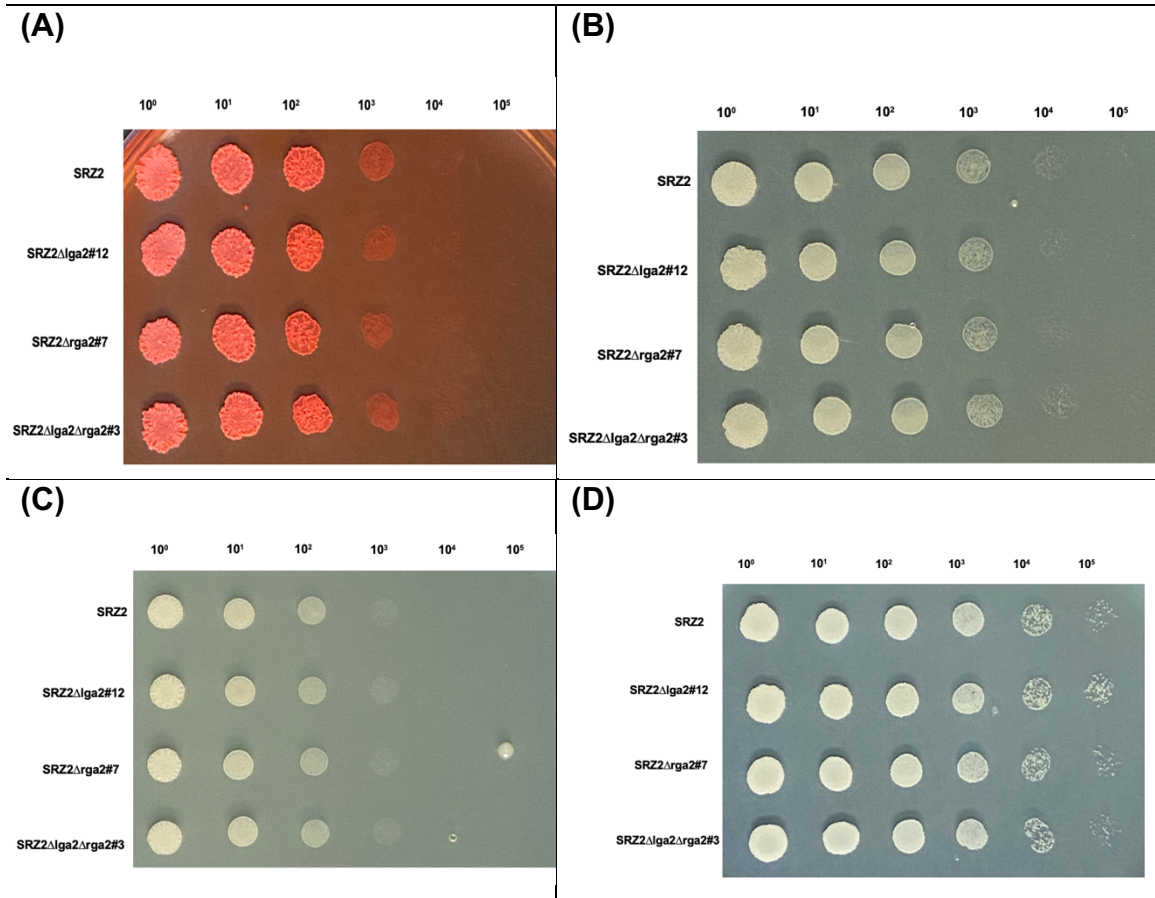


Supplemental Figure 4. Southern blot analysis to confirm deletion of target genes in SRZ. The deletion constructs for Lga2, Lga2/Rga2 and AOX were used as hybridization probes by PCR amplification using Q5 High-Fidelity DNA Polymerase (New England Biolabs) and subsequent digoxigenin (DIG) labelling using DIG-High Prime DNA Labelling Mix (Roche AG). In each panel, a schematic representation of expected bands is illustrated for both WT (above each gel) and deletion mutant (below each gel) strains for the determination of target gene replacement with the corresponding disruption construct. The lowest amount of gDNA detected by the DIG-labelled probes was approximated by pipetting serial dilutions of the unlabeled deletion constructs and hybridizing them with the labelled deletion construct. Detection was strong at 0.2 $\mu\text{g}/\mu\text{L}$ for all three Southern blots performed. (A) Southern blot for verification of Lga2 deletion mutants, in which gDNA was digested with NdeI, producing a single band 7781 bp (indicated in red) in size in WT strains and 2916 bp and 5176 bp (indicated in blue and green, respectively) in size in successful mutants. (B) Southern blot for verification of Lga2/Rga2 double mutants, in which gDNA was digested with NsiI, producing a single band 13262 bp (indicated in red) in size in WT strains and two bands 9453 bp and 2891 bp (indicated in blue and green, respectively) in size in successful mutant strains. Note that the band corresponding to WT gDNA was very faint and is not indicated in the photograph. (C) Southern blot for verification of AOX deletion mutants, in which gDNA was digested with PvuI, producing a single band of hybridization 11152 bp (indicated in red) in size in WT strains and two bands 2985 bp and 8744 bp (indicated in blue and green, respectively) in size in successful mutant strains.

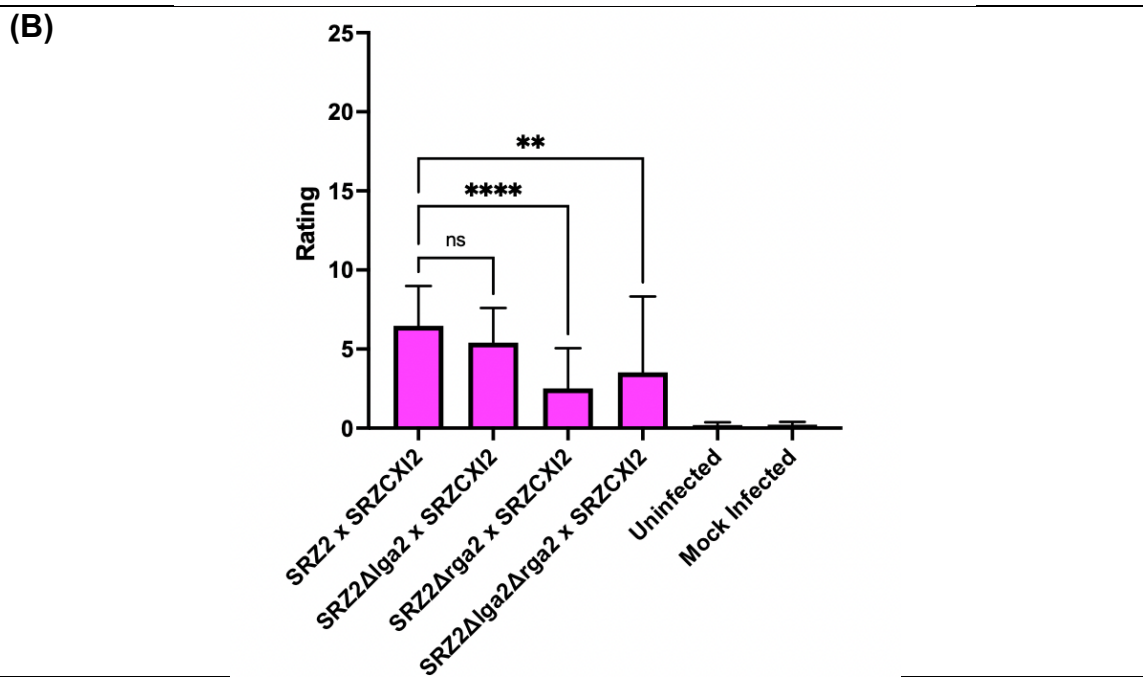
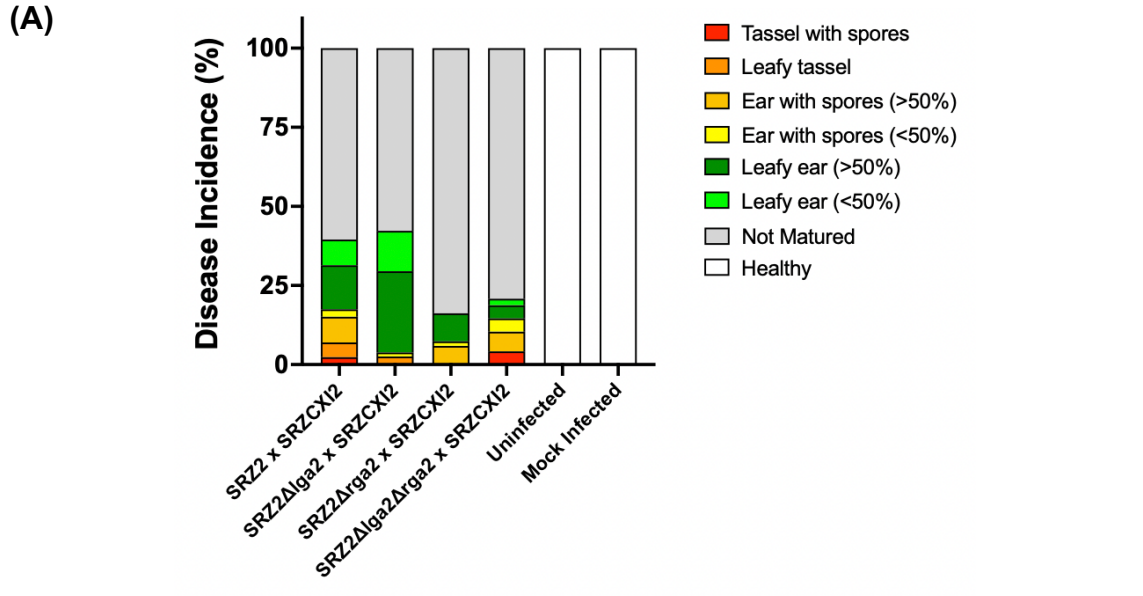




Supplemental Figure 5 – Mating reactions for Lga2/Rga2 mutants. Assessment of conjugation (A-I) and analysis of colony edges for determination of dikaryon formation (J-R) are indicators of successful mating between compatible partners: (A/J) SRZ2Δlga2#12, (B/K) SRZ2Δlga2#12 x SRZ1, (C/L) SRZ2Δlga2#12 x SRZCX12, (D/M) SRZ2Δrga2#7, (E/N) SRZ2Δrga2#7 x SRZ1, (F/O) SRZ2Δrga2#7 x SRZCX12, (G/P) SRZ2Δlga2Δrga2#3, (H/Q) SRZ2Δlga2Δrga2#3 x SRZ1, (I/R) SRZ2Δlga2Δrga2#3 x SRZCX12.

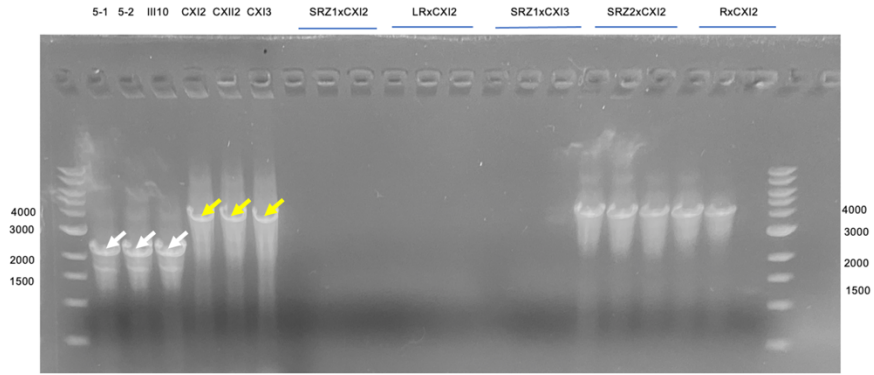


Supplemental Figure 6 – Growth of Lga2/Rga2 mutants on stress media. 10-fold dilutions of WT and Lga2/Rga2 mutant strains were spotted onto PD agar, supplemented with 100 μM CR (A), 1M sorbitol (B), 1M NaCl (C) and 1.5 mM H₂O₂ (D). Plates were photographed 48 hours post-inoculation.

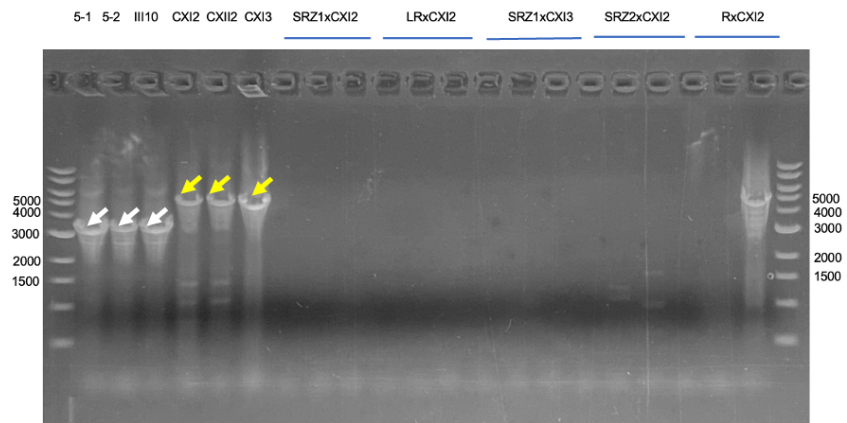


Supplemental Figure 7 – Assessment of pathogenicity of Lga2/Rga2 mutants on maize. (A) Mutant and WT strains of SRZ were used to infect maize seedlings. Test groups consisted of 10-14 plants and symptoms were scored 7-8 wpi according to the ranking score illustrated in Figure 3. (B) Mean disease severity indexes were calculated based on the individual symptoms ranking. Bars represent averages of biological within each group, with standard errors indicated. Comparisons were made between WT crosses and their corresponding AOX deletion mutant crosses, with statistical significance indicated on top of bars. For statistical comparisons, $p \geq 0.05$ = not significant (ns), $p \leq 0.05$ = weakly significant (*), $p \leq 0.01$ = significant (**), $p \leq 0.001$ = very significant (***) and $p \leq 0.0001$ = extremely significant (****).

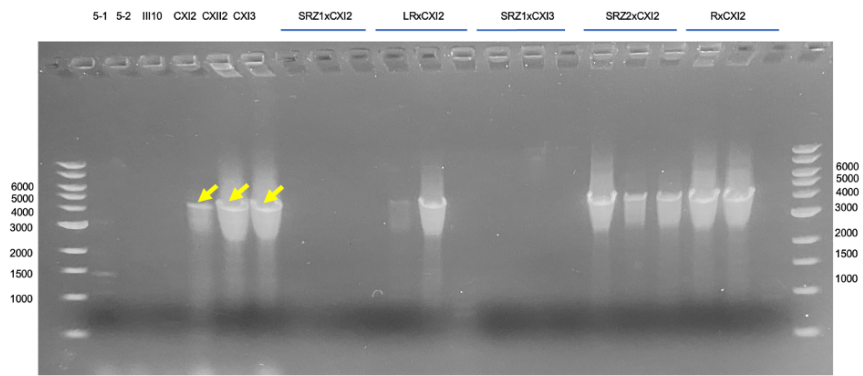
(A)



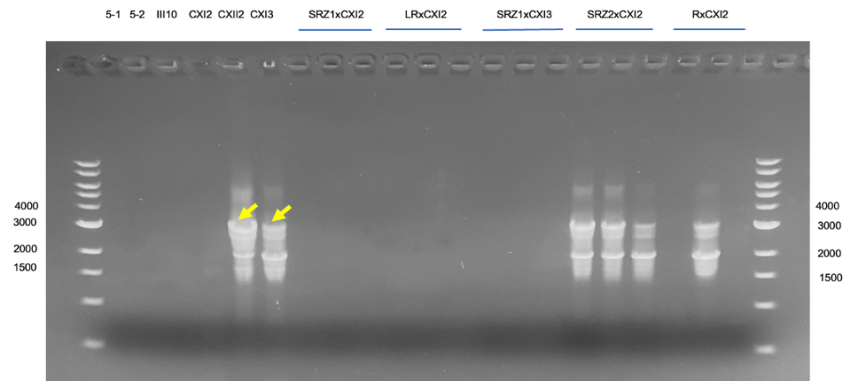
(B)

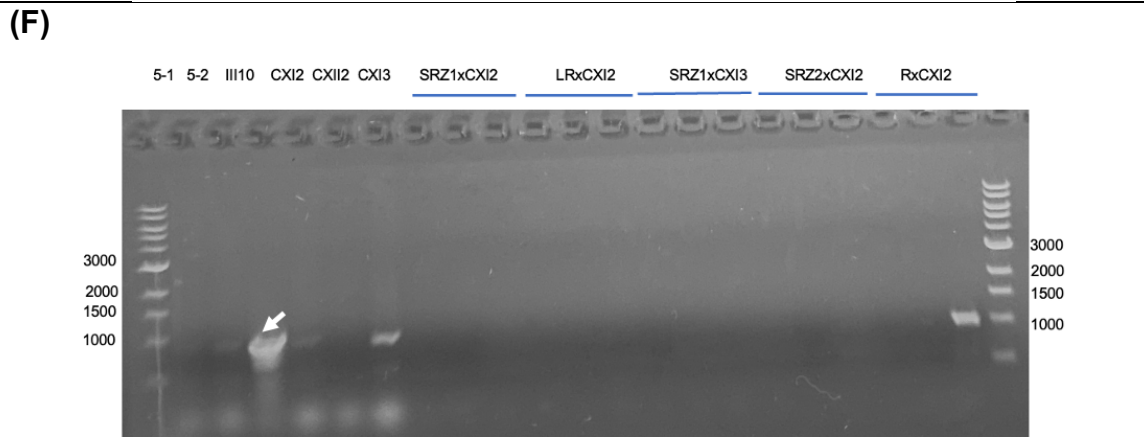
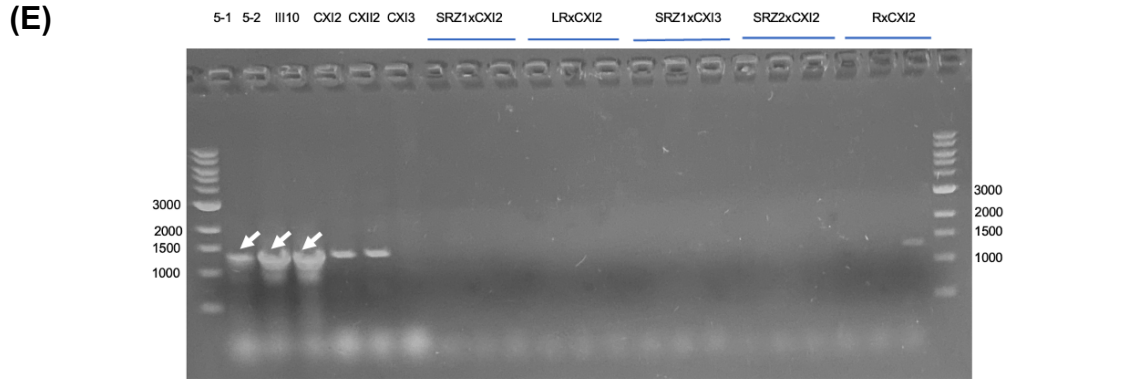


(C)



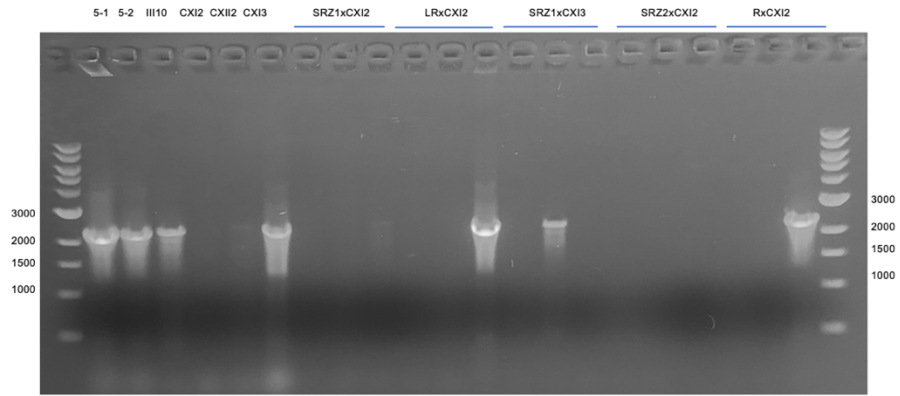
(D)



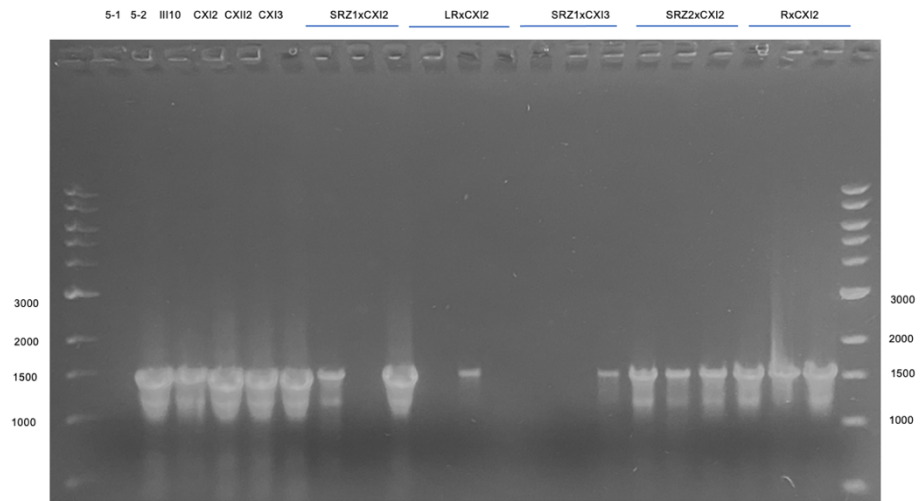


Supplemental Figure 8 – Gel electrophoresis for the determination of SRZ mitotype based on *cox1* polymorphic region. 5-1 = SRZ2, 5-2 = SRZ1, LR = Lga2/Rga2 deletion mutant, R = Rga2 deletion mutant. Three biological replicates were performed for each cross tested, corresponding to three separate mtDNA extractions. White arrows correspond to bands produced exclusively in German strains, while yellow arrows correspond to bands produced exclusively in Chinese strains. (A) oHM127/131, German = 2420, Chinese = 4165 bp. (B) oHM119/115, German = 3603 bp, Chinese = 5347 bp. (C) oHM115/116, Chinese only = 4154 bp. (D) oHM133/136, Chinese only = 3115 bp. Note that SRZCXI2 did not produce the expected band. Experiment was repeated to ensure this was due to technical issues in the preparation of the PCR reaction, and not an actual finding (not shown). (E) oHM112/128, German only = 1347 bp. Note that Chinese strains SRZCXI2 and SRZCXII2 produced bands, but these were faint and looked slightly larger than the expected size. One replicate of the teliospore produced in “RxCXI2” also produced this nonspecific band. (F) oHM112/113, German only = 1071 bp. Note that only SRZIII10 produced a clear band. Experiment was repeated to ensure that this amplification also occurred for the remaining German strains 5-1 and 5-2 (not shown). The Chinese strains produced faint bands that were slightly larger than the expected size. One replicate of the teliospore produced in “RxCXI2” also produced this unexpected band.

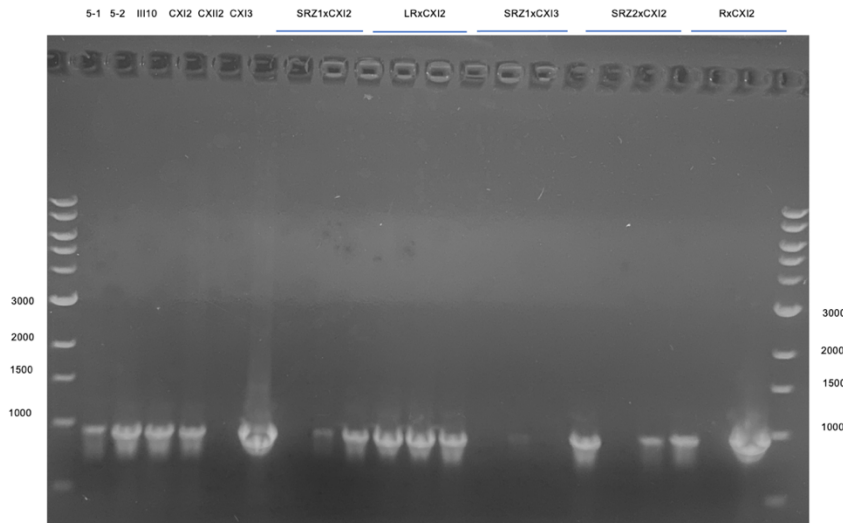
(A)



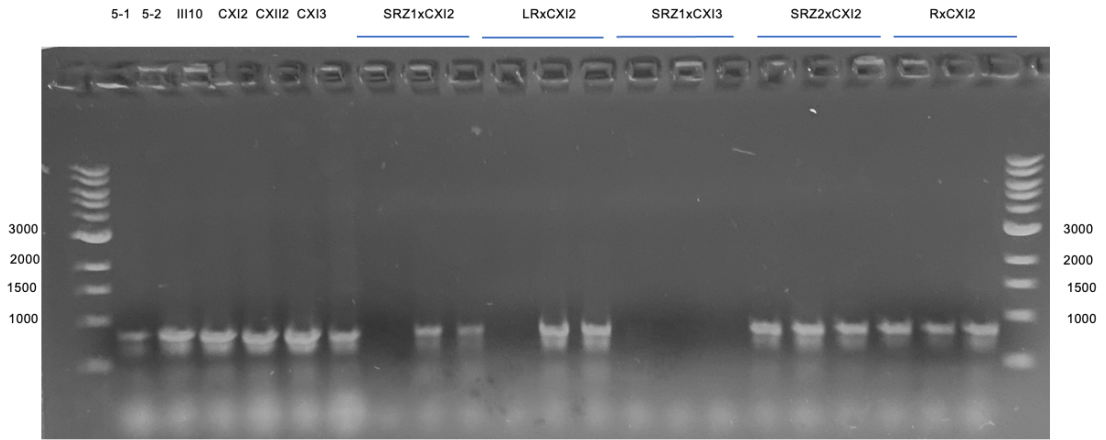
(B)



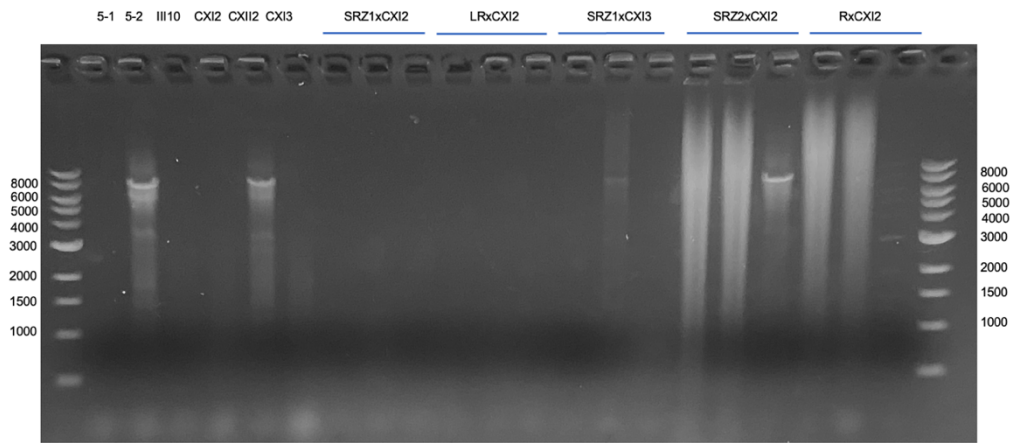
(C)



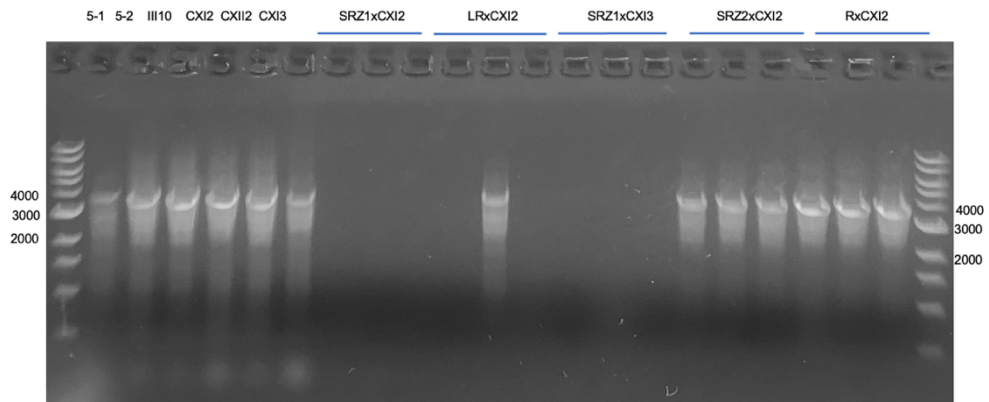
(D)



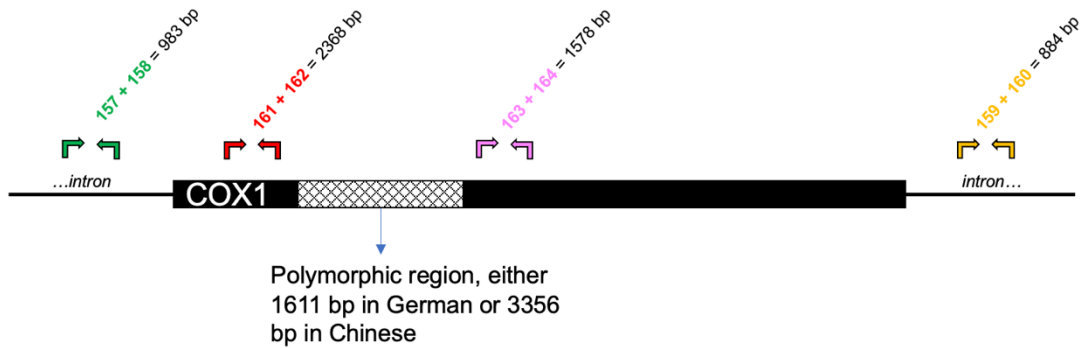
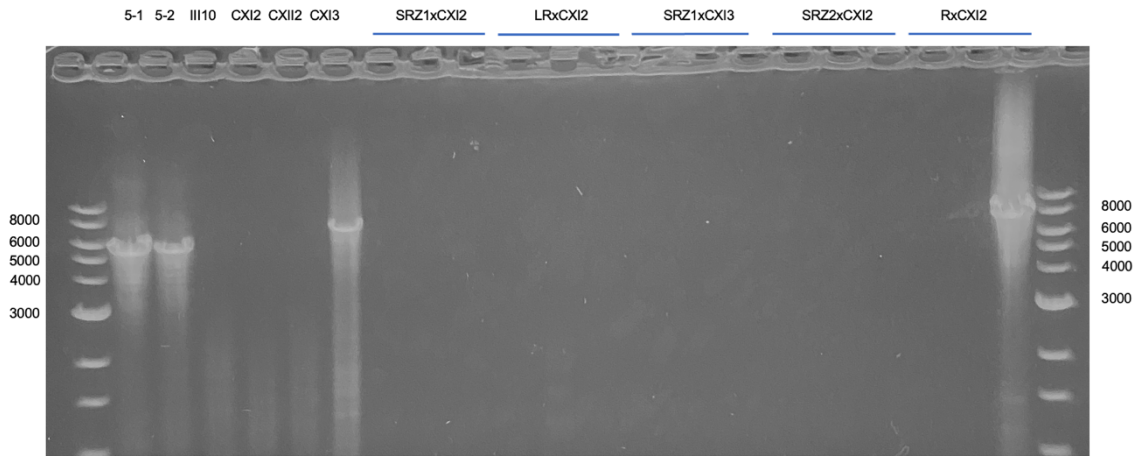
(E)



(F)

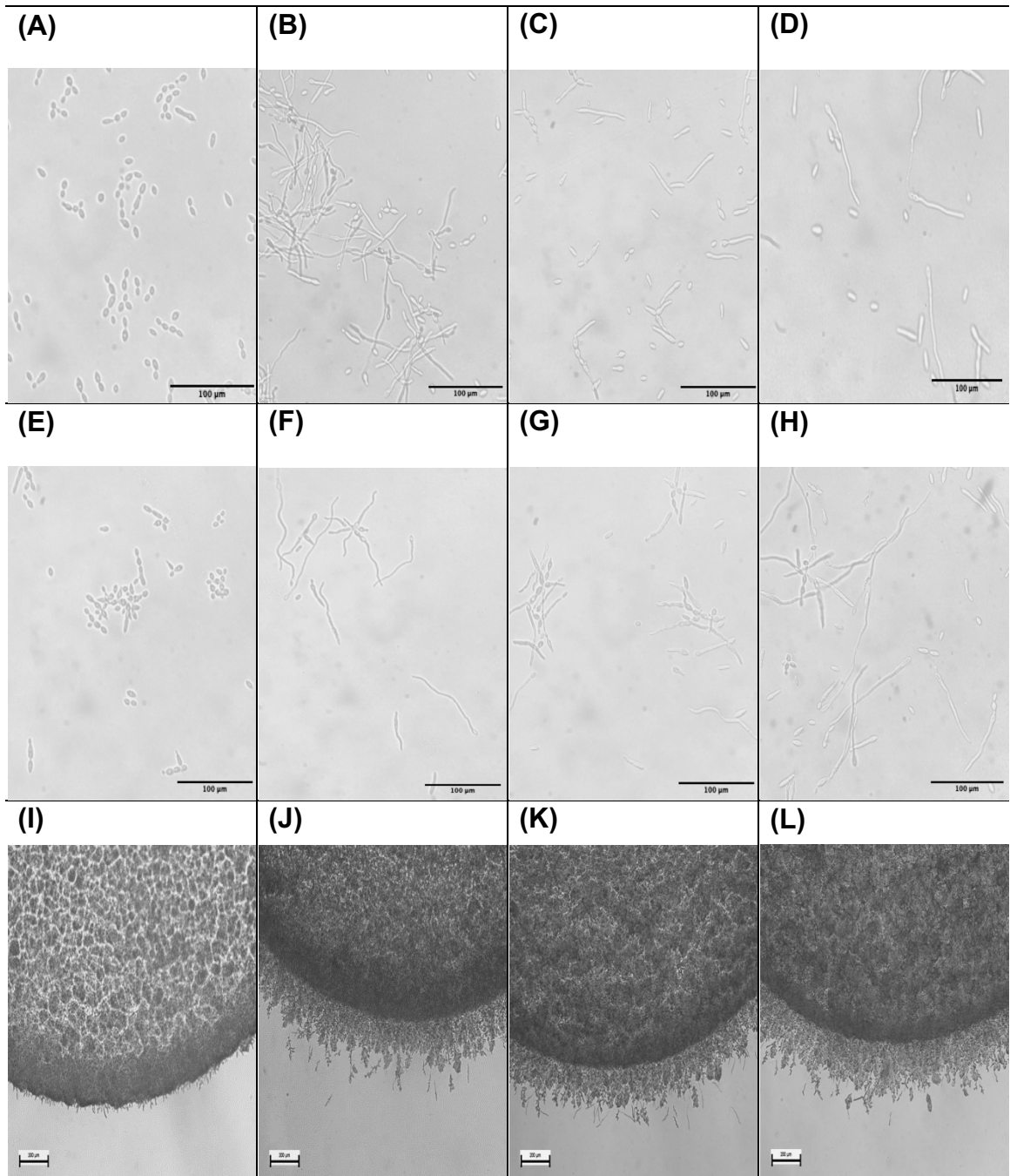


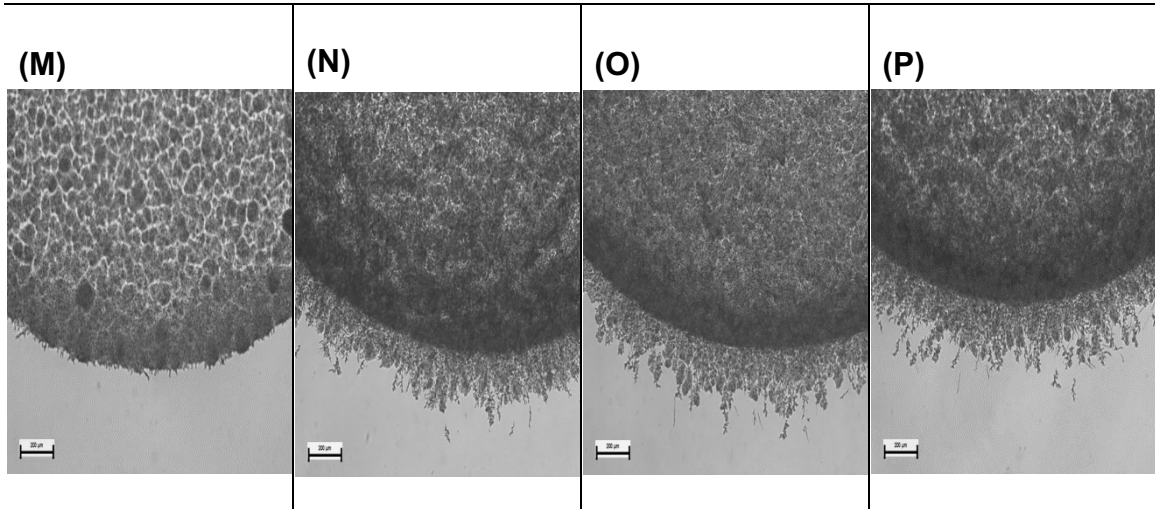
(G)



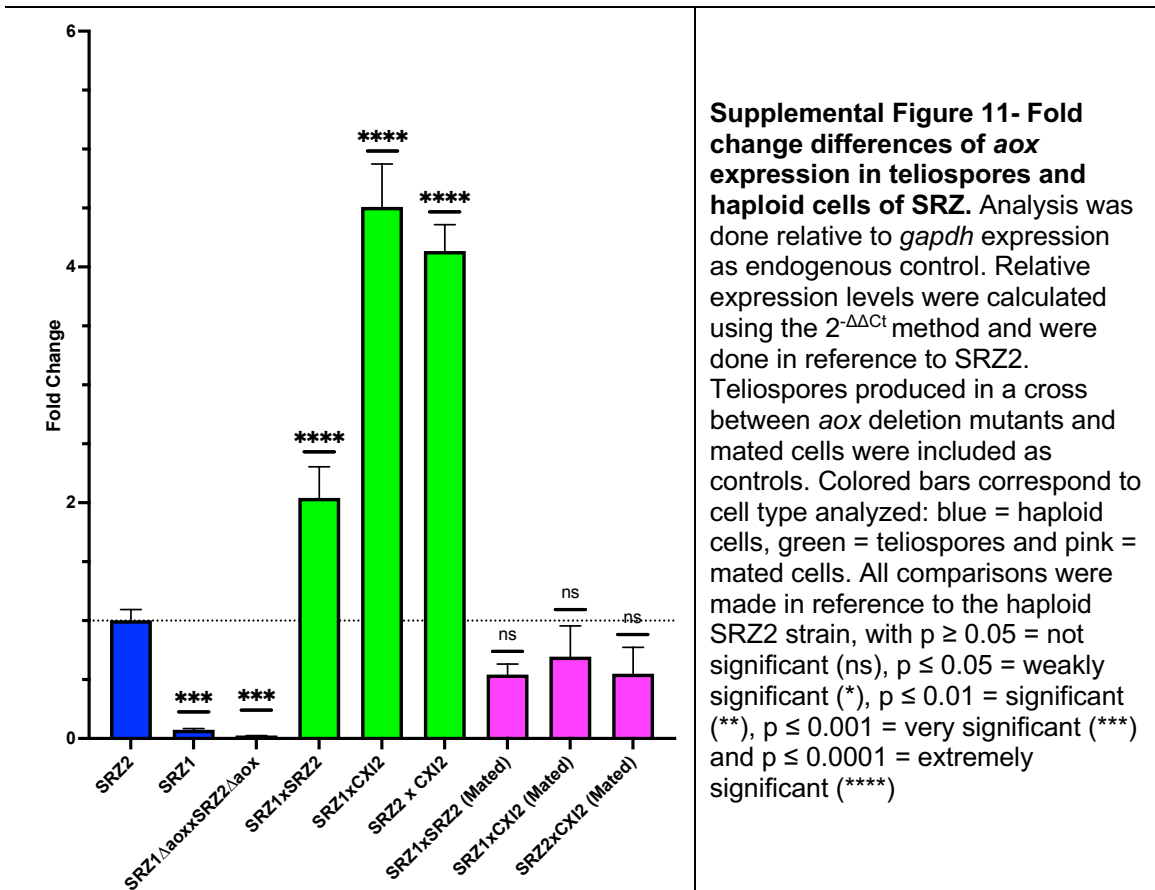
(H)

Supplemental Figure 9 – Gel electrophoresis for the exploration of the vicinity of the polymorphic region of *cox1*. 5-1 = SRZ2, 5-2 = SRZ1, LR = Lga2/Rga2 deletion mutant, R = Rga2 deletion mutant. Three biological replicates were performed for each cross tested, corresponding to three separate mtDNA extractions. (A) oHM161/162 = 2368 bp. (B) oHM163/164 = 1578 bp. (C) oHM157/158 = 983. (D) oHM159/160 = 884 bp. (E) oHM163/160 = 8241 bp. (F) oHM157/162 = 3992. (G) oHM161/164, German = 5941 bp, Chinese = 7686 bp. (H) Schematic representation of COX1 polymorphic region and corresponding primer binding sites.





Supplemental Figure 10 – Additional mating reactions of AOX mutants. Assesment of conjugation: (A) unmated/incompatible control, SRZ2, (B) SRZ2xSRZ1, (C) SRZ2 x SRZCXI2, (D) SRZ1 x SRZCXI2, (E) unmated/incompatible mutant control, $\Delta aox\#4$, (F) SRZ2 $\Delta aox\#1$ x SRZ1 $\Delta aox\#2$, (G) SRZ2 $\Delta aox\#1$ x SRZCXI2 $\Delta aox\#4$, (H) SRZ1 $\Delta aox\#2$ x SRZCXI2 $\Delta aox\#4$. Analysis of colony surfaces to determine dikaryon formation: (I) unmated/incompatible control, SRZ2, (J) SRZ2 x SRZ1, (K) SRZ2 x SRZCXI2, (L) SRZ1 x SRZCXI2, (M) unmated/incompatible mutant control, SRZCXI2 $\Delta aox\#4$, (N) SRZ2 $\Delta aox\#1$ x SRZ1 $\Delta aox\#2$, (O) SRZ2 $\Delta aox\#1$ x SRZCXI2 $\Delta aox\#4$, (P) SRZ1 $\Delta aox\#2$ x SRZCXI2 $\Delta aox\#4$.



Supplemental Figure 11- Fold change differences of aox expression in teliospores and haploid cells of SRZ. Analysis was done relative to *gapdh* expression as endogenous control. Relative expression levels were calculated using the $2^{-\Delta\Delta C_t}$ method and were done in reference to SRZ2. Teliospores produced in a cross between *aox* deletion mutants and mated cells were included as controls. Colored bars correspond to cell type analyzed: blue = haploid cells, green = teliospores and pink = mated cells. All comparisons were made in reference to the haploid SRZ2 strain, with $p \geq 0.05$ = not significant (ns), $p \leq 0.05$ = weakly significant (*), $p \leq 0.01$ = significant (**), $p \leq 0.001$ = very significant (***) and $p \leq 0.0001$ = extremely significant (****)

CURRICULUM VITAE

Hector E. Mendoza

Louisville, KY 40204 ■ mikin18@hotmail.com ■ (917) 623-7525 ■
linkedin.com/in/hecmendoza

Education

2021 **PhD Biology**. University of Louisville, Advisor: Michael H. Perlin, GPA:
3.832

2015 **BA Biology**. CUNY Queens College, *Cum Laude*, GPA: 3.552

Publications

Primary research:

Wallen, R. M., Richardson, K., Furnish, M., **Mendoza, H.**, Dentinger, A., Khanal, S., & Perlin, M. "Differential Roles for *Ustilago maydis* b Locus Components in Haploid Cells vis-à-vis Nutritional Availability." *Journal of Fungi* 2021(7): 135. DOI: 10.3390/jof7020135

Khanal, S., Schroeder, L., Nava-Mercado, O. A., **Mendoza, H.** & Perlin, M. H. "Role for nitrate assimilatory genes in virulence of *Ustilago maydis*." *Fungal Biology*. 2021. <https://doi.org/10.1016/j.funbio.2021.04.010>.

Reviews:

Mendoza, H., Perlin, M. H., Schirawski, J. 2020. "Mitochondrial inheritance in phytopathogenic fungi: Everything is known, or is it?" *International Journal of Molecular Sciences* 2021(11): E3883. DOI: 10.3390/ijms21113883

Presentations

2021 Biology Department Awards (University of Louisville).

“Investigating inheritance mechanisms of mitochondria in the smut fungus *Sporisorium reilianum*”.

2019 Smut Convergence Mini Conference (Bochum, Germany).
“Implications of a degradation-mediated mitochondrial inheritance system”.

Grants and Awards

2021 Institutional Research and Academic Career Development Awards (IRACDA) Post-Doctoral Program, University of Michigan (Declined)

2021 Biology Department Presentation Award, University of Louisville (\$100)

2021 Doctoral Dissertation Completion Award, Graduate School, University of Louisville (\$10,000)

2020-2021 Dissertation Scholar Fellowship Award, Southern Regional Education Board (SREB) (\$25,000)

2017-2019 Diversity Assistantship, Graduate School, University of Louisville (\$66,000)

2019 Biology Department Teaching Assistant Award, University of Louisville (\$500)

2017 Graduate Network in A&S Research Fund, College of Arts & Sciences, University of Louisville (\$500)

2017 A&S Research and Creative Activities Grant, College of Arts & Sciences, University of Louisville (\$1000)

Pedagogy

BIOL 240 Unity of Life Honors Recitation (2020), University of Louisville

BIOL 244 Principles of Biology Laboratory (2018), University of Louisville

BIOL 331 Genetics and Molecular Biology Laboratory (2017-2018), University of Louisville

Mentorship

Graduate Students

2021-Present **Otniel Nava-Mercado** (UofL '22) – Gene expression analysis in *Ustilago maydis* as it relates to its tetrapolar mating-type system and nitrogen availability.
Outcomes: Master's project in progress.

Undergraduate Students

2020-Present **Luke Schroeder** (UofL '21) – Investigating disease resistance to *Ustilago maydis* in wild strains of maize.
Outcomes: Senior thesis in progress.

2019-Present **Emma Lamb** (UofL '21) – Exploring mitochondrial respiration in *Sporisorium reilianum*.
Outcomes: Senior thesis in progress, Summer Research Opportunity Program 2021 (SROP) poster presentation.

2018-2019 **Caroline Culver** (UofL '20) – Characterization of a putative alternative oxidase (AOX) in *Sporisorium reilianum*.
Outcomes: Senior thesis completed in 2020, conference presentation in Bochum, Germany.